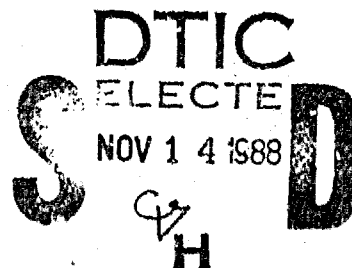Pressure Variation Over a
Solid Wavy Surface

Prepared by
David James Courtemanche
Thomas J. Hanratty, Project Supervisor
for
The Office of Naval Research, Arlington, VA 2217
Contract N00014-82-K-0324
Project NR 657-728

Report 8

Department of Chemical Engineering
University of Illinois
Urbana, Illinois
61801

DTIC
ELECTE
NOV 1 4 1988
H

October, 1988

·88 11 14 067

REPORT DOCUMENTATION PAGE		READ INSTRUCTIONS BEFORE COMPLETING FORM
1. REPORT NUMBER Report 8	2. GOVT ACCESSION NO.	3. RECIPIENT'S CATALOG NUMBER
4. TITLE (and Subtitle) Pressure Variation Over a Solid Wavy Surface		5. TYPE OF REPORT & PERIOD COVERED Progress 1987-1988
		6. PERFORMING ORG. REPORT NUMBER
7. AUTHOR(s) Courtemanche, David J. and Thomas J. Hanratty, Project Supervisor		8. CONTRACT OR GRANT NUMBER(s)
9. PERFORMING ORGANIZATION NAME AND ADDRESS Department of Chemical Engineering University of Illinois, 1209 West California St. Urbana, IL 61801		10. PROGRAM ELEMENT, PROJECT, TASK AREA & WORK UNIT NUMBERS NR 657-728
11. CONTROLLING OFFICE NAME AND ADDRESS		12. REPORT DATE 1988, October
		13. NUMBER OF PAGES 95
14. MONITORING AGENCY NAME & ADDRESS(if different from Controlling Office) Office of Naval Research Arlington, Virginia 22217		15. SECURITY CLASS. (of this report)
		15a. DECLASSIFICATION/DOWNGRADING SCHEDULE

16. DISTRIBUTION STATEMENT (of this Report)

17. DISTRIBUTION STATEMENT (of the abstract entered in Block 20, if different from Report)

18. SUPPLEMENTARY NOTES

19. KEY WORDS (Continue on reverse side if necessary and identify by block number)

Pressure, turbulence, wavy surfaces

20. ABSTRACT (Continue on reverse side if necessary and identify by block number)

See Reverse

DD FORM 1473 1 JAN 73   EDITION OF 1 NOV 65 IS OBSOLETE
S/N 0102-014-6601 |

Surface pressure variations for turbulent flow over solid wavy surfaces with a wavelength of 2 inches were studied. Measurements were made over waves of two amplitudes, 0.0123 inches and 0.03125 inches. The water flow rate and viscosity were varied so that a range of dimensionless wave numbers (scaled with the friction velocity and the kinematic viscosity) of α^+ = 0.0011 to 0.020 were covered.

alpha(+)

Pressure profiles are described using a three harmonic fit. A linear response, for which only a single harmonic is needed, was observed for all α^+ for the small amplitude wave and for small α^+ for the large amplitude wave.

Of particular interest is the large phase shift of the pressure profile observed with increasing α^+. These results are used to test the quasi-laminar model for flow over wavy surfaces, widely used to predict wave generation and drag on small amplitude waves.

Keywords Surface Pressure Turbulence Wavy Surfaces. jndk

DTIC
COPY
INSPECTED

Accession For	
NTIS GRA&I	☑
DTIC TAB	☐
Unannounced	☐
Justification	

By_____
Distribution/
Availability Codes

Dist	Avail and/or Special
A-1	

REPORT DOCUMENTATION PAGE		READ INSTRUCTIONS BEFORE COMPLETING FORM
1. REPORT NUMBER	2. GOVT ACCESSION NO.	3. RECIPIENT'S CATALOG NUMBER
4. TITLE (and Subtitle)		5. TYPE OF REPORT & PERIOD COVERED
		6. PERFORMING ORG. REPORT NUMBER
7. AUTHOR(s)		8. CONTRACT OR GRANT NUMBER(s)
9. PERFORMING ORGANIZATION NAME AND ADDRESS		10. PROGRAM ELEMENT, PROJECT, TASK AREA & WORK UNIT NUMBERS
11. CONTROLLING OFFICE NAME AND ADDRESS		12. REPORT DATE
		13. NUMBER OF PAGES
14. MONITORING AGENCY NAME & ADDRESS(If different from Controlling Office)		15. SECURITY CLASS. (of this report)
		15a. DECLASSIFICATION/DOWNGRADING SCHEDULE

16. DISTRIBUTION STATEMENT (of this Report)

17. DISTRIBUTION STATEMENT (of the abstract entered in Block 20, if different from Report)

18. SUPPLEMENTARY NOTES

19. KEY WORDS (Continue on reverse side if necessary and identify by block number)

20. ABSTRACT (Continue on reverse side if necessary and identify by block number)

DD FORM 1473 EDITION OF 1 NOV 65 IS OBSOLETE
1 JAN 73
S/N 0102-014-6601 |

Pressure Variation Over a

Solid Wavy Surface

Prepared by

David James Courtemanche
Thomas J. Hanratty, Project Supervisor

for

The Office of Naval Research, Arlington, VA   2217
Contract N00014-82-K-0324
Project NR 657-728

Report 8

Department of Chemical Engineering
University of Illinois
Urbana, Illinois
61801

October, 1988

TABLE OF CONTENTS

v

LIST OF TABLES

LIST OF FIGURES

CHAPTER 1

INTRODUCTION

The study of flow over wavy surfaces has attracted attention since the work of Helmholtz in 1868. As the research in the area progressed the models became more sophisticated, allowing for larger amplitude waves, incorporating turbulent stresses and interactions between the turbulence and the wave.

In this study pressure profiles were measured over a wavy surface for turbulent flow in a rectangular water channel. Using a voltage response pressure transducer the differential pressure was measured at thirty-two locations along a two inch wavelength. All pressures were referenced to the upstream crest. The results of this study are compared to several other experimental and theoretical works.

The motivation for this research is threefold. First, it allows models of turbulence that have been studied over simpler geometries (flow over a flat plate, for instance) to be tested under different conditions. This gives further insight into the physics of turbulence. The second reason for this work is to gain an understanding of the surface forces over a wavy interface. This information can be used in studying wave generation. The third, is to gain knowledge of the effect of the presence of the wave on form drag. Previous studies have indicated that the wave can reduce skin friction. It is therefore necessary to know the increase in form drag to determine if the overall drag is actually reduced by the presence of the wavy surface.

CHAPTER 2

LITERATURE REVIEW

The first model for flow over small amplitude waves was proposed by Helmholtz (1868). This neglected viscous effects and solved the equations of motion linearized around a uniform mean velocity. The change in cross-sectional area of flow, due to the presence of the wave, induces a variation in the mean flow along the wave surface. Due to the Bernoulli effect this produces a pressure variation 180° out of phase with the wave surface.

Miles (1957) dealt with the generation of surface waves by a parallel shear flow. The only effect of turbulence in this model was the presence of a non-uniform velocity profile u=u(y) characteristic of a turbulent flow. A mechanism for the generation of waves was developed using the inviscid Orr-Sommerfeld equation. The maximum surface pressure was calculated to shift from the trough towards the downstream crest. Neither the Helmholtz nor the Miles model allowed for surface shear stresses because of the neglect of viscosity.

Benjamin (1959) and Miles (1959) concurrently reformulated the problem in curvilinear coordinates, so as to reduce the restrictions on the allowable amplitude of the perturbation. These models also include the dominant viscous term of the full Orr-Sommerfeld equation. The inclusion of the viscosity was found to have an effect on the phase relationship of the pressure distribution. These models do, however, neglect wave-induced variations of turbulent stresses and, therefore, are not complete.

Thorsness (1975) also worked in curvilinear coordinates, using several turbulence models to incorporate wave-induced turbulent stresses. Model A is basically the same as the quasilaminar approach used by Benjamin. Model C accounts for Reynolds stress due to the wave through a turbulent viscosity based on the van Driest mixing length model of Loyd, Moffat, and Kays (1970). Model D also used mixing length considerations. This model, however, takes into account the effect of the acceleration and deceleration of the flow on the turbulence by allowing the van Driest viscous layer thickness parameter to be a function of the wall pressure gradient. Model D was found to give better agreement with experiment than the other models.

All models discussed to this point are linear and limited to small amplitudes. These models do not allow for separation of flow. Abrams (1979) used a nonlinear boundary layer analysis to predict occurrence of separation and to extend the range of calculations to larger amplitude waves. He also introduced an effective pressure gradient into Model D to account for the fact that the flow cannot adjust to the pressure gradient instantaneously.

In further work Abrams (1984) observed that shear stress could vary with distance from the wave boundary due to the presence of pressure gradients. For this reason he introduced local shear stresses into Model D, which had previously recognized only wall shear stresses. This resulted in Model D*. In this work he dealt with small amplitude waves and therefore used linearized equations similar to Thorsness.

Frederick (1986) developed a nonlinear computer code for use with finite amplitude waves. Using spectral methods in the direction of flow and finite difference methods in the normal direction, the code solves the

nonlinear Reynolds-averaged Navier-Stokes equations. The code modifies the boundary layer program of McLean (1983) to the flow geometry of waves on the lower wall of a rectangular channel.

Experimental studies of pressure variation over solid, stationary, sinusoidal surfaces was first undertaken by Motzfeld (1937) in a wind tunnel using a wavelength of 30 cm and $2a_d/\lambda$ =.05, .10. The smaller amplitude wave gave a sinusoidal pressure variation that was 180° out of phase with the solid wave. The larger amplitude had a pressure response that was asymmetric, the peak shifted slightly downstream from the trough.

Zagustin, Hsu, Street, and Perry (1966) conducted experiments in an open water channel. Wall surface pressure measured over 2 and 3 foot wavelengths with $2a_d/\lambda$ =.04 and .02, respectively, showed linear response.

Kendall (1970) made windtunnel measurements over a 4 inch wavelength with $2a_d/\lambda$ =.0625. The wavy surface was formed by a smooth neoprene rubber sheet which was mechanically deformed by a series of cams into twelve sinusoidal waves. These waves could be made to move with or against the airflow at controlled speeds. He also obtained a sinusoidal pressure variation. Saeger and Reynolds (1971), who also worked with moving waves, obtained a sinusoidal pressure variation for $2a_d/\lambda$ =.0094.

Sigal (1971) made measurements in a wind tunnel over aluminum sheeting deformed into sinusoidal waves. Wavelengths of 12 and 6 inches with $2a_d/\lambda$ =.055 were used, with five waves in each wavetrain. The pressure distributions were sinusoidal.

Hsu and Kennedy (1971) made measurements of airflow in a wavy walled pipe. By forming fiberglas over wooden mandrels they constructed pipes

having average inner diameter of .0408 feet and $2a_d/\lambda$ =.022 and .011. Direct comparison of results is questionable here due to the differences in channel and pipe geometry.

Lin, Walsh, and Balasubramanian (1984) studied drag in a 15 inch low turbulence wind tunnel. Their studies included a variety of wave forms. Four of these were sinusoidal with λ=1 inch. Values of $2a_d/\lambda$ were 0.01, 0.02,0.03, and 0.04. A 0.5 inch wavelength with $2a_d/\lambda$ =0.023 and a 2 inch wavelength with $2a_d/\lambda$ =0.005 were also used. This study used a long wavetrain (35 waves) so as to ensure fully developed flow. The measurements did not show a sinusoidal pressure distribution for all waves.

In this lab pressure measurements over large amplitude waves were done by Zilker (1976), Buckles (1979), and Kuzan (1983). These waves definitely produced large separated flow and are therefore not comparable to the present study.

Cook (1970) studied flow over waves with $2a_d/\lambda$ =.05. There were 10 waves in the wavetrain. This wave amplitude is likely to produce separation at lower Reynolds numbers. Evidence for this exists in the nonlinearity of the pressure profiles. Studies reported by the other investigators with $2a_d/\lambda$ of this value or higher were all at larger Reynolds numbers and thus nonseparated.

Niederschulte (1988) conducted experiments under almost identical conditions to the present work. In the current study measurements were made over the twenty-second wave of a twenty-four wave train. Niederschulte's were made over wave eight of twelve. For $2a_d/\lambda$ =.03125 the range of dimensionless wave number, $\alpha^+= 2\pi v/\lambda u^*$, was the same for both studies.

Unfortunately the water tunnel employed in Niederschulte's work became unusable due to age and deterioration soon after measurements over a wave with $2a_d/\lambda = .0123$ had begun.

CHAPTER 3

THEORY

A. Governing Equations

In order to predict turbulent flow properties over a wavy surface of finite amplitude the nonlinear Reynolds-averaged Navier-Stokes equations are considered. In cartesian coordinates the two-dimensional, steady state momentum equations for incompressible flow are as follows:

$$u\frac{\partial u}{\partial x} + v\frac{\partial u}{\partial y} = -\frac{1}{\rho}\frac{\partial p_d}{\partial x} + \nu\left[\frac{\partial^2 u}{\partial x^2} + \frac{\partial^2 u}{\partial y^2}\right] + \frac{\partial}{\partial x}\overline{(-u'u')} + \frac{\partial}{\partial y}\overline{(-u'v')} \qquad (3.1)$$

$$u\frac{\partial v}{\partial x} + v\frac{\partial v}{\partial y} = -\frac{1}{\rho}\frac{\partial p_d}{\partial y} + \nu\left[\frac{\partial^2 v}{\partial x^2} + \frac{\partial^2 v}{\partial y^2}\right] + \frac{\partial}{\partial x}\overline{(-u'v')} + \frac{\partial}{\partial y}\overline{(-v'v')} \qquad (3.2)$$

Here ρ is the density, p_d, the dimensional surface pressure, ν, the kinematic viscosity, u, u' and v, v', the time-averaged and fluctuating velocities in the x and y directions, respectively. The turbulence model for the Reynolds stress terms, used to close the equations, will be discussed in section C.

The boundary conditions for the top wall and the wave surface are no slip and no penetration. These can be stated as follows:

$$u(x, a_d \cos \alpha x) = v(x, a_d \cos \alpha x) = 0 , \qquad (3.3)$$

$$u(x,y_t) = v(x,y_t) = 0, \qquad (3.4)$$

where y_t is the coordinate of the top wall of the channel. The wave surface is described by:

$$y = a_d \cos \alpha x, \qquad (3.5)$$

with a_d being the wave amplitude, $\alpha = 2\pi/\lambda$, the wave number, and λ, the wave length. In the horizontal direction the periodicity of the wave surface dictates the following boundary conditions:

$$u(0,y) = u(\lambda,, y),$$ (3.6)

$$v(0,y) = v(\lambda,, y).$$ (3.7)

B. Numerical Method of Frederick

Linearized theories introduce the wavy properties of the flow into the solution by proposing that flow variables consist of a wave-averaged component and a periodic perturbation term. By substituting these variables into the momentum equations and eliminating second order terms in the perturbation, the solution of problem is greatly simplified. This imposes restrictions on the amplitude of the wave that are most likely not strictly met in the present study.

Frederick (1986) dealt with this problem through the use of a nonlinear channel code. The code is used to solve the momentum equations (3.1) and (3.2) expressed in stream function-vorticity form. The stream function, ψ, and the vorticity, ω, are defined by

$$u = \frac{\partial \psi}{\partial y}$$ (3.8)

$$v = -\frac{\partial \psi}{\partial x}$$ (3.9)

$$\omega = \frac{\partial v}{\partial x} - \frac{\partial u}{\partial y}$$ (3.10)

In order to facilitate computations the physical domain $0 <= x <= \lambda$ and $a_d \cos \alpha x <= y <= y_t$ are mapped onto the rectangular region $0 <= \epsilon <= 2\pi$, $0 <= \eta <= \eta_t$. The mapping is achieved by the following orthogonal transformation:

$$\alpha x = \epsilon + \sum_{i=1}^{\infty} \frac{b_i}{i} \sin i\epsilon \left[\frac{\cosh i(\eta_t - \eta)}{\sinh i\eta_t} \right] \qquad (3.11)$$

$$\alpha y = \eta + b_0 - \sum_{i=1}^{\infty} \frac{b_i}{i} \cos i\epsilon \left[\frac{\sinh i(\eta_t - \eta)}{\sinh i\eta_t} \right] \qquad (3.12)$$

The coefficients b_i are chosen to approximate the wave surface at $\eta = 0$. For the waves dealt with in his work Frederick found eleven terms sufficient. An additional stretching scheme was used in the η coordinate to give better resolution near the upper and lower boundaries, where the velocity gradients are largest.

The vertical derivatives (those with respect to η) were evaluated by standard finite difference approximations. The horizontal periodicity of the flow field allows the stream function and vorticity to be easily represented by a Fourier series. Due to the simplicity of calculating Fourier derivatives the same resolution can be achieved with roughly half as many grid points as are needed with a finite difference scheme. For these reasons the horizontal derivatives were evaluated using spectral methods.

Once the stream function was calculated the cartesian velocity was recovered by the chain rule equation:

$$u(x,y) = \frac{\partial \psi}{\partial y} = \frac{\partial \psi}{\partial \eta} \frac{\partial \eta}{\partial y} + \frac{\partial \psi}{\partial \epsilon} \frac{\partial \epsilon}{\partial y} \qquad (3.13)$$

For more detail on the numerical method refer to Frederick (1986).

C. Model for Turbulent Stresses

The Reynolds stress terms in equations (3.1) and (3.2) can be modeled with an isotropic eddy viscosity:

$$\overline{-u'u'} = \frac{1}{\rho} R_{xx} = v_t \, 2 \, S_{xx} = v_t \, 2 \, \frac{\partial u}{\partial x} \tag{3.14}$$

$$\overline{-v'v'} = \frac{1}{\rho} R_{yy} = v_t \, 2 \, S_{yy} = v_t \, 2 \, \frac{\partial v}{\partial y} \tag{3.15}$$

$$\overline{-u'v'} = \frac{1}{\rho} R_{xy} = v_t \, 2 \, S_{xy} = v_t \left(\frac{\partial u}{\partial y} + \frac{\partial v}{\partial x} \right) \tag{3.16}$$

where R_{ii} is the time-averaged stress tensor, S_{ii} is the time-averaged rate of strain tensor, and v_t is the turbulent eddy viscosity.

Reynolds and Tiederman (1967) modeled the eddy viscosity as

$$\frac{v_t}{v} = \frac{1}{2} \left\{ 1 + \frac{4}{9} \kappa^2 \left(\frac{y' u^*}{\upsilon} \right)^2 \left(1 - \frac{y'}{2h} \right)^2 \left[3 - 4 \frac{y'}{h} + 2 \left(\frac{y'}{h} \right)^2 \right]^2 \right.$$

$$\left. \left[1 - \exp\left(\frac{-y' \tau^{.5}}{\rho^{.5} \upsilon A} \right) \right]^2 \right\}^{.5} - \frac{1}{2} \tag{3.17}$$

where h is the average half channel height, κ is the von Karman constant, y' is distance to either the wave surface or the top wall (whichever is closer), τ is the local shear stress, A is the van Driest parameter (a measure of the thickness of the viscous wall region).

The van Driest parameter is evaluated using Model D* developed by Thorsness (1975) and Abrams (1984). Model D* accounts for the fact that the viscous wall region thickens with increasing negative pressure gradient and thins with increasing positive pressure gradient. Loyd, Moffat, and Kays

(1970) suggest the following functional dependence of A on the dimensionless pressure gradient, $p^+ = (dp_d/dx)(\upsilon/\rho u*^3)$:

$$A = \overline{A} \, [\, 1 + p^+ K_1 + p^{+^2} K_2 + ...]$$

(3.18)

where A is the flat channel value of A and K_1 and K_2 are empirical constants. For the nonequilibrium condition present with flow over waves an effective pressure gradient, p^+_{eff}, should be used in (3.18). The effective pressure gradient is defined as follows, with K_L being an empirical lag constant:

$$\frac{\partial p^+_{eff}}{\partial x^+} = \frac{p^+ - p^+_{eff}}{K_L}$$

(3.19)

The results of this nonlinear analysis are compared with the experimental data of the present study.

CHAPTER 4

EXPERIMENTAL EQUIPMENT AND PROCEDURES

A. Flow System

All measurements in this study were made in the rectangular water channel designed and built by Niederschulte (1988). The system consists of an enclosed horizontal loop approximately 50 feet in length and 30 feet in height, through which water circulates in a counter-clockwise direction, as pictured in Figure (4.1). The loop has a capacity of ∼1400 gallons and is connected to two tanks, one of 1000 gallons and one of 1650 gallons, for storage of test fluids. The system was constructed using 316 or 304 stainless steel, plexiglas, PVC, rubber, or rubber-lined steel to avoid corrosion.

At the far left of Figure (4.1) is a 480 gallon reservoir tank which contains heating and cooling coils, providing temperature control for the channel. With careful adjustment of the heating/cooling water flow rate the temperature of the loop can be maintained to one-tenth degree centigrade. A small, one-half horsepower pump can be used to circulate the contents fo this tank through a bank of $5\mu m$ water filters.

The tank empties to the inlets of the channel's two pumps, which are plumbed in parallel and are run only one at a time. The smaller pump is a five horsepower Worthington 6CNG84 centrifugal, 316 stainless steel model with a six-inch intake and six-inch horizontal discharge. The larger pump is located in a lower level of the building to isolate its vibrations. This pump is a 316

13
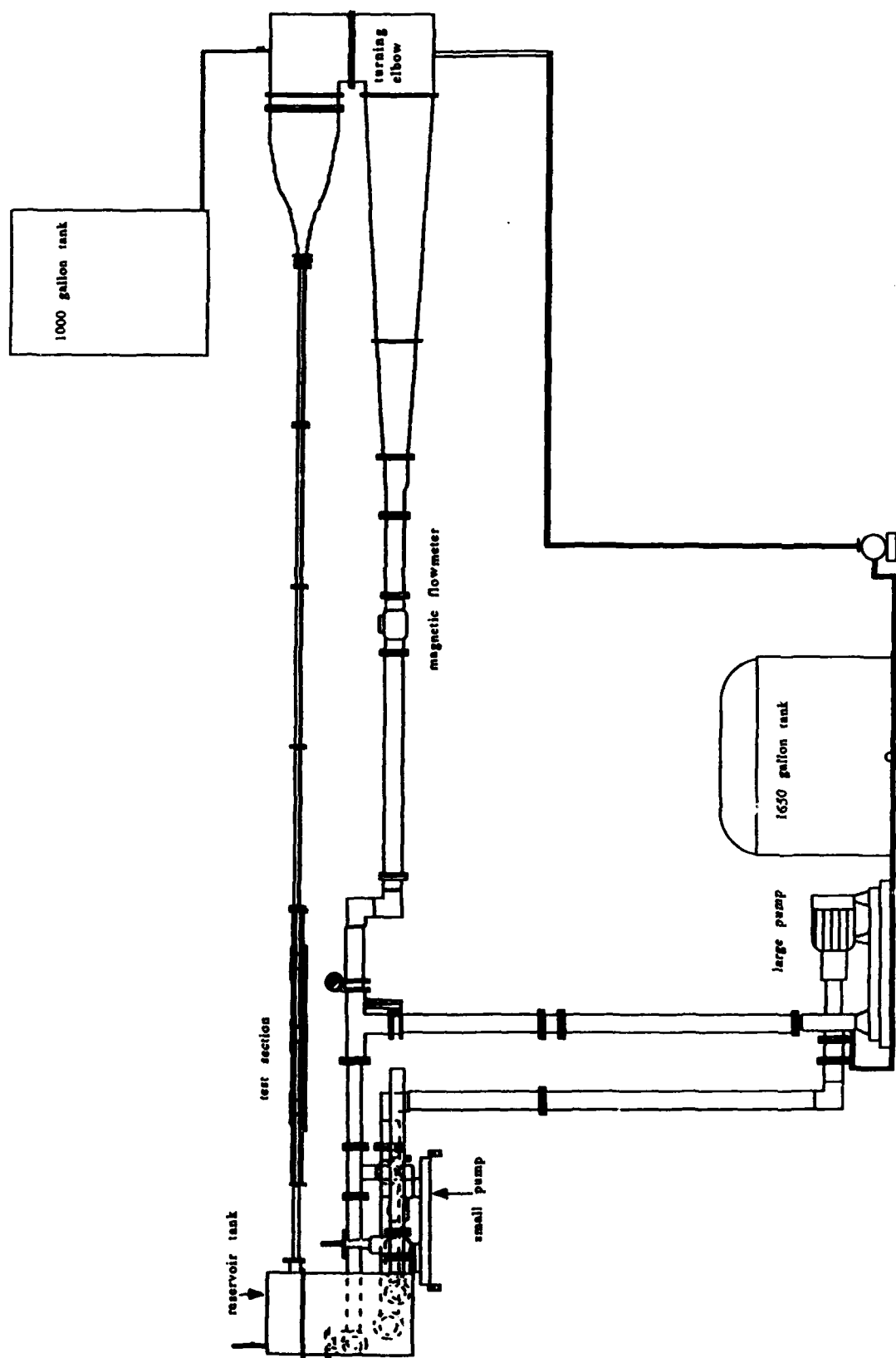
Figure 4.1 Side View of Flow System

1000 gallon tank

turning elbow

magnetic flowmeter

test section

reservoir tank

small pump

large pump

1650 gallon tank

stainless steel Worthington model 1050-D with eight-inch horizontal intake and six-inch vertical discharge. It has a 60 horsepower motor.

The parallel pump design allows for a wide range of flowrates. The small pump is capable of operating the channel through the range of 40 g.p.m. to 800 g.p.m. or Reynolds numbers (based on bulk velocity, half-channel height, and water) of 2400 to 45,000. The large pump can deliver 2750 g.p.m. which produces a Reynolds number of 160,000. Both pumps discharge to tees in the channel/bypass line. The bypass line leads directly back to the reservoir tank and contains a diaphragm valve to control its flow rate. The channel line contains a butterfly valve to control flow rate to the channel. Manipulation of the two valves allows the system to be run anywhere from total recirculation (between the reservoir tank and the pump) to maximum channel flow.

The channel line, made of eight-inch PVC piping, contains a magnetic flowtube. The Foxboro M/2800 series flow tube measures flow using the principles of magnetic inductance. The advantages of this form of measurement are its accuracy (one-half percent of full scale range) and low head loss. Another major advantage is the fact that this flow measurement is independent of temperature, density, and viscosity of the fluid used. The flowtube outputs its reading to both an analog meter and the data acquisition system of the computer.

The flow is expanded from 8 inch diameter to 22 x 30 inches and enters the turning elbows of the system. The elbows are designed to decrease frictional losses and undesirable disturbances resulting from abrupt turning of the fluid. A honeycomb is used to straighten the flow and reduce the

intensity of the turbulence. After the honeycomb is a nozzle system that changes the cross section of the loop from 22 x 30 inches to 2 x 24 inches.

The channel consists of four 70 inch 304 stainless steel segments, each with internal cross section of 2 x 24 inches, leading to the test section. The test section, made of stainless steel and plexiglas, has the same inner dimensions as the channel segments. Deviations from stated cross sectional dimensions were limited to 0.010 inches for the first three channel segments, 0.002 inches for the final segment, and 0.0002 inches for the test section. (Test section tolerance excludes plexiglas components.) The bottom wall of the test section consists of three plexiglas plates. In this study sinusoidal waves and pressure taps were machined onto the plates. The plates will be discussed in greater detail in section B.

The test section empties into the reservoir tank, completing the enclosed flow circuit. The design criteria, dimensions, and construction of the flow system are described in detail in the PhD thesis of Niederschulte (1988).

B. Pressure Apparatus

The equipment used to measure of pressure variation over a wave consists of four major components: plexiglas plates with a sinusoidal surface and pressure taps, a pressure transducer and demodulator, a header device to connect the taps to the transducer, and a device to calibrate the output of the transducer.

The plexiglas plates were built by Bill Knight of the University of Illinois Chemical Sciences Machine Shop. The plexiglas slabs were first machined flat and square. Shoulders for mounting the plates were created by

removing material from the perimeter of the slab to leave a 1 inch wide border of 1/2 inch thickness. (The thickness of the shoulder was increased for strength by applying 3 inch wide by 1 inch thick plexiglas pieces to the underside of the finished plate.) Clearance holes for 1/4 inch bolts were drilled 1/2 inch from the outer edge of the shoulder. These holes were spaced 2 inches apart. Between the clearance holes and the body of the slab an O-ring groove was milled to facilitate sealing.

The sinusoidal surfaces were formed with specially milled cutting tools. Each cutting tool was formed such that its cutting edge was a complete sine wave with an additional 1/16 wave period on each end. The plates were set up on a horizontal milling machine and the waves were cut one at a time in the spanwise direction. The additional length of the cutting tool over one period allowed the machinist to overlap the waves, reducing machining lines. The 0.03125 amplitude waves were machined onto all three plates of the test section in anticipation of use in other research projects. The 0.0123 waves were machined only onto the first two plates, using an existing flat plate downstream. The downstream plate should not affect the pressure measurements, which are done over the second plate.

The plates were polished one wave at a time, spanwise across the entire length of the wave. Great care was taken to remove as little material as possible and to distribute polishing equally to crests and troughs. Polishing was accomplished using progressively finer agents: 500A, 600A wet-dri sandpaper; 2/0, 3/0, 4/0 emery paper; and finally suspensions of aluminum oxide in deionized water (with 15μ, 9.5μ, and 5μ particles). The final finish was glasslike in appearance.

The pressure taps run from the crest of the twenty-second wave to the crest of the twenty-third wave in either a twenty-four wave train (amplitude = 0.0123 inches) or a thirty-six wave train (amplitude = 0.03125 inches). The taps are 0.040 inch diameter holes drilled through the wave surface. On the back surface of the plate the taps are enlarged to 0.127 inches. This enlargement allows the insertion of 1/8 inch stainless steel tubing necessary for connection of the taps to the pressure transducer. The taps meet the criteria outlined by Shaw (1960) for minimizing measurement error.

The layout of the pressure taps is shown in Figure (4.2). There are thirty-three taps, allowing thirty-two differential pressure measurements. All measurements were referenced to the upstream crest. The taps are spaced 1/16 inch apart in the streamwise direction and 1/8 inch apart in the spanwise direction. The arrangement of the taps (four sets of eight, each set at an angle of 45° to the streamwise direction) allows measurements to be made with a streamwise resolution of 0.0625 inches, yet maintains a full inch distance between taps along the same spanwise location. The pressure tap layout in centered on the channel's centerline.

A well one inch deep by two inches wide by three inches long was machined into the back of the waveplate, centered around the taps. Stainless steel tubing, ranging in length approximately from two inches to ten inches, was inserted into each tap and arranged for convenient connection to the header device. The well was filled with epoxy, sealing the tubing with the plate and anchoring the tubing arrangement. A short length of tygon tubing was sealed onto each piece of stainless steel tubing with General Electric RTV
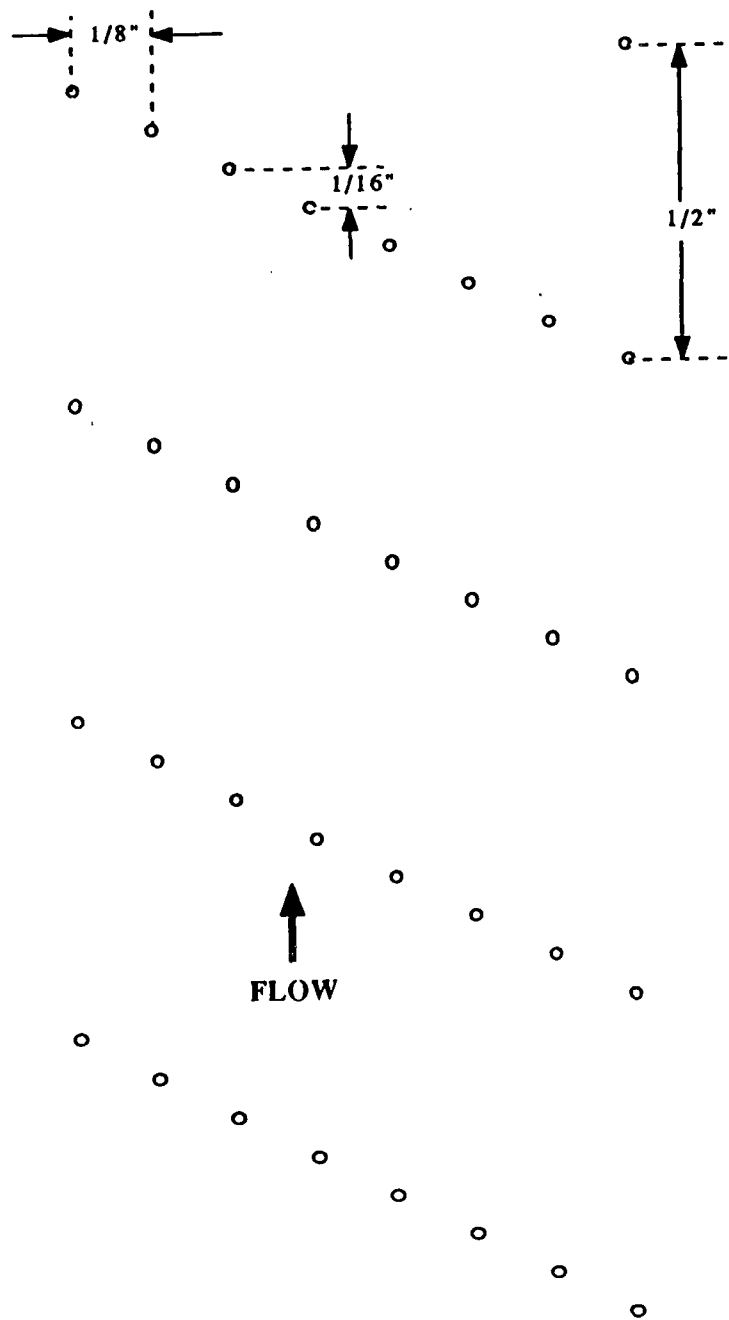
Figure 4.2 Pressure Tap Layout

silicone sealant. The tygon tubing is used to connect the steel tubing to the pressure header.

The pressure header is shown in Figure (4.3). This was built by Niederschulte and modified for the present study. It was built with 1/8 inch stainless steel tubing and Swagelock fittings mounted on a plexiglas frame. The header consists of ten lines with a valve in each line. One line leads directly to the low pressure inlet of the transducer. This line is connected to the tap at the upstream crest as reference for all measurements. The other nine lines are connected in parallel to the high pressure inlet of the transducer. Eight of these lines are used to connect one row of taps to the transducer. The ninth line can be used as a bleed line to remove air bubbles.

Differential pressure was measured with a model CJVR pressure transducer and a model CJCD-4111 carrier demodulator, both manufactured by C.J. Enterprises. The CJVR has a full scale output of ±5 volts and depending on the pressure diaphragm used, a pressure range of ±0.5 or±2.5 inches of water.

The pressure transducer's output was quite sensitive to vibration and position. For this reason the transducer was anchored to the header device with a hose clamp. The header was firmly bolted to the optical traverse used by Niederschulte (1988) in his laser doppler experiments. The traverse is a large, heavy structure designed to prevent vibrational effects from reaching that which is mounted on it.

A calibration device was constructed (also by Niederschulte) in order to obtain the imposed-pressure/voltage-output relationship for the pressure transducer at the conditions of a given run. The calibrator included two 1/8 inch glass tubes. One of these was connected via the header to the reference
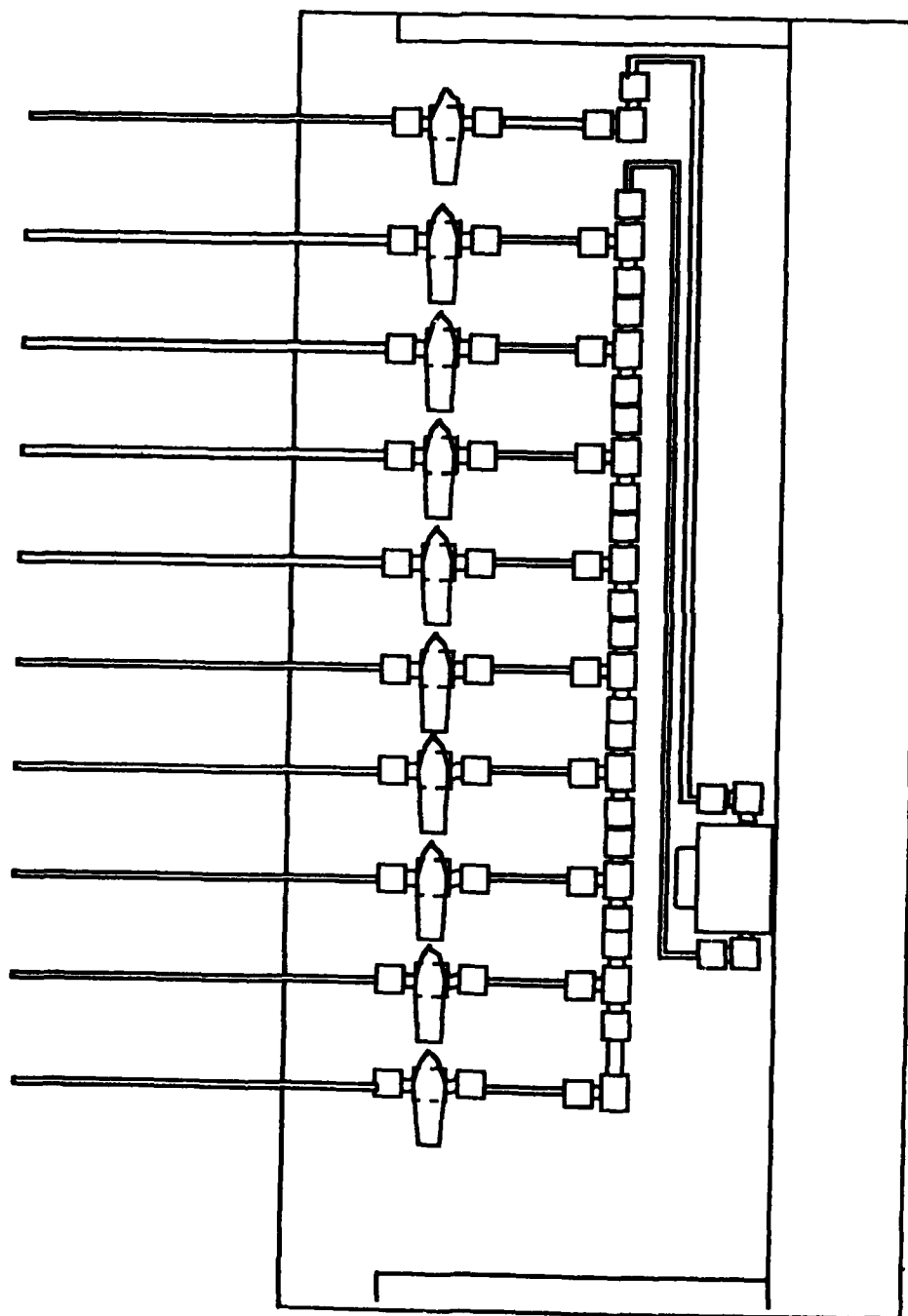
Figure 4.3 Pressure Valve Header

side of the transducer, the other was connected (also via the header) to the measurement side of the transducer. The lines were filled with deionized water and air bubbles were bled out through bleed screws in the pressure transducer. By adding water to one tube or the other their relative height of water, and thus the differential pressure, could be set at a desired level. A steel scale graduated in 1/64 inch increments was mounted next to each tube. The calibrator was leveled with a bulls-eye level mounted in its base. The body of the calibrator was precision machined stainless steel such that the two scales were vertical and at the same relative height if the bubble in the bulls-eye level was centered. Therefore the imposed head could be accurately measured. The calibration device is shown in Figure (4.4). By varying the head and sampling the voltage output a linear calibration relationship was found for the transducer.

C. Experimental Procedures

Measurements were made using either water or a solution of dextrose in water as the operating fluid. The use of fluids of different viscosities allowed measurements to be made over a wide range of dimensionless wave numbers, $\alpha^+ = 2\pi\upsilon/\lambda u^*$. The flow loop was initially filled with the desired fluid. Before any runs were made with that fluid the flow loop was run at various speeds for several days in an effort to remove as much entrained air as possible.

Once the flow rate had been selected for a given run the loop was configured to be run with the appropriate pump. Monitoring the flowrate with the magnetic flowmeter, the bypass and butterfly valves were adjusted until the desired flow was achieved. The heating or cooling water was run to
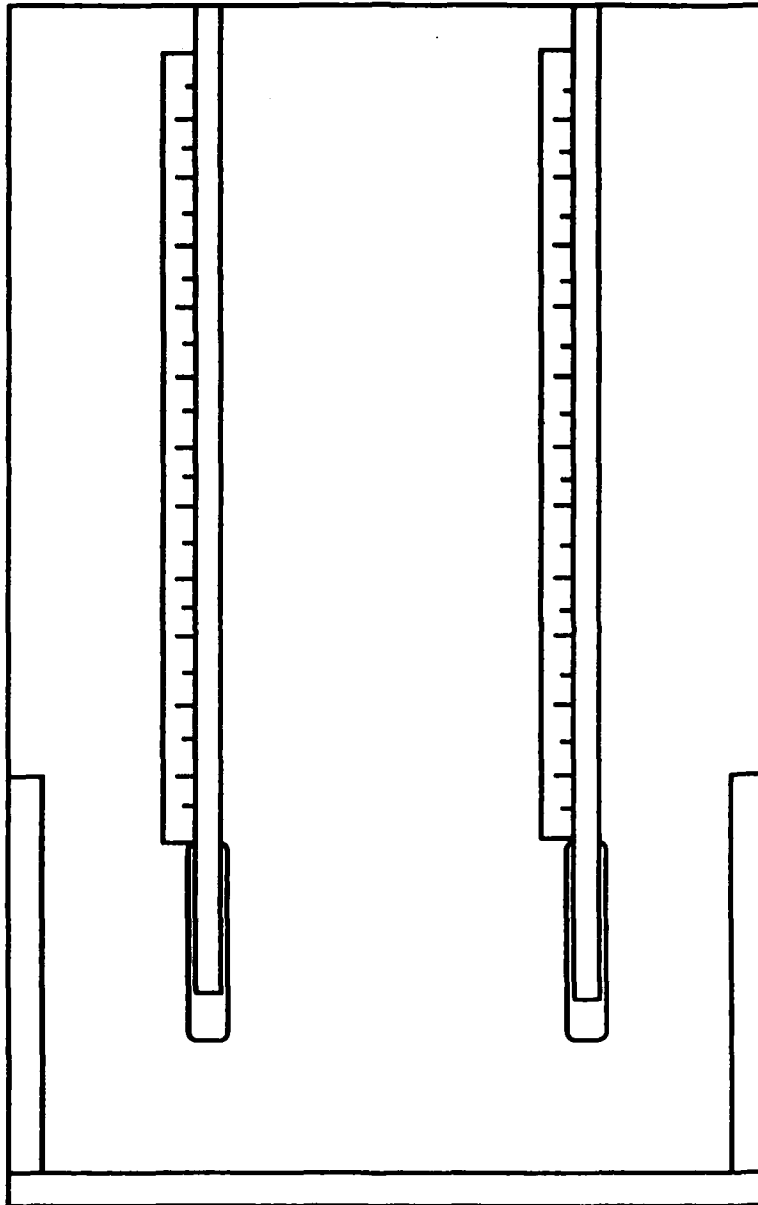
Figure 4.4 Calibration Device

bring the fluid temperature to 25° C and then adjusted and monitored until the fluid held that temperature.

Once the flow system was set the pressure taps for the downstream crest and the trough were connected to the header and any air in the lines was bled. These two taps are where the extremes in the pressure profile occur. The span adjust and zero adjust of the carrier demodulator were adjusted to place the pressure range occurring over the wave at approximately 80% of full scale.

The calibration device was connected to the header and any air bled out. If the operating fluid was dextrose, all dextrose was bled out also. Fifteen different heads were imposed and the voltage was sampled.

The first set of eight pressure taps and the reference tap were connected to the header, and bled to remove air (and water introduced by the calibration, if the operating fluid was dextrose). The pressure at each tap location was measured by opening the valve on its connecting line and sampling the pressure transducer's voltage output. A twelve bit analog to digital converter manufactured by Metra-Byte Corporation was used to collect the data on an IBM AT Personal Computer. Spectral analysis of several data sets indicated that random noise overpowered signal at approximately 50 Hz. Stable averages were obtained with sample times of 100 seconds. The voltages were sampled at 100 Hz for 150 seconds. The voltages were also monitored with a digital voltage meter. In this manner erroneous voltages due to air bubbles in the lines could be detected, the line bled, and the point retaken. After all eight taps were sampled the next set was connected and the process repeated. After all four sets were finished a second calibration was conducted.

The relationship between imposed differential pressure and voltage output was linear. The correlation coefficient was always above 0.980. The deviation from a correlation of 1.00 was due to scatter in the points as opposed to any curvature in the relationship of imposed differential pressure versus voltage output. The two calibrations agreed within two percent of one another with regard to the slope of the plot. The intercept of the line often changed from one calibration to the other. It was observed that the excessive bleeding necessary for the connection of the calibration device sometimes caused a shift in the output voltage. These shifts were not noticed with the changing of the pressure taps within a run as they require considerably less bleeding of the lines. As a result the intercept chosen for analyzing the data was the one that would position the pressure profile so that the differential pressures seemed most reasonable. It is important to note that the intercept only affects the zeroth order harmonic, or DC component. This component has no effect on the quantities calculated in this study, such as phase angles and amplitudes of the profile, or drag coefficients. A sample calibration is shown in Appendix C.

Data was stored in binary form on the hard disc of the IBM. A Fortran program (Press.For, see Appendix B) on the IBM was used to unpack the data to standard ASCII form as voltages. The program then converted the voltages to pressure with the linear relation obtained from calibration. The pressures were non-dimensionalized by dividing through by $\rho u*^2$, where $u*$ is the friction velocity (equal to the square root of the wall shear stress divided by density). The mean pressure gradient (that which would be present in a flat channel) was removed by assuming a linear pressure drop across the two inch

wavelength. The magnitude of the drop was assumed to be described by the relation

$$\frac{d\left(\dfrac{p_d}{\rho u^{*2}}\right)}{d\left(\dfrac{x u^{*}}{\nu}\right)} = \frac{\nu}{h u^{*}} \qquad (4.1)$$

from the correlations of Dean(1978). Plotting files of non-dimensionalized pressure versus location on the wave were the output of this program. The plotting files were networked to a Digital Equipment Company microVax. On the Vax another Fortran program (Fit3u.for, see Appendix B) fit the pressure profiles to three harmonics through Fourier analysis. The harmonic files and the data files were accessed by an Apple Macintosh computer for plotting.

CHAPTER 5

RESULTS

Differential pressure profiles were measured for eight different Reynolds numbers over the 0.03125 inch amplitude wave and for ten Reynolds numbers over the 0.0123 inch amplitude wave. Figures (5.1-5.8) show the profiles measured over the 0.03125 inch wave and figures (5.9-5.18) show the profiles measured over the 0.0123 inch wave. These figures show differential pressure $(p - p_{crest})$ nondimensionalized with fluid density, ρ, and the square of the friction velocity, u^*, plotted versus streamwise location along the wave, nondimensionalized with the wavelength, λ. The friction velocity is defined as

$$u^* = u_b \ (C_f/2)^{0.5} \tag{5.1}$$

where u_b is the bulk velocity and C_f is the friction factor. The friction factor is obtained through the correlation of Dean(1978) for flow through a rectangular channel (this correlation is based on smooth walls)

$$C_f = 0.0614 \ Re^{-0.25} \tag{5.2}$$

where Re is the Reynolds number based on half channel height. The experimental data and run conditions are tabulated in Appendix A.

The pressure profiles were found to depend on the dimensionless wave number, $\alpha^+ = 2\pi v/\lambda u^*$, and the dimensionless amplitude of the wave surface, $a^+ = a_d u^*/v$. The pressure response can be characterized as

$$p(x/\lambda) = \sum a_i \ \cos(2\pi x/\lambda + \theta_i) \tag{5.3}$$

where θ_i is the phase angle between the pressure response and the wave surface. A positive phase angle indicates the pressure maximum is shifted

upstream from the wave crest. The profiles taken at the three smallest α^+ for the 0.03125 inch wave have a linear response and are adequately described by one term in equation (5.1). The rest are adequately described by three terms. Over the 0.0123 inch wave all the profiles except that for the highest α^+ are adequately described by one term. In order to compare the a_i of runs using working fluids of different kinematic viscosity it is necessary to look at the ratio a_i/a^+. (The relationship of a_1 and θ_1 to α^+ and a^+ will be covered in Chapter 6.)

Figures (5.1-5.4) show the profiles taken over the 0.03125 inch wave using water as the working fluid. Figure (5.1) was taken at a Reynolds number of 41,600 and α^+ of 0.0016. The ratio a_1/a^+ is 0.55 and the phase θ_1 is 167°. This profile is described quite well by a linear response, the amplitude of the second harmonic being three percent of the first. This value is due more to experimental scatter the any distortion of the profile. The curve created using three harmonics falls directly over that using a single harmonic term.

Figure (5.2) is the profile taken at a Reynolds number of 30,400 and α^+ of 0.0021. The ratio a_1/a^+ is 0.625 and θ_1 is 171°. This profile is also linear with a_2/a_1 equal to 0.03. The three harmonic curve falls almost exactly over the one harmonic curve.

Figure (5.3) was obtained at a Reynolds number of 21,600 and α^+ of 0.0029. The ratio a_1/a^+ is 0.77 and θ_1 is 168°. The second harmonic amplitude is six percent of the first. In this case the three harmonic curve diverges from the single harmonic curve, particularly near the crests of the wave surface. This is considered a borderline linear/nonlinear profile. Note that, in this profile (as well as the other profiles to come), although the additional

harmonic terms may take on significant amplitudes their relative phases are such that they affect the shape of the profile without causing significant change to the magnitude of the profile. In other words, even though the curve created using three harmonic terms differs from the single harmonic curve, the first amplitude term a_1, adequately describes the magnitude of the pressure response.

Figure (5.4) is the profile taken at a Reynolds number of 14,900 and α^+ of 0.0040. The amplitude ratio a_1/a^+ is 0.82 and θ_1 is 169°. This profile is nonlinear with a_2/a_1 equal to 0.11. Although nonlinearity has set in the phase is still similar to that of the linear profiles.

Figures (5.5-5.8) show the profiles taken over the 0.03125 inch wave using dextrose solution as the working fluid. Figure (5.5) is the profile taken at a Reynolds number 4690 and α^+ of 0.0108. The amplitude ratio a_1/a^+ is 1.40 and θ_1 is 150°. The profile is quite nonlinear with a_2/a_1 equal to 0.14. The phase shift is now significantly lower than that observed for the smaller α^+ runs.

Figure (5.6) shows the profile measured at a Reynolds number of 3250 and α^+ equal to 0.0150. The ratio a_1/a^+ is 1.49 and θ_1 is 149°. The second harmonic amplitude is eighteen percent of the first harmonic's. The figure (5.7) is the profile taken at a Reynolds number of 3220 and α^+ equal to 0.0151. This run was made to establish the level of reproducibility of the experiments. The ratio a_1/a^+ is 1.57 and θ_1 is 144°. The second harmonic's amplitude is fourteen percent of the first's. The ratio a_1/a^+ agrees to 5.1% and the phase angle agrees to 5°. Both profiles are nonlinear and have similar shapes.

Figure (5.8) shows the profile taken at a Reynolds number of 2360 and α^+ equal to 0.0198. The ratio a_1/a^+ is 1.56 and θ_1 is 146°. The ratio a_2/a_1 is 0.20 and the profile is highly nonlinear.

Figures (5.9-5.12) show the profiles obtained over the 0.0123 inch wave using water as the working fluid. Figure (5.9) is the profile from the run taken at a Reynolds number of 66,400 and α^+ equal to 0.0011. The ratio a_1/a^+ is 0.432 and θ_1 is 173°. The ratio a_2/a_1 is 0.06. This is probably inflated due to experimental scatter as the three harmonic profile follows the one harmonic profile very closely.

Figure (5.10) was measured at a Reynolds number of 43,900 and α^+ equal to 0.00154. The amplitude ratio a_1/a^+ is 0.502 and θ_1 is 172°. The amplitude of the second harmonic is four percent of the first and the profile is very linear.

Figure (5.11) is the profile measured at a Reynolds number of 32,100 and α^+ equal to 0.0020. The ratio a_1/a^+ is 0.568 and θ_1 is 172°. The amplitude of the second harmonic is again four percent of the first and the profile is linear.

Figure (5.12) shows the pressure profile taken at a Reynolds number of 21,400 and α^+ equal to 0.0029. The value of a_1/a^+ is 0.670 and θ_1 is 172°. The ratio a_2/a_1 is 0.08, but this is due mostly to experimental scatter as the profile is linear.

Figures (5.13-5.18) show the profiles taken over the 0.0123 inch wave using dextrose solution as the working fluid. Figure (5.13) shows the pressure profile obtained at a Reynolds number of 15,000 and α^+ equal to 0.0039. The ratio a_1/a^+ is 0.993 and θ_1 is 163°. The second harmonic amplitude is six

percent that of the first and the profile is linear. The profile phase has begun to shift from the low α^+ values.

Figure (5.14) was taken at a Reynolds number of 9450 and α^+ equal to 0.0059. The ratio a_1/a^+ is 1.033 and θ_1 is 162°. The value of a_2/a_1 is 0.05 and the pressure response is linear.

Figure (5.15) the profile measured at a Reynolds number of 6730 and α^+ equal to 0.0079. The ratio a_1/a^+ is 1.172 and θ_1 is 157°. The ratio of a_2/a_1 is 0.09 and the profile is a borderline linear/nonlinear pressure response.

Figure (5.16) shows the measured profile at Reynolds number 5200 and α^+ equal to 0.0099. The ratio a_1/a^+ is 1.203 and θ_1 is 162°. This is another borderline profile with the amplitude of the second harmonic being eight percent of the first. Figure (5.17) is the profile taken at a Reynolds number of 5120 and α^+ equal to 0.0101. The ratio a_1/a^+ is 1.159 and θ_1 is 156°. The second harmonic has an amplitude that is six percent that of the first and the profile is also borderline. The amplitudes, a_1, agree to three percent. The variation is θ_1 is perhaps due to one or two erroneously low points over the 0.4 to 0.5 x/λ range in figure (5.16).

Figure (5.18) shows the pressure profile measured at a Reynolds number of 3300 and α^+ equal to 0.0148. The ratio a_1/a^+ is 1.420 and θ_1 is 164°. This is a larger than expected phase angle. One explanation is that with a_2/a_1 equal to 0.12 this is the first truly nonlinear profile measured over the 0.123 inch wave. The three harmonic curve (which follows the data well), has its maxima located to the right of the one harmonic maxima. This indicates the true phase angle is lower than θ_1.

It should be noted that some of the profiles contain an erroneous zeroth order harmonic, shifting the profile up or down by a constant amount. This is due to the calibration difficulties discussed in the chapter on Experimental Equipment and Procedures. This shift does not affect the amplitudes or phases of the profile nor does it affect the form drag coefficients calculated in the next chapter.
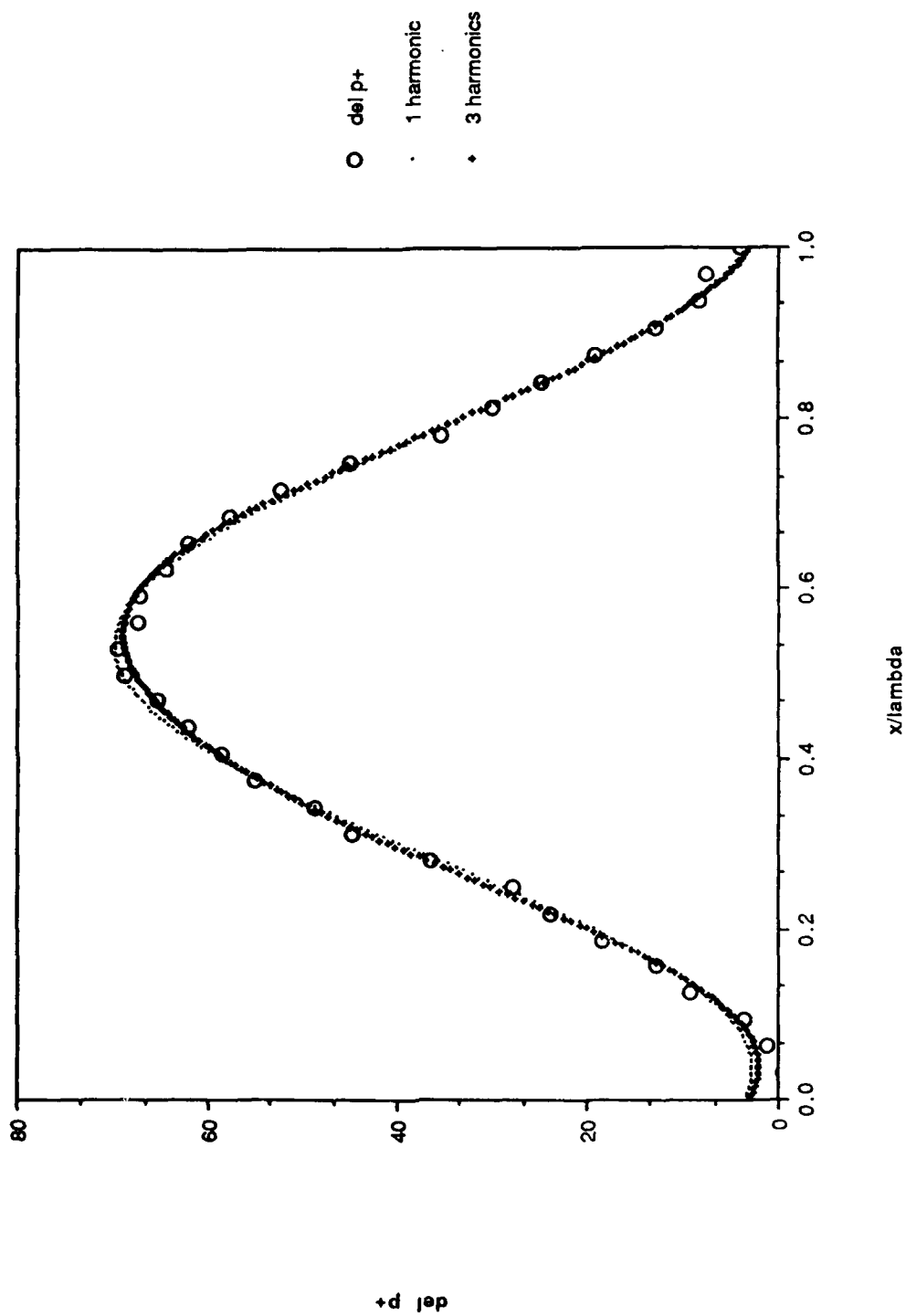
Figure 5.1 Pressure Profile $2a_d/\lambda = 0.03125$, $\alpha^+ = 0.0016$
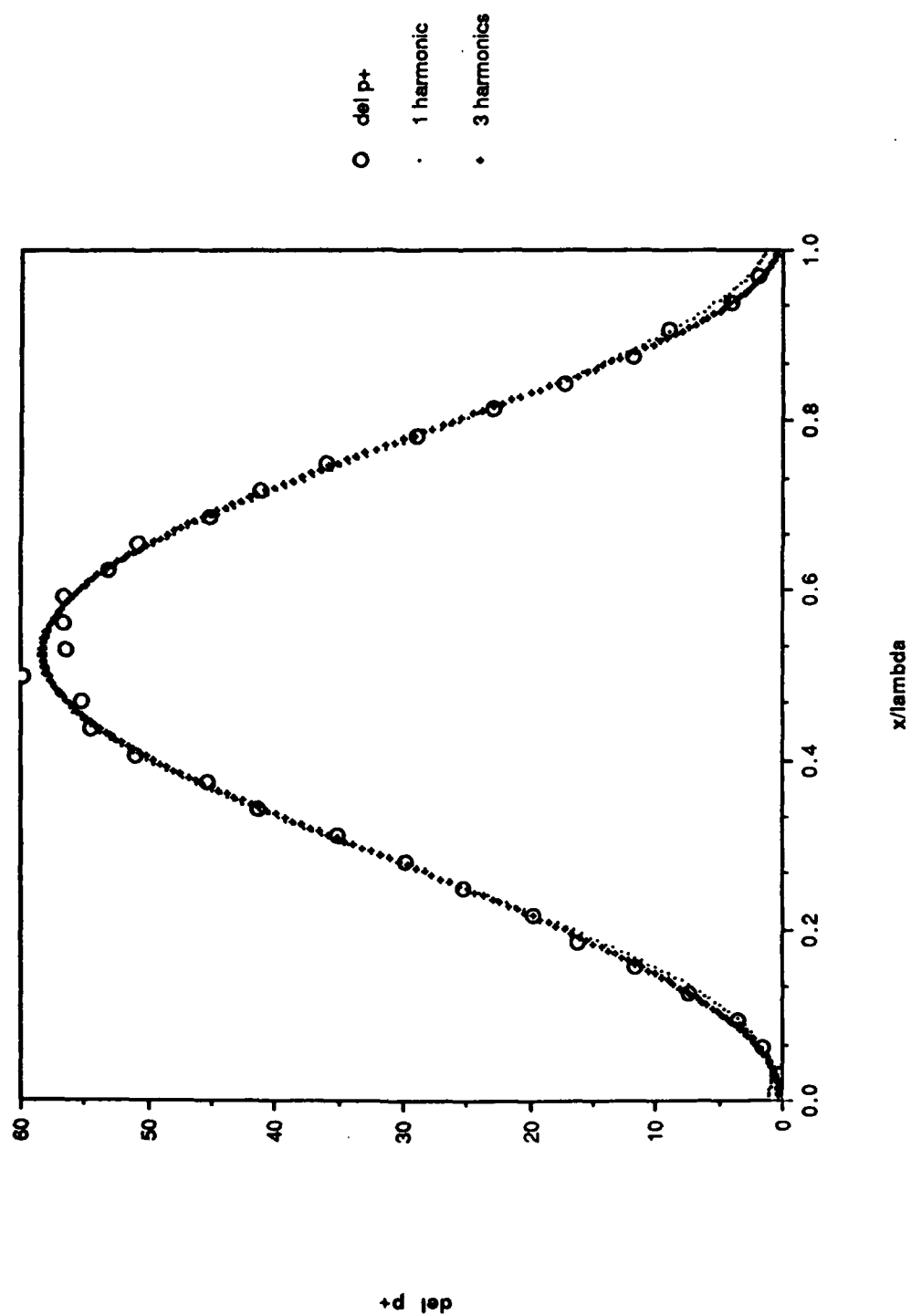
Figure 5.2 Pressure Profile $2a_d/\lambda = 0.03125$, $\alpha^+ = 0.0021$
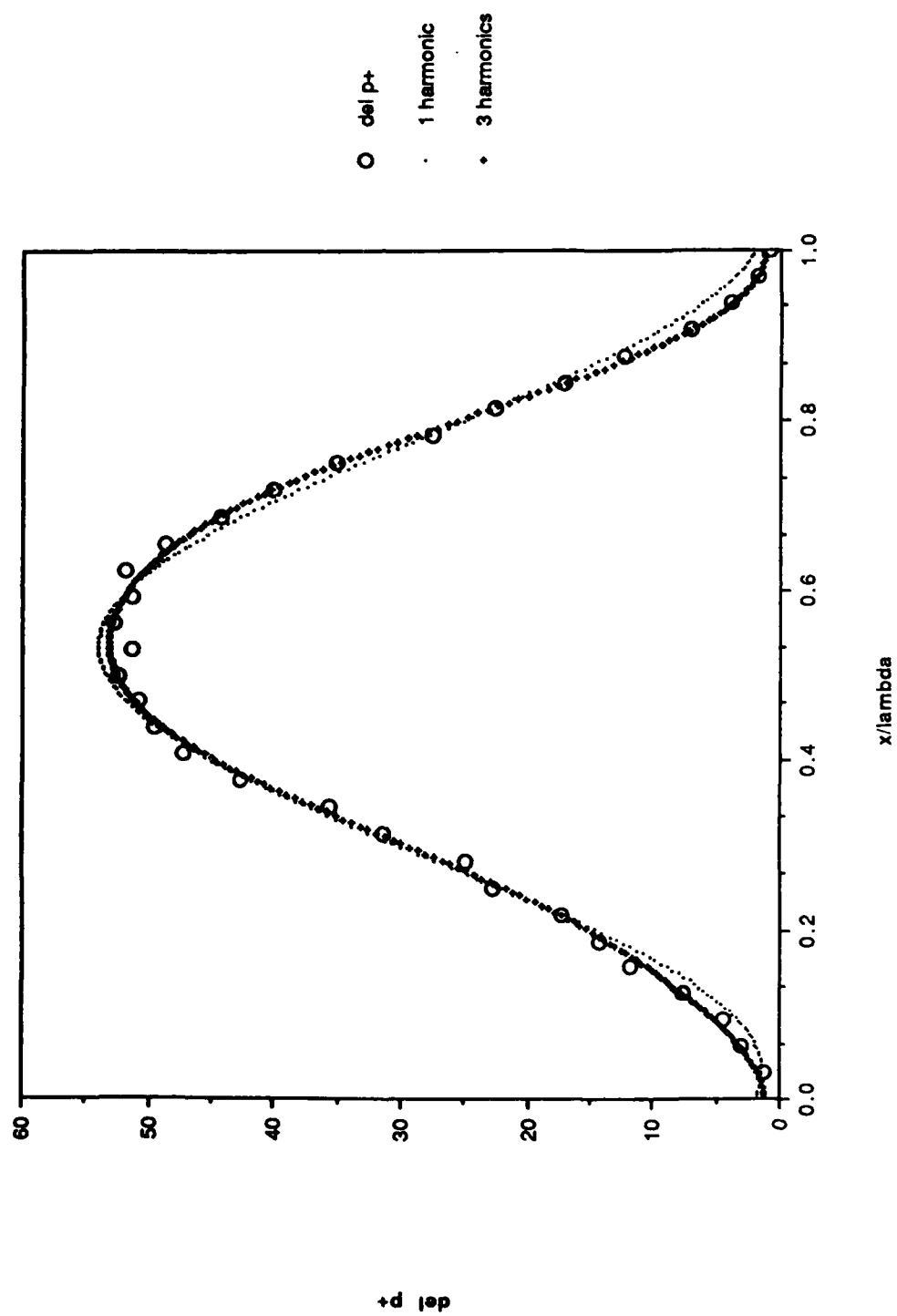
Figure 5.3 Pressure Profile $2a_d/\lambda = 0.03125$, $\alpha^+ = 0.0029$
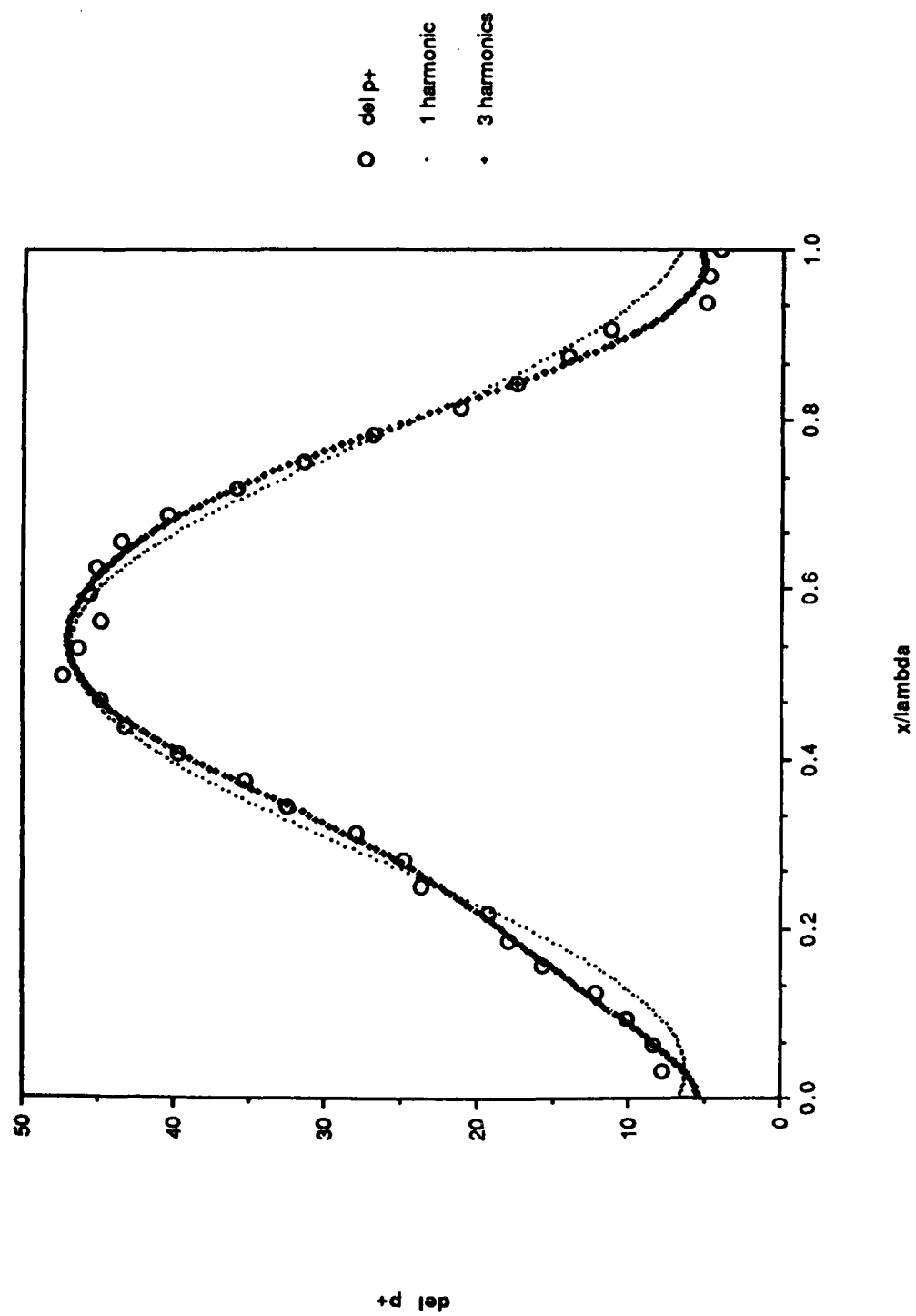
Figure 5.4 Pressure Profile $2a_d/\lambda = 0.03125$, $\alpha^+ = 0.0040$
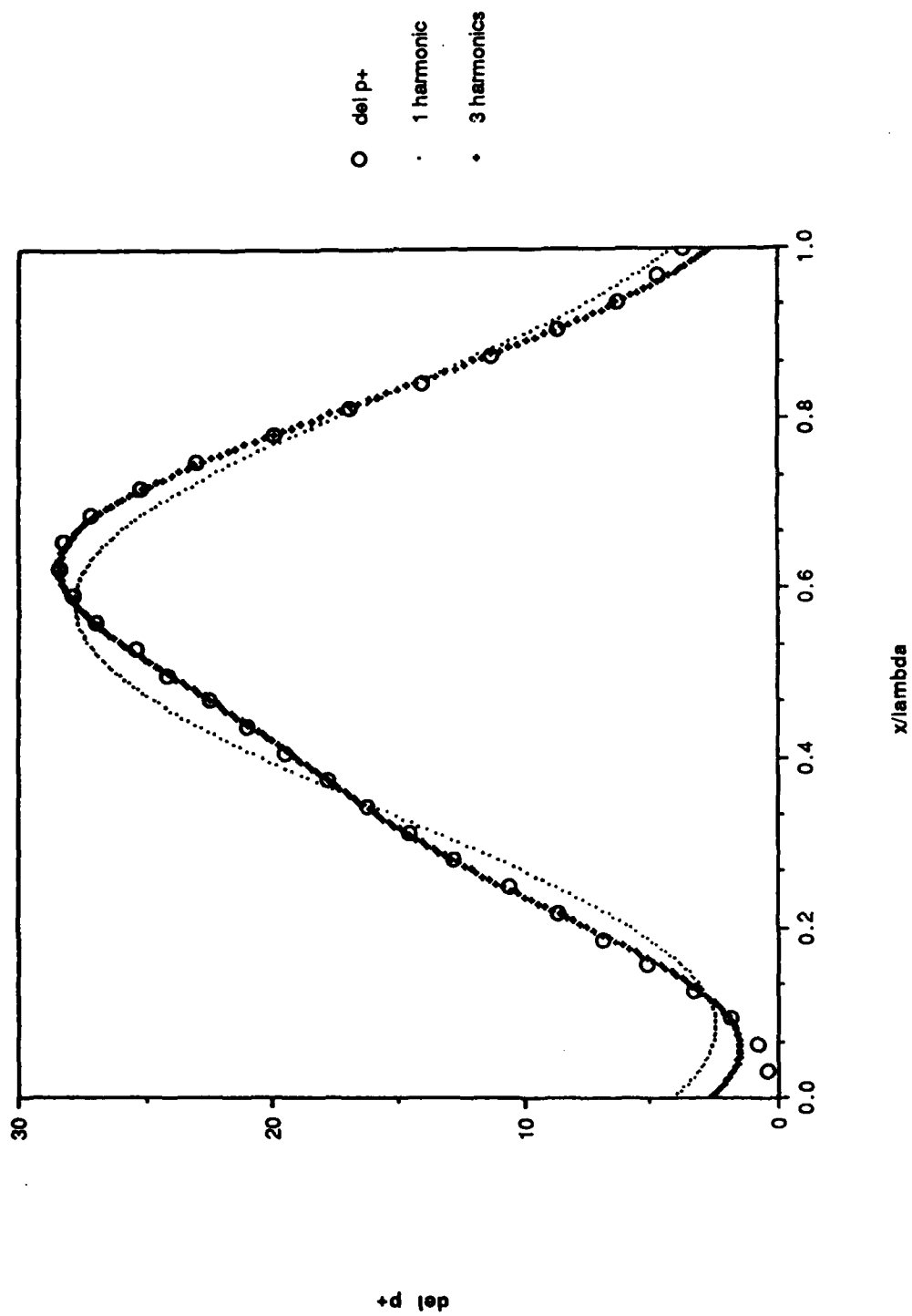
Figure 5.5 Pressure Profile $2a_d/\lambda = 0.03125$, $\alpha^+ = 0.011$
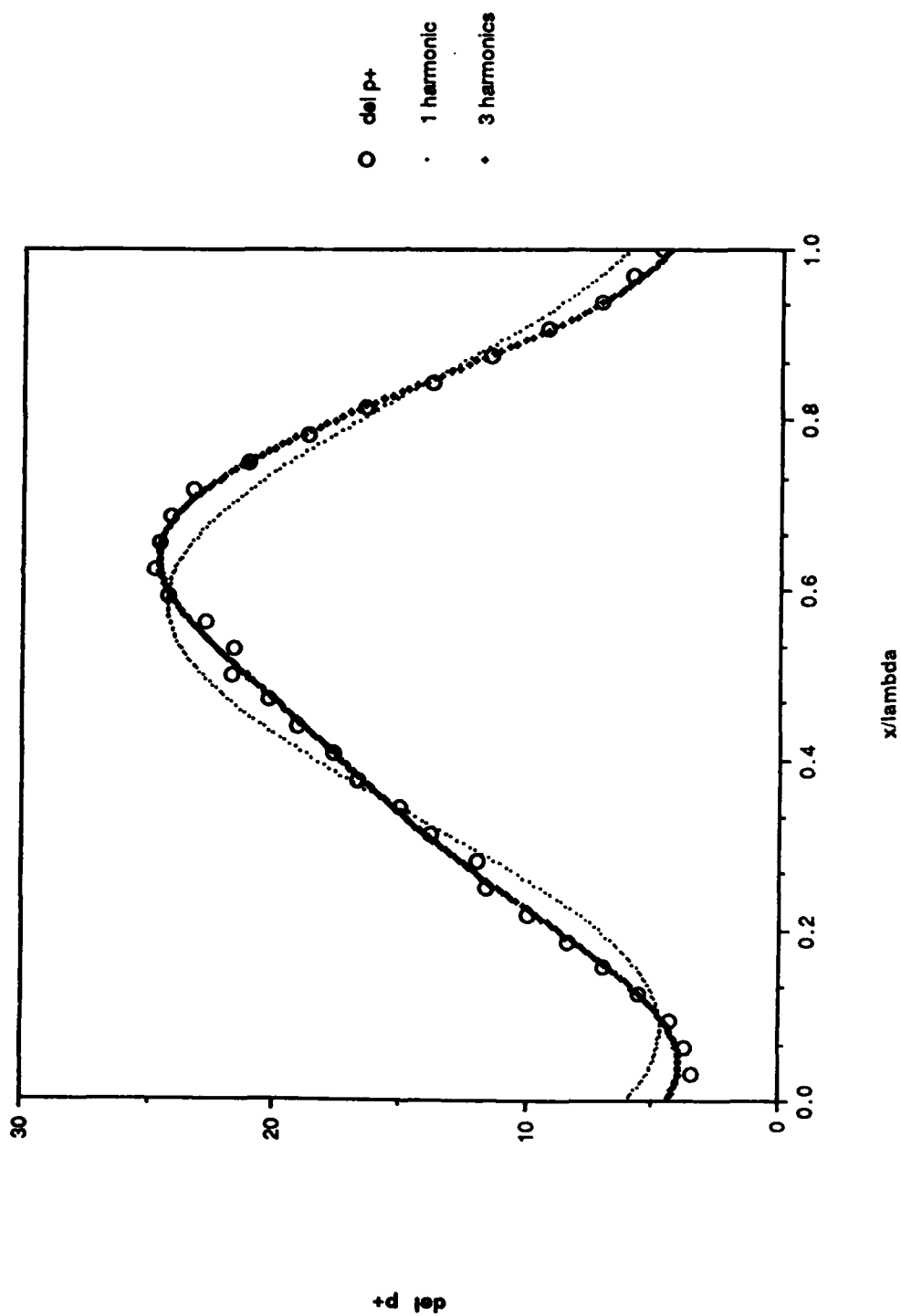
Figure 5.6 Pressure Profile $2a_d/\lambda = 0.03125$, $\alpha^+ = 0.015$
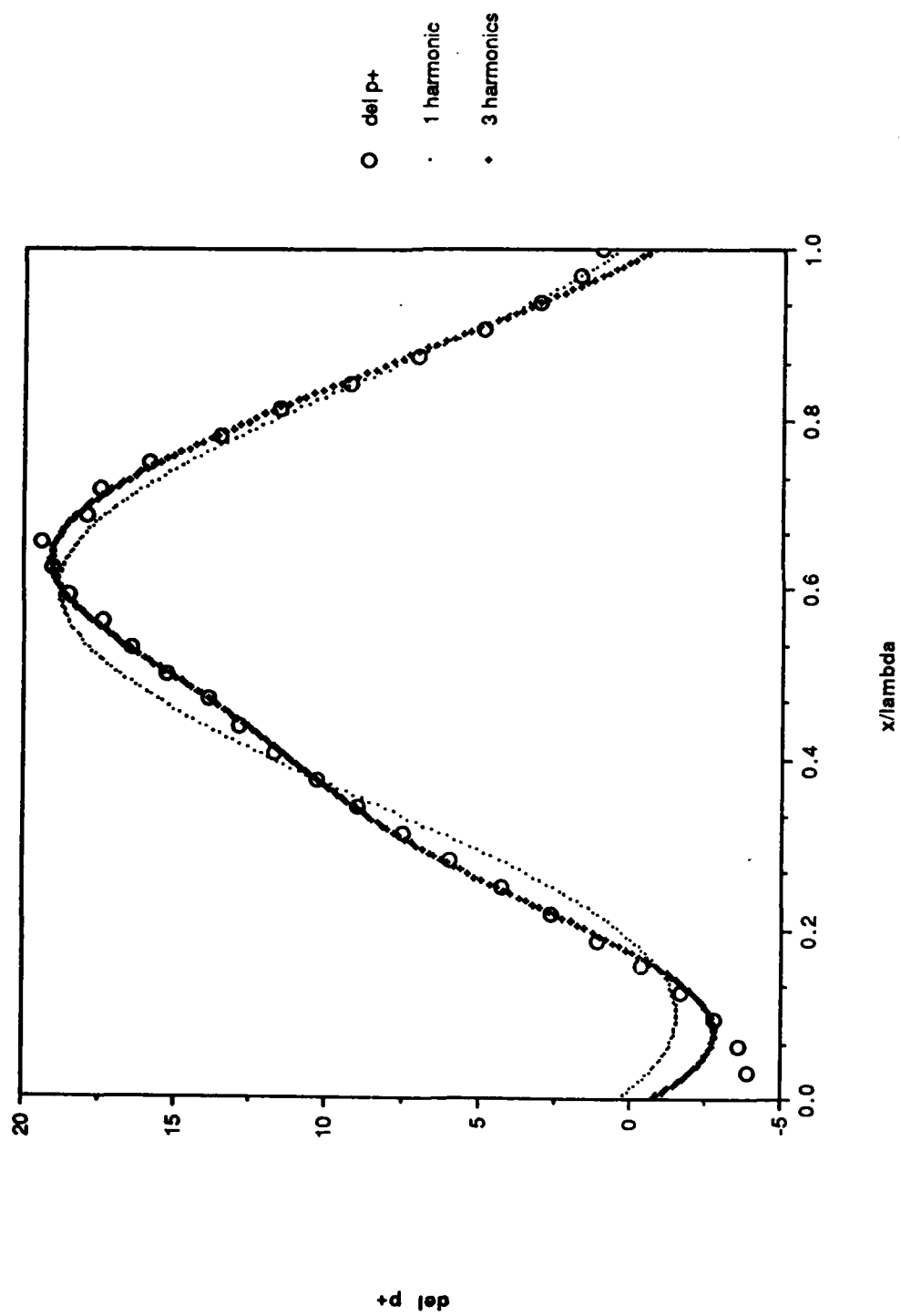
Figure 5.7 Pressure Profile $2a_d/\lambda = 0.03125$, $\alpha^+ = 0.015$
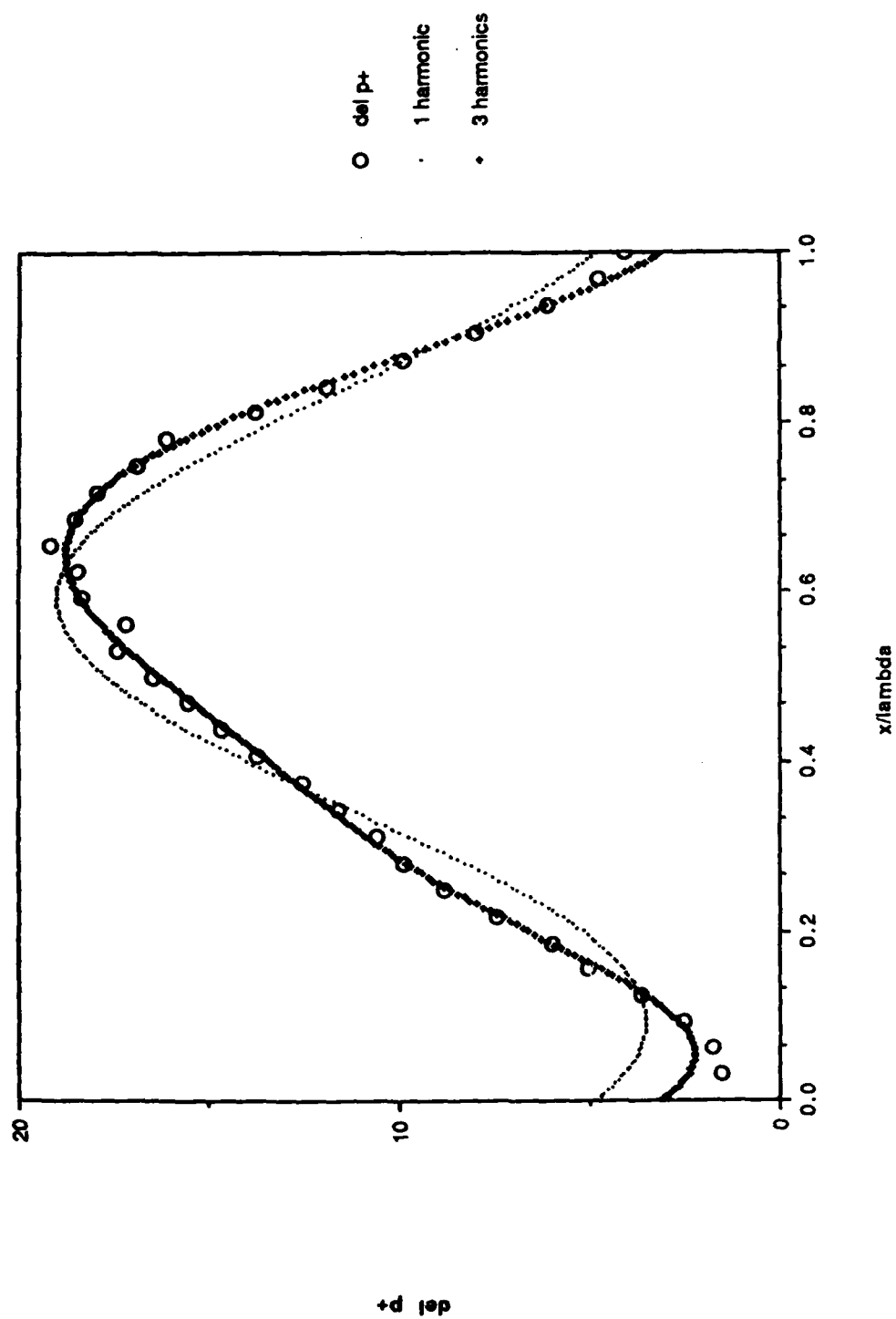
Figure 5.8 Pressure Profile $2a_d/\Lambda = 0.03125$, $\alpha^+ = 0.020$
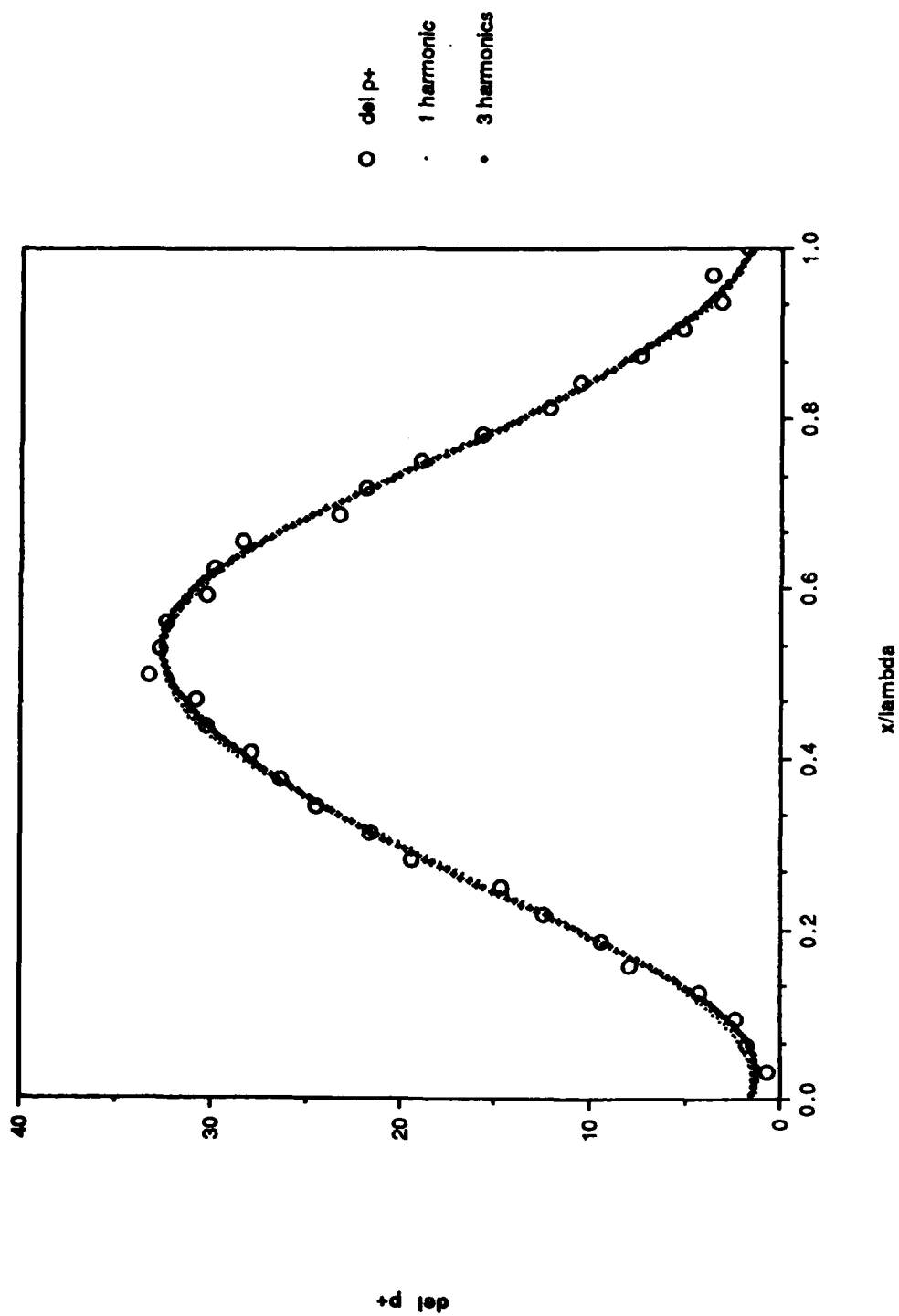
Figure 5.9 Pressure Profile $2a_d/\lambda = 0.0123$, $\alpha^+ = 0.0011$
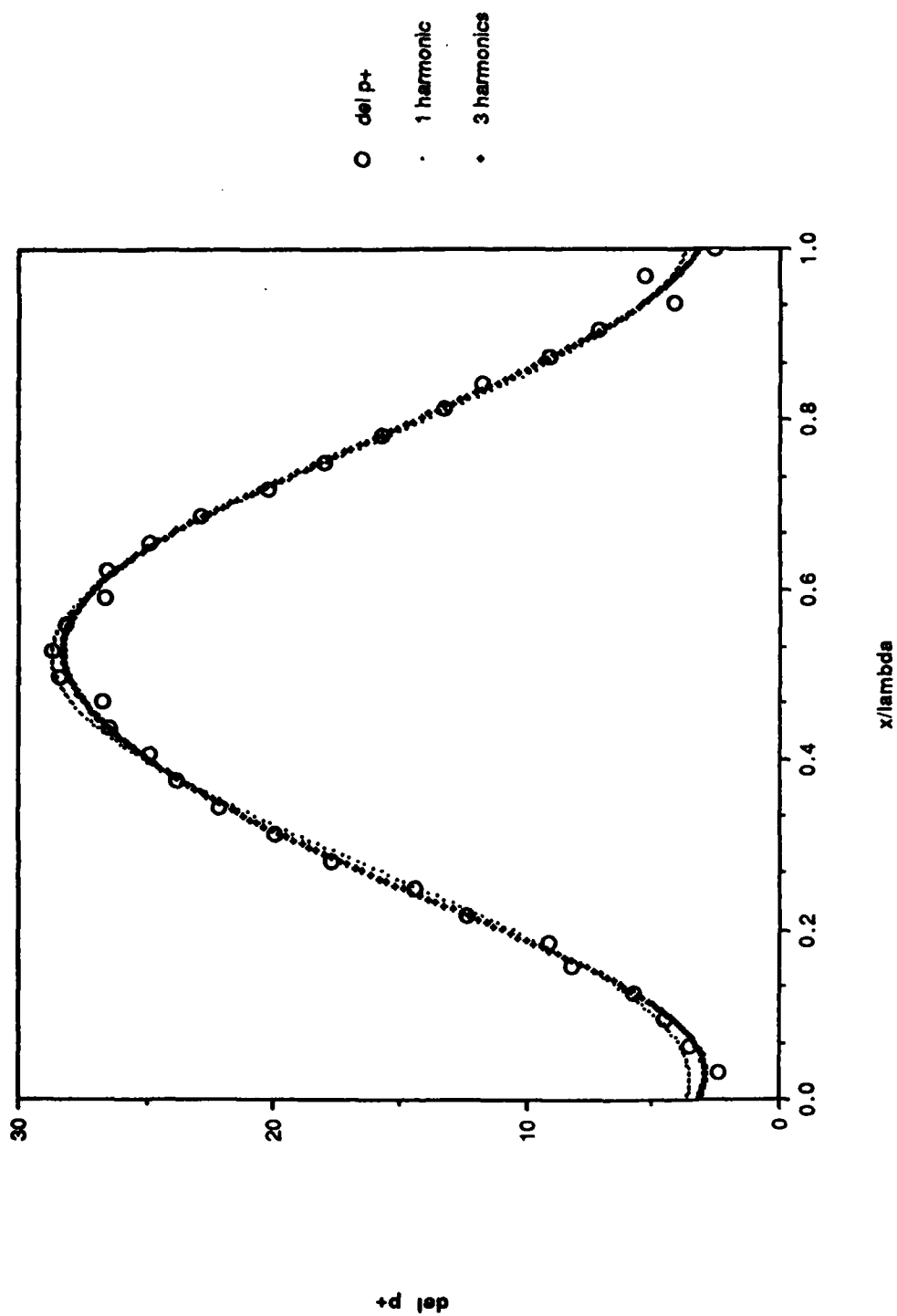
Figure 5.10   Pressure Profile $2a_d/\lambda = 0.0123$, $\alpha^+ = 0.00154$
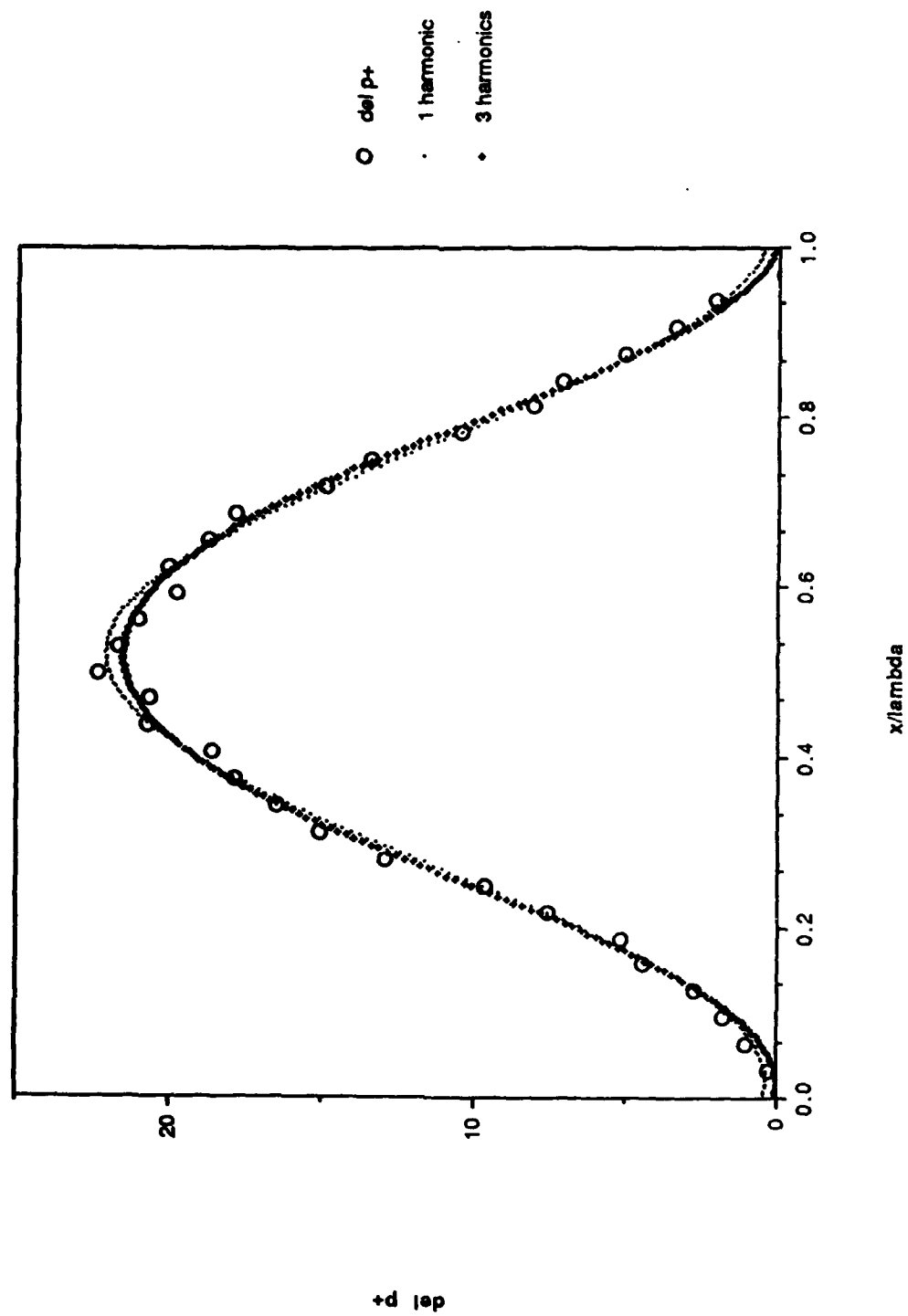
Figure 5.11 Pressure Profile $2a d/\lambda = 0.0123$, $\alpha^+ = 0.0020$

Figure 5.12 Pressure Profile $2a_d/\lambda = 0.0123$, $\alpha^+ = 0.0029$
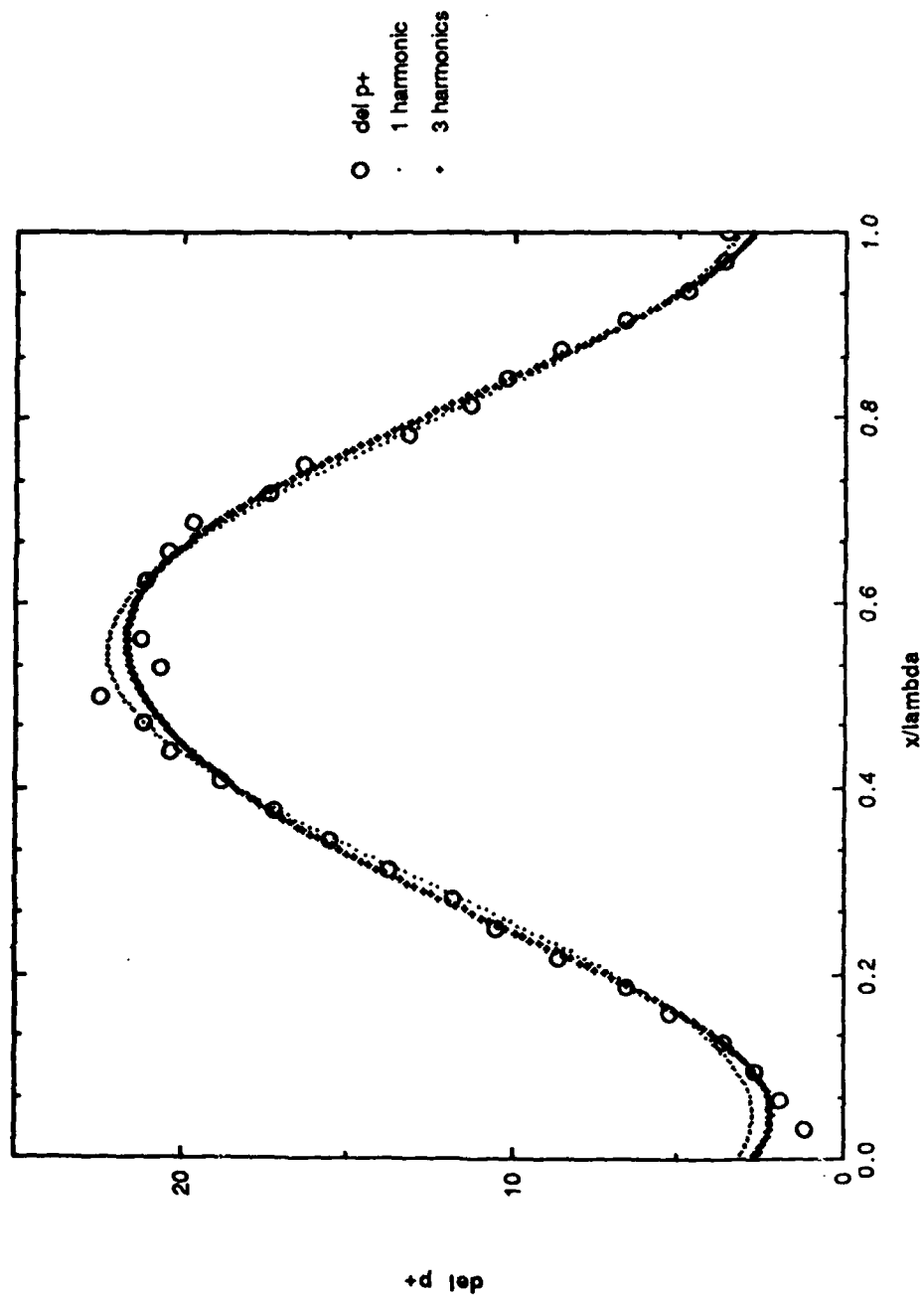
Figure 5.13 Pressure Profile $2a_d/\Lambda = 0.0123$, $\alpha^+ = 0.0039$

44

O del p+

· 1 harmonic

♦ 3 harmonics

15

5

-5

0.0   0.2   0.4   0.6   0.8   1.0

x/lambda

del p+
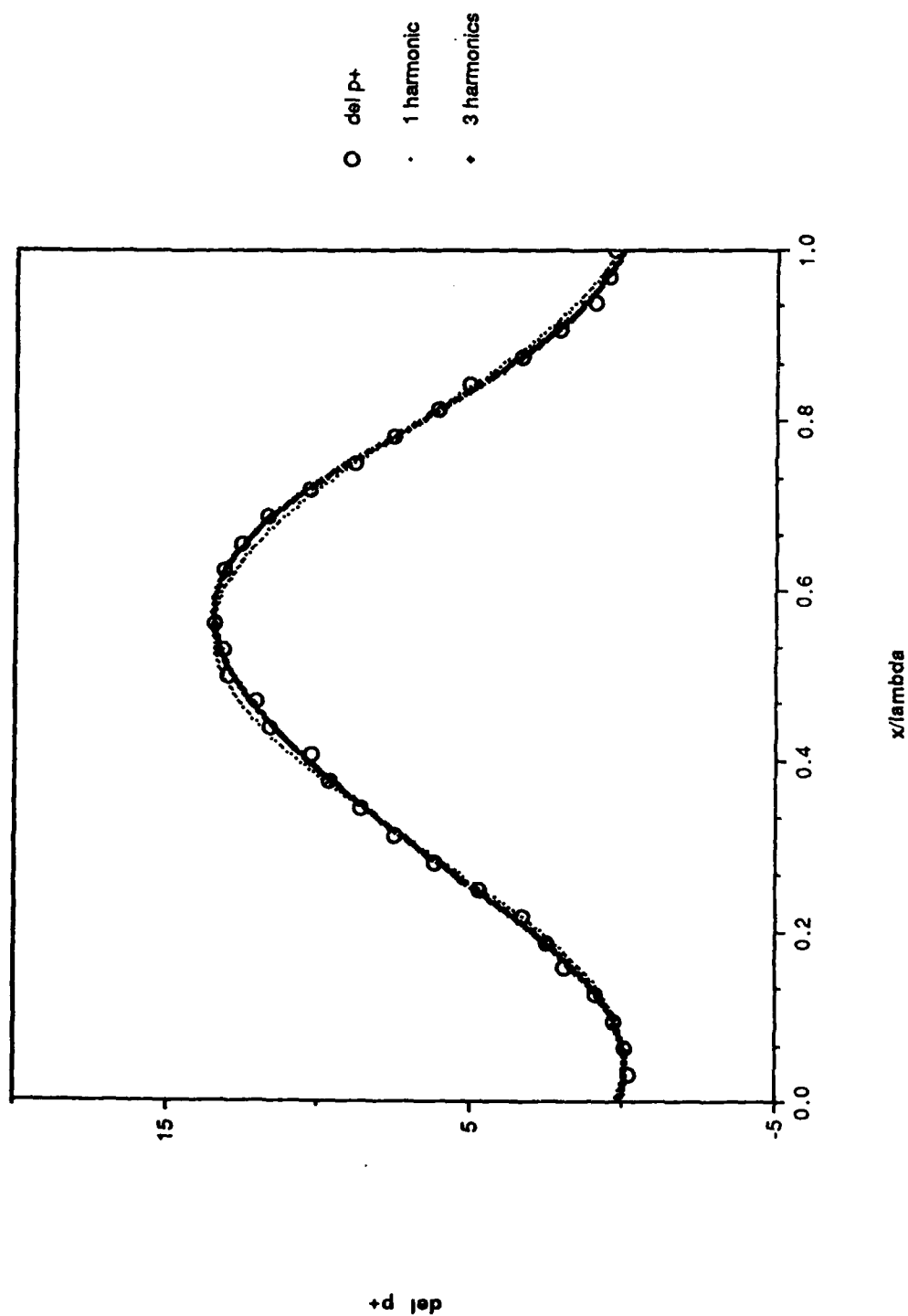
Figure 5.14   Pressure Profile $2a_d/\lambda = 0.0123$, $\alpha^+ = 0.0059$
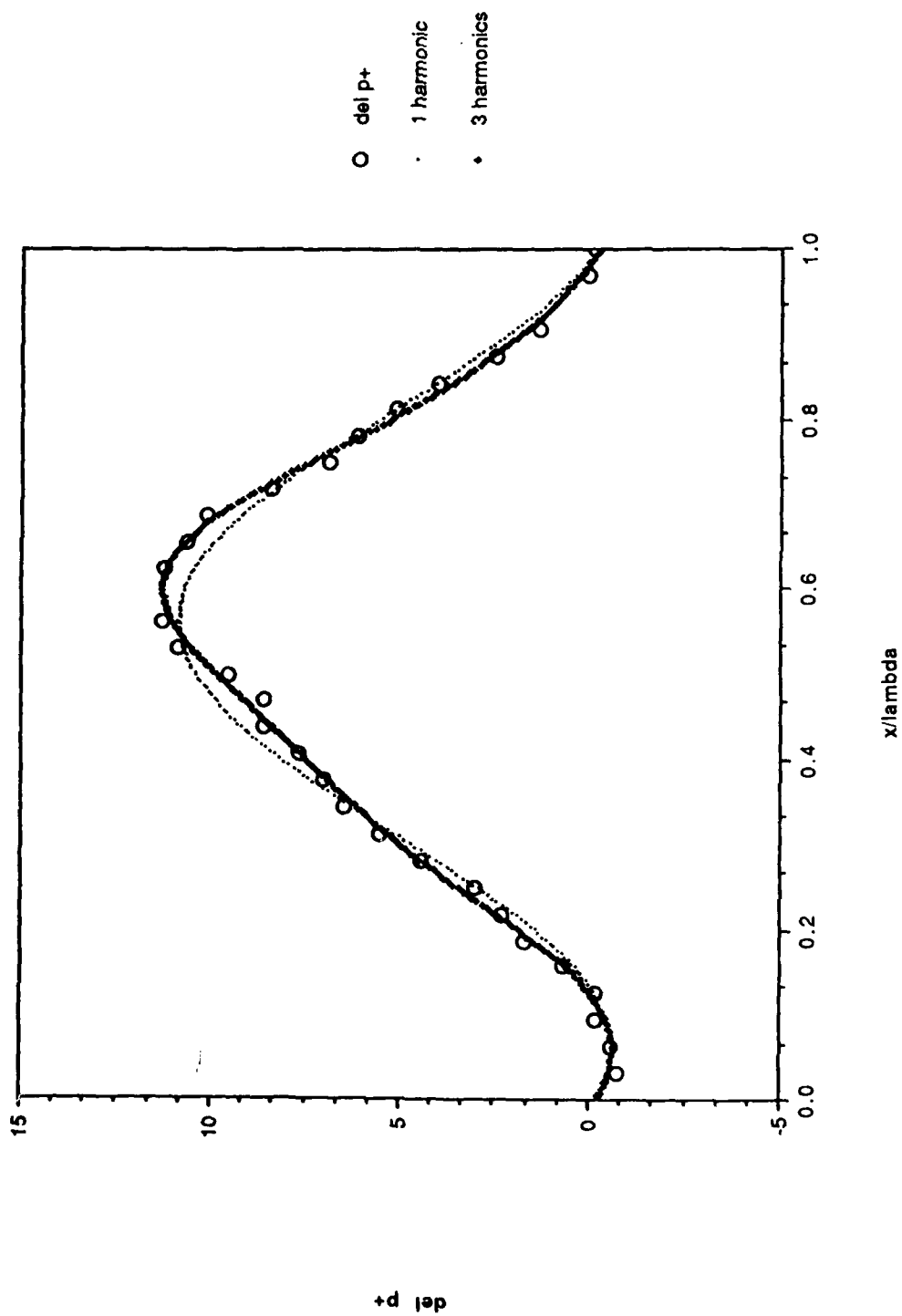
Figure 5.15 Pressure Profile $2\pi d/\lambda = 0.0123$, $\alpha^+ = 0.0079$

del p+

○ del p+

· 1 harmonic

⊹ 3 harmonics

x/lambda
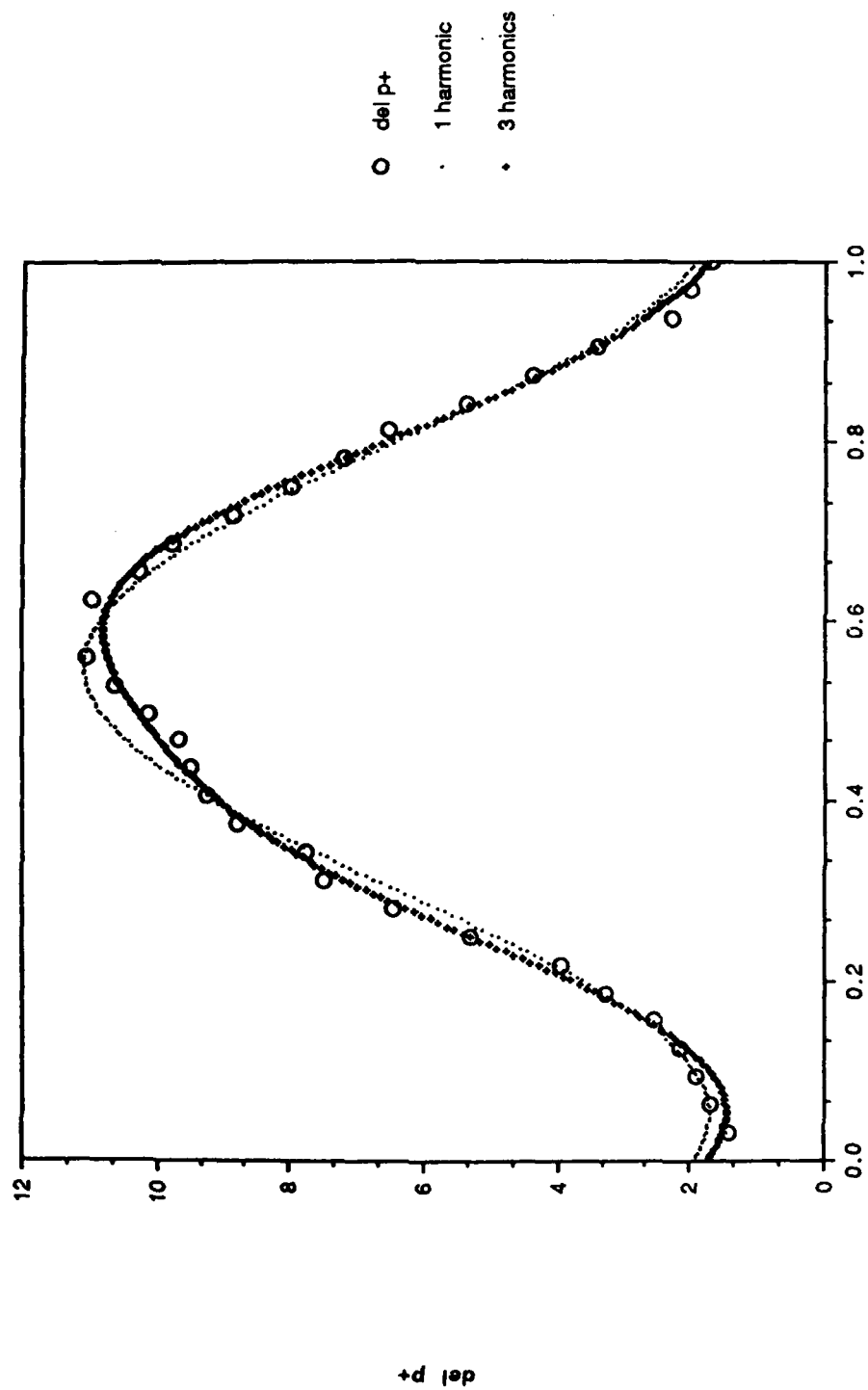
Figure 5.16   Pressure Profile $2a_d/\lambda = 0.0123$, $\alpha^+ = 0.0099$

del p+

O   del p+

·   1 harmonic

•   3 harmonics

x/lambda
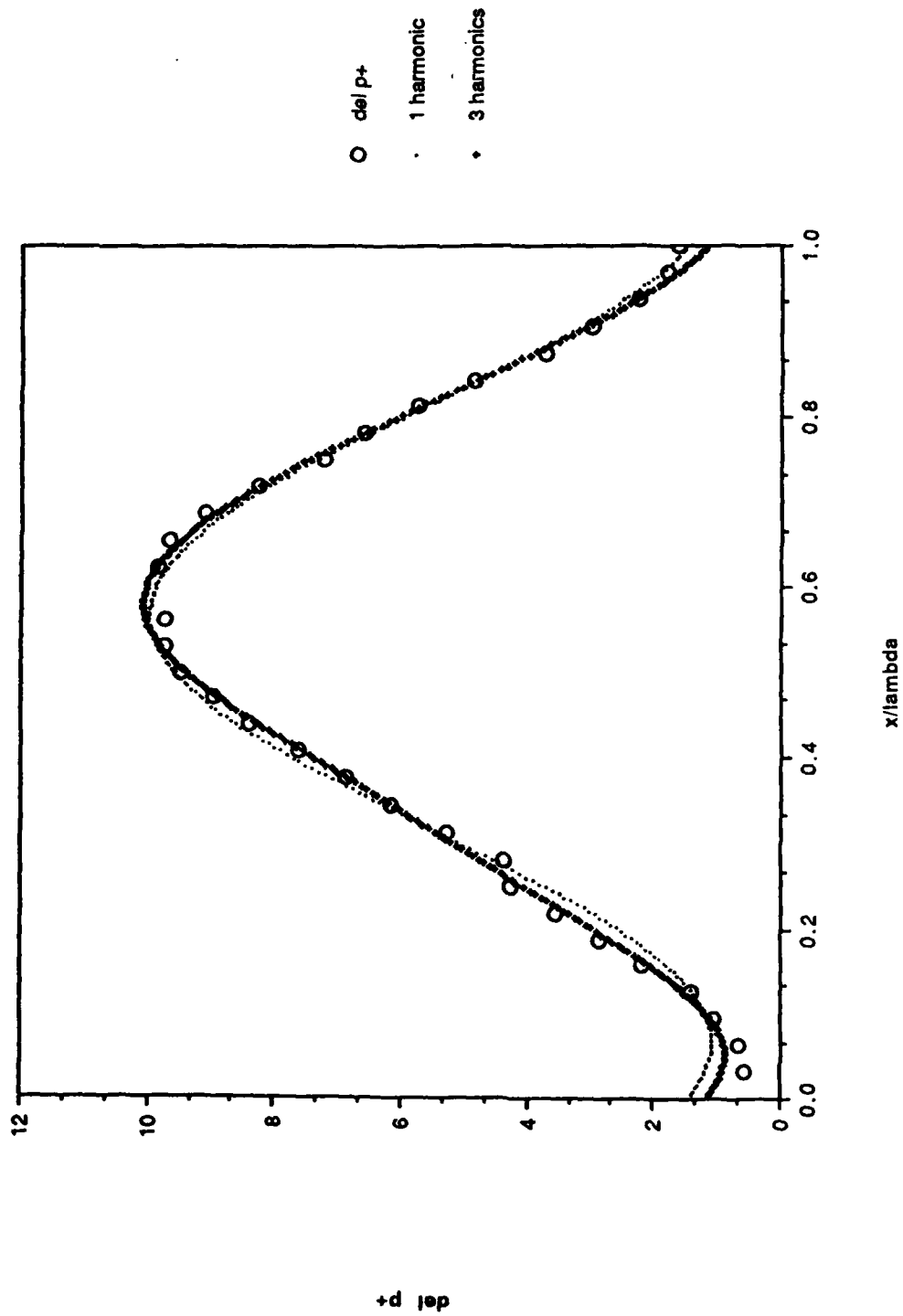
Figure 5.17   Pressure Profile $2a_d/\lambda = 0.0123$, $\alpha^+ = 0.0101$
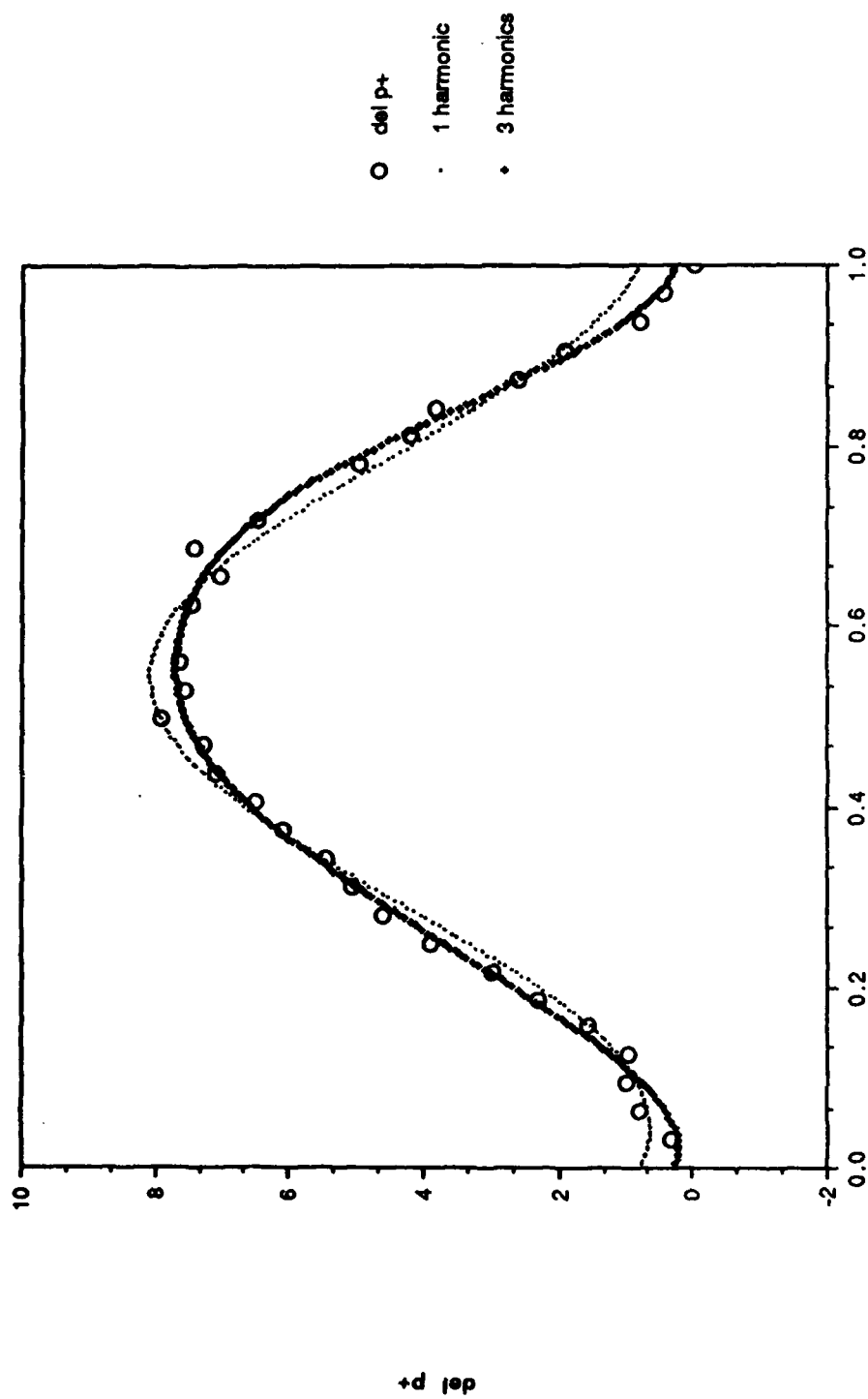
Figure 5.18 Pressure Profile $2a_d/\lambda = 0.0123$, $\alpha^+ = 0.0148$

CHAPTER 6

DISCUSSION OF RESULTS

The measurements made in this study covered a wider range of the dimensionless wave number, α^+, than any of the previous experimental studies. Because of this they are of great use in evaluating the various theoretical works discussed in the literature survey. The pressure response to flow over a wavy surface can be summarized by the ratio of the first harmonic amplitude to the dimensionless wave amplitude, a_1/a^+, and the phase angle of the first harmonic, θ_1. At larger dimensionless wave numbers the shape of the pressure response is markedly distorted from the simple one harmonic approximation. By comparing profiles taken over the same wave at α^+ that are almost the same, the level of reproducibility can be seen as roughly five percent for first harmonic amplitude, a_1, and five degrees for the phase angle, θ_1. The variation in magnitude and phase of the actual measured profile from the linear, one harmonic approximation is within these tolerances (for all but the highest α^+). This is not to say that these profiles are exactly linear, but only that a_1/a^+ and θ_1 are appropriate for comparison.

The data from the work of Lin *et al* (1984), Niederschulte(1988), and this study are summarized in Table (6.1). Figure (6.1) compares the amplitude ratio, a_1/a^+, of these experimental studies with linear predictions from Thorsness(1975) using Model A, Abrams(1984) using Model D*, and the nonlinear analysis of Frederick(1986). Figure (6.2) compares phase angles, θ_1, in a similar fashion. In both of the figures and the table, the work of Lin *et al*

Source	a_d	λ	α^+	a^+	a_1	θ_1	a_2	θ_2	a_3	θ_3	a_1/a^+	a_1/a_2
NASA	0.0104"	1"	0.0027	24.12	17.06	167.9	1.36	-157.5	0.48	-30.0	0.707	0.08 B
NASA	0.0104"	1"	0.0033	19.72	15.17	166.0	1.21	-150.8	0.40	-43.4	0.769	0.08 B
NASA	0.0104"	1"	0.0043	15.14	13.08	163.9	1.22	-156.1	0.44	-44.5	0.864	0.09 N
NASA	0.0104"	1"	0.0063	10.40	11.03	160.4	1.18	-145.1	0.20	-32.2	1.061	0.11 N
NASA	0.0197"	1"	0.0027	46.00	30.04	169.9	2.29	-121.9	1.77	-37.8	0.6350	0.08 N
NASA	0.0197"	1"	0.0033	37.60	26.43	168.3	2.53	-115.7	1.45	-47.5	0.7029	0.10 N
NASA	0.0197"	1"	0.0043	28.85	22.58	165.8	2.77	-110.7	0.85	-38.0	0.7827	0.12 N
NASA	0.0197"	1"	0.0063	19.83	17.98	161.1	3.18	-123.5	0.73	-19.0	0.9067	0.18 N
NASA	0.0100"	2"	0.0014	23.39	9.56	173.4	0.33	33.5	0.11	49.5	0.4087	0.03 L
NASA	0.0100"	2"	0.0017	19.04	8.96	177.8	0.33	35.5	0.20	52.0	0.4706	0.04 L
NASA	0.0100"	2"	0.0022	14.67	8.04	176.2	0.24	48.3	0.23	19.6	0.5480	0.03 L
NASA	0.0100"	2"	0.0031	10.09	7.02	173.4	0.26	2.20	0.12	34.4	0.6954	0.04 L
NASA	0.0150"	1"	0.0027	34.98	23.64	169.9	0.78	-149.5	0.78	-150.6	0.6758	0.03 L
NASA	0.0150"	1"	0.0033	28.60	20.92	167.8	1.04	-123.9	0.60	-160.0	0.7315	0.05 L
NASA	0.0150"	1"	0.0043	21.94	18.07	165.4	1.46	-119.1	0.54	174.6	0.8236	0.08 B

L = linear   B = borderline linear/nonlinear   N = nonlinear   * = data unavailable

Table 6.1 SUMMARY OF EXPERIMENTAL DATA

Source	ad	λ	α+	a+	a1	θ1	a2	θ2	a3	θ3	a1/a+	a1/a2
NASA	0.0150"	1"	0.0063	15.08	14.39	161.7	1.58	-129.6	0.38	148.3	0.9542	0.11 N
Nieder	0.03125"	2"	0.00191	51.32	24.49	166.8	0.83	-177.2	0.21	-107.3	0.477	0.03 L
Nieder	0.03125"	2"	0.00213	46.17	25.08	165.5	0.81	-158.0	0.33	93.7	0.5432	0.03 L
Nieder	0.03125"	2"	0.00216	45.54	26.70	168.2	1.09	-165.8	0.34	-67.2	0.5863	0.04 L
Nieder	0.03125"	2"	0.00216	45.54	25.83	163.6	0.87	-153.5	0.23	-24.9	0.5672	0.034 L
Nieder	0.03125"	2"	0.00216	45.53	25.27	164.0	2.24	-164.5	0.74	-140.6	0.5550	0.09 B
Nieder	0.03125"	2"	0.00220	44.56	23.49	167.2	0.92	-156.7	0.22	-110.6	0.5271	0.04 L
Nieder	0.03125"	2"	0.00913	10.74	17.97	154.0	2.76	-143.4	*	*	1.6718	0.15 N
Nieder	0.03125"	2"	0.0141	6.95	12.61	146.9	2.35	-166.0	*	*	1.814	0.19 N
Nieder	0.03125"	2"	0.0167	5.90	11.14	148.8	1.91	-162.5	0.42	15.1	1.890	0.17 N
Nieder	0.03125"	2"	0.0171	5.76	10.94	145.5	1.93	-173.7	0.21	21.6	1.901	0.18 N
Nieder	0.03125"	2"	0.0206	4.77	7.94	143.4	1.47	-175.5	0.18	142.1	1.663	0.18 N
Nieder	0.03125"	2"	0.0225	4.37	6.81	142.6	1.23	-176.3	*	*	1.557	0.18 N
Nieder	0.0123"	2"	0.0108	3.58	7.00	160.5	0.45	-140.3	*	*	1.957	0.07 L
This study	0.03125"	2"	0.0016	60.8	33.62	167.2	0.97	-177.5	0.52	35.9	0.553	0.03 L
This study	0.03125"	2"	0.0021	46.2	28.82	170.5	0.82	-132.2	0.45	-127.6	0.625	0.03 L

L = linear   B = borderline   linear/nonlinear   N = nonlinear   * = data unavailable

Table 6.1 SUMMARY OF EXPERIMENTAL DATA, continued

Source	ad	λ	α+	a+	a₁	θ₁	a₂	θ₂	a₃	θ₃	a₁/a+	a₁/a₂
This study	0.03125"	2"	0.0029	34.3	26.32	168.0	1.47	-122.3	1.06	-87.5	0.767	0.06 L
This study	0.03125"	2"	0.0040	24.8	20.3	168.9	2.23	-109.0	1.04	-124.0	0.819	0.11 N
This study	0.03125"	2"	0.0108	9.06	12.7	150.0	1.83	-161.8	0.46	51.8	1.402	0.14 N
This study	0.03125"	2"	0.0150	6.57	9.80	149.5	1.77	-161.7	0.08	-1.2	1.492	0.18 N
This study	0.03125"	2"	0.0151	6.51	10.20	144.0	1.39	173.4	0.53	60.47	1.567	0.14 N
This study	0.03125"	2"	0.0198	4.95	7.74	146.2	1.57	174.8	0.23	134.6	1.564	0.20 N
This study	0.0123"	2"	0.0011	36.0	15.54	173.2	0.10	176.1	0.41	78.9	0.432	0.06 L
This study	0.0123"	2"	0.0015	25.1	12.59	171.5	0.52	158.2	0.22	84.6	0.502	0.04 L
This study	0.0123"	2"	0.0020	19.1	10.86	172.2	0.47	169.2	0.13	-53.1	0.568	0.04 L
This study	0.0123"	2"	0.0029	13.4	8.98	171.8	0.74	-175.5	0.27	-169.3	0.670	0.08 L
This study	0.0123"	2"	0.0039	9.85	9.78	163.0	0.60	158.0	0.10	28.1	0.993	0.06 L
This study	0.0123"	2"	0.0059	6.57	6.79	161.8	0.37	-133.1	0.08	11.8	1.033	0.05 L
This study	0.0123"	2"	0.0079	4.88	5.72	157.4	0.52	-126.7	0.32	44.2	1.172	0.09 B
This study	0.0123"	2"	0.0099	3.90	4.69	161.5	0.38	175.4	0.17	9.76	1.203	0.08 B
This study	0.0123"	2"	0.0101	3.84	4.45	156.2	0.28	-147.0	0.13	121.4	1.159	0.06 B
This study	0.0123"	2"	0.0148	2.62	3.72	163.9	0.45	-179.5	0.11	-133.8	1.420	0.12 N

L = linear   B = borderline   linear/nonlinear   N = nonlinear   * = data unavailable

Table 6.1 SUMMARY OF EXPERIMENTAL DATA, continued

alpha+

a I/a +
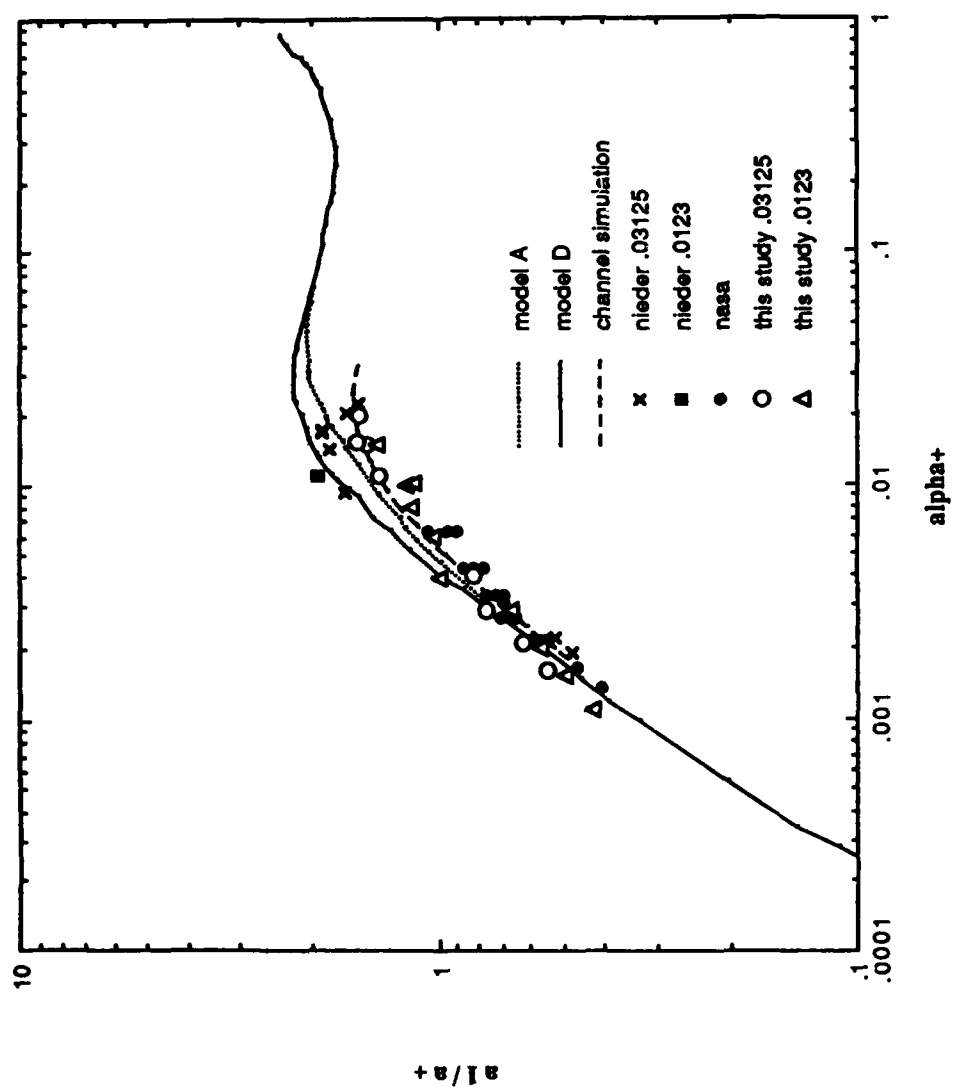
Figure 6.1 Comparison of Amplitude Ratios
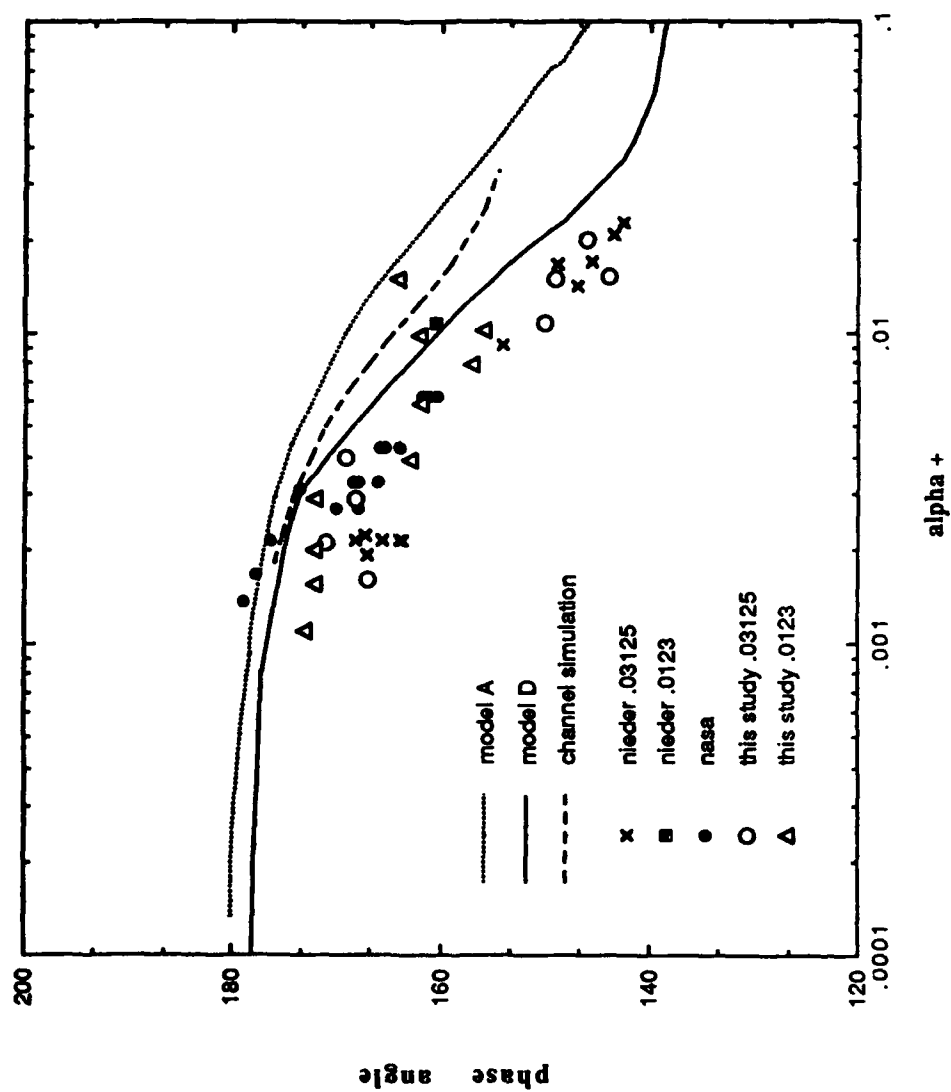
Figure 6.2 Comparison of Phase Angles

is referenced as NASA and the work of Niederschulte is referenced as Nieder.

Lin *et al* measured pressure over waves with similar $2a_d/\lambda$ to the present work. They cover an α^+ range of 0.0027 to 0.0063. The amplitude ratios are in good agreement with the present study, generally within the reproducibility of the work. The phase angles agree for α^+ above 0.0022. Below that, however, the NASA data indicates a faster approach to the expected asymptote of $\theta_1 = 180°$. A possible cause for this disagreement is the different dimensions of the flow system used in the two studies. The NASA data was obtained in a wind tunnel where the top and bottom walls were fifteen inches apart. The water channel in this study has a distance of two inches between the top and bottom walls, which can be compared to a boundary layer thickness.

The data of Niederschulte falls into two regions: The first was obtained with water over α^+ of 0.00191 to 0.0022; the second was obtained with dextrose solution over α^+ of 0.00913 to 0.02245. The data taken in the lower α^+ region agree well with the present results in amplitude ratio, a_1/a^+. The phase angles are somewhat lower (approximately four percent) than those obtained in this study. The phase angle measured at α^+ equal to 0.0016 over the 0.03125 inch wave in this study does agree with Niederschulte's results,though.

The phase angles from Niederschulte's high α^+ measurements agree quite well with those of the present work. A comparison of the shape of profiles from the two studies at similar α^+ shows remarkable similarity considering the data were collected in two different flow systems, using different wave plates and differing arrangements for connecting the pressure taps to the pressure transducer.

The amplitudes of Niederschulte's high α^+ data present some difficulty. The values of a_1/a^+ are a much as fifteen percent higher as measured by Niederschulte. The amplitude ratio also reaches a maxima at α^+ equal to 0.0171. The amplitude ratio measured over the 0.0123 inch wave does not agree with the 0.03125 inch wave data.

It appears that Niederschulte's amplitude data are suspect. The first argument supporting this statement is the abruptness of the drop in amplitude after the maxima is reached. Also, the values at the two highest α^+ agree with the current study, although that may only be coincidence. Secondly, the data point taken over the 0.0123 inch wave does not agree with his other data, while the data from the two wave amplitudes agree quite well in the present study. Finally the data of the current study follow a recognizable trend over a wide range of α^+. The low α^+ data of Niederschulte are effectively clumped into two data points, making trends very difficult to discern. The high α^+ data shows very little pattern. Based on the similarity of Niederschulte's profile shapes to the current study, it may be concluded that the profiles were measured accurately, but the pressure transducer's voltage output to imposed differential pressure relationship was incorrectly calibrated throughout the high α^+ runs. These runs were all made using dextrose solution, which makes calibration more difficult as the need to bleed the lines of the pressure header is increased due to the presence of the dextrose.

The phase angles of this study are best represented, among the models considered, by Abrams' linear calculations using Model D*. All of the experimental data presented here follow the shape of Abrams' curve but are shifted a few degrees lower than his predictions. The notable exceptions are

the phase angles at α^+ equal to 0.0099 and 0.0148 over the 0.0123 inch wave, which are significantly higher. The phase angle at α^+ equal to 0.0101 (which should be the same as that of α^+ equal to 0.0099) falls where expected from the trend of the data.

The amplitude ratio predictions of Frederick's channel simulation are in excellent agreement with the experimental data of this study. The NASA data appear in a range where all three theoretical models predict similar results. The data of Niederschulte don't agree with any of the models, but this has already been discussed.

As stated in the introduction, one motivation for researching flow over a wavy surface is the reduction of drag. Skin friction can be reduced by imposing a wavy boundary on the flow. The wavy surface, however, will inevitably increase form drag. If the increase in form drag is larger than the decrease in skin friction then no gain is made.

It is of interest, therefore, to see if a drag coefficient calculated using the one harmonic approximation to the pressure profile gives an accurate representation of the form drag or if it is necessary to use the actual pressure profile in the calculation. A nondimensional drag coefficient was calculated by dividing the form drag the wave exerts on the fluid by the effective area (the area present in the absence of a wave, equal to the wavelength times the width) and ρu^{*2}.

$$C_p = 1/\lambda \rho u^{*2} \int p_d \sin \beta \, dl \qquad (6.1)$$

where $\beta = \arctan(dy/dx$ of the wave surface) and dl is the differential distance along the wave surface. The drag coefficients were calculated using both the one harmonic fit of the pressure profile (a linear approximation to the

measured profile) and the three harmonic fit (which follows the data very closely).

The calculated drag coefficients are plotted in Figure (6.3). The coefficients for the 0.0123 inch wave show close agreement between those calculated using the one harmonic approximation and those using the more accurate three harmonic fit. The agreement is not as close for the 0.03125 inch wave were the two calculations generally differ by fifteen percent. This is reasonable since the one harmonic fit and the three harmonic fit tend to be quite similar for the 0.0123 wave and not as similar for the 0.03125 wave. The one harmonic calculation may still be appropriate for the 0.03125 inch wave as the more exact calculation gives a larger coefficient for some of the cases and a smaller coefficient in the rest of the cases. Also included in the graph is a form drag coefficient calculated by Frederick. It is in good agreement with those of this study.

Another important consideration in flow over a wavy surface is the possibility of flow separation, or areas of stagnant flow on the downward sloping face of the wave. Separated flow is predicted when the surface shear stress is allowed to reach zero. In his nonlinear analysis Abrams (1979) mapped the boundary between separated and nonseparated flow as $2a_d/\lambda$ versus α^+. Figure (6.4) shows where the data of this study lie on that map. As seen on the map all of the flows studied over the 0.0123 inch amplitude wave should be nonseparated. The pressure profiles support this as none of them are truly distorted. The map predicts that flow over the 0.03125 inch amplitude wave should separate above an α^+ of approximately 0.006. The data support this prediction also. The profiles for α^+ below 0.003 are quite symmetric. The
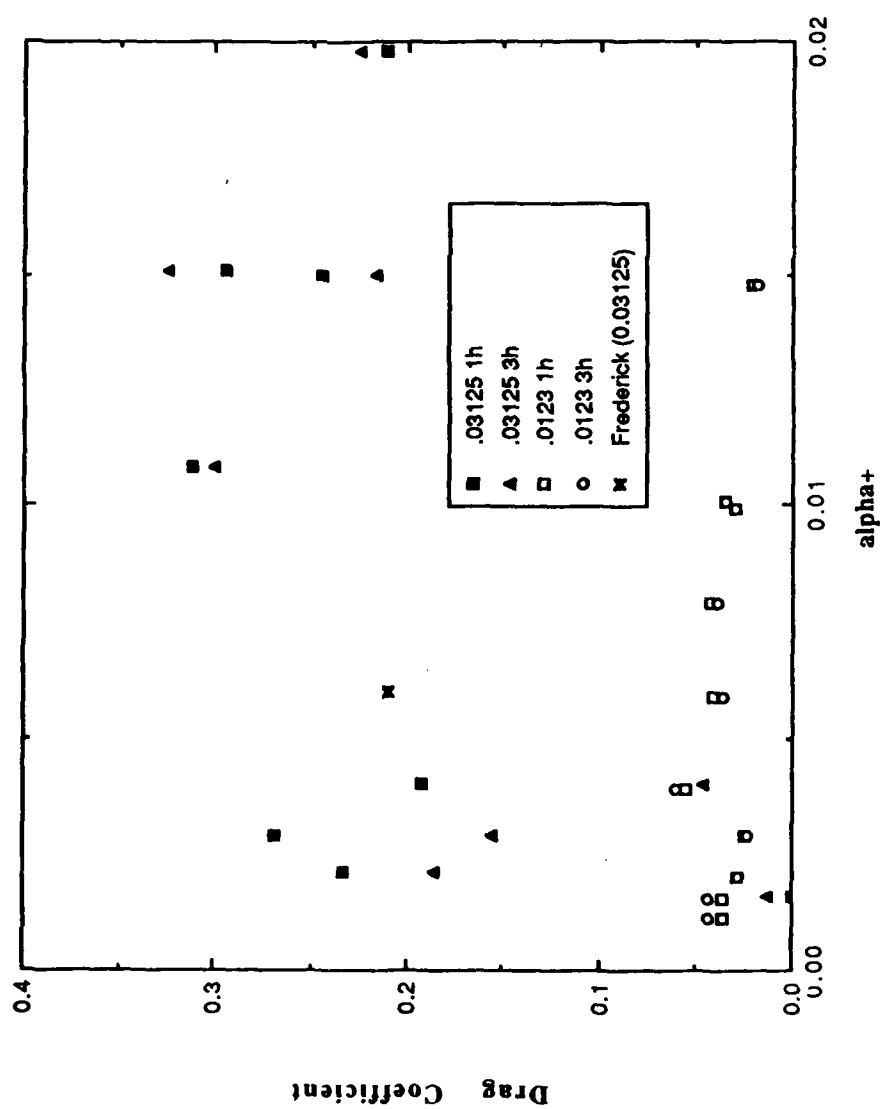
Figure 6.3 Calculated Drag Coefficients versus Alpha+
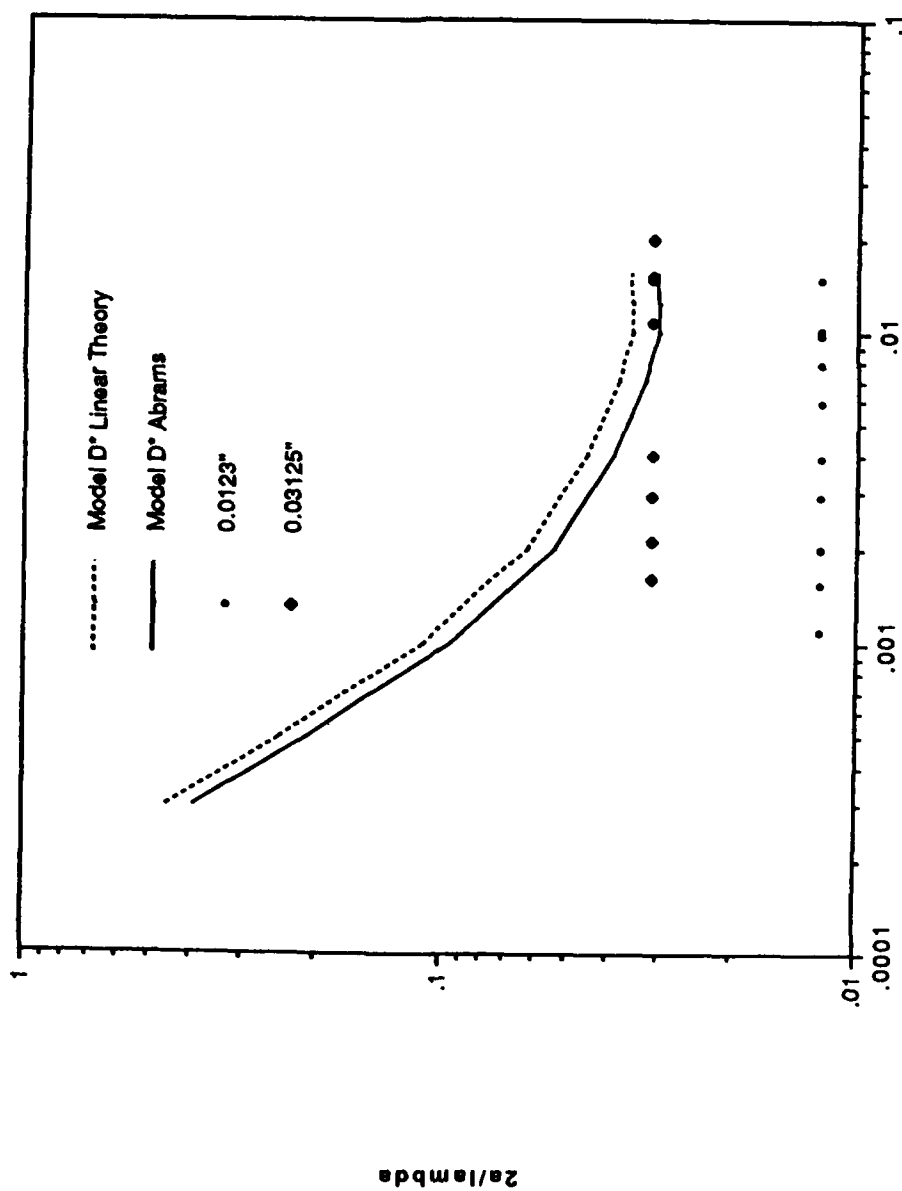
Figure 6.4 Flow Regime Map

profile at α^+ equal to 0.004 begins to show some distortion. The rest of the profiles are at α^+ greater than 0.01 and are all distorted. This distortion could be due to a separated zone.

In conclusion, it is in the high α^+ regions that linear approximations should break down. In this region the nonlinear predictions of amplitude by Frederick match the experimental data best. Surprisingly, the predictions of phase angle that match the experimental data best are from the linear calculations using Model D* by Abrams.

Although it appears that the amplitude of the surface waves in this study are large enough to necessitate nonlinear calculations, the pressure response seems to be satisfactorily described as a first approximation with a linear (one harmonic) approach. This statement can be supported by the observance that the pressure response's amplitude and phase as reported by the one harmonic approximation are within the experimental reproducibility of the measurements to the actual amplitude and phase of the data. Also supporting this statement is the general agreement of form drag coefficients calculated using the one harmonic approximation to those calculated using the three harmonic fit (which follows the data very closely). The presence of nonsymmetric pressure profiles only in the regions where separation is predicted by theory tends to support these predictions.

APPENDIX A

Tabulated   Data

TABLE A.1 PRESSURE DATA $2a_d/\lambda = 0.03125$, $\alpha^+ = 0.0016$

Date: June 3,1988

Fluid: Water   Temp: 25° C   Density: 0.997 g/cm^3 v: 0.00896 cm^2/s

u^*: 6.871 cm/s a^+: 60.8   Re: 41,600

slope: 0.3906   intercept: -0.3678

Harmonic 1:   amplitude= 33.6   phase= +167°

Harmonic 2:   amplitude= 0.97   phase= -177°

Harmonic 3:   amplitude= 0.52   phase= +36°

x value/lambda	Differential Pressure	Average Voltage
3.125E-02	-3.875E-01	9.198E-01
6.250E-02	1.104E+00	9.890E-01
9.375E-02	3.440E+00	1.099E+00
1.250E-01	9.284E+00	1.379E+00
1.563E-01	1.282E+01	1.548E+00
1.875E-01	1.847E+01	1.819E+00
2.188E-01	2.369E+01	2.260E+00
2.813E-01	3.644E+01	2.680E+00
3.125E-01	4.467E+01	3.076E+00
3.438E-01	4.869E+01	3.268E+00
3.750E-01	5.507E+01	3.574E+00
4.063E-01	5.858E+01	3.741E+00
4.375E-01	6.218E+01	3.913E+00
4.688E-01	6.541E+01	4.066E+00
5.000E-01	6.902E+01	4.238E+00
5.313E-01	6.958E+01	4.262E+00
5.625E-01	6.763E+01	4.164E+00
5.938E-01	6.726E+01	4.144E+00
6.250E-01	6.456E+01	4.010E+00
6.563E-01	6.204E+01	3.884E+00
6.875E-01	5.775E+01	3.673E+00
7.188E-01	5.229E+01	3.406E+00
7.500E-01	4.504E+01	3.051E+00
7.813E-01	3.531E+01	2.576E+00
8.125E-01	2.992E+01	2.312E+00
8.438E-01	2.466E+01	2.054E+00
8.750E-01	1.914E+01	1.784E+00
9.063E-01	1.268E+01	1.467E+00
9.375E-01	8.239E+00	1.245E+00
9.688E-01	7.451E+00	1.208E+00
1.000E+00	4.076E+00	1.041E+00

TABLE A.2 PRESSURE DATA $2a_d/\lambda = 0.03125$, $\alpha^+= 0.0021$

Date: May 29,1988

Fluid: Water   Temp: 25° C   Density: 0.997 g/cm^3 ν: .0.00896 cm^2/s

u^*: 5.216 cm/s a^+: 46.2   Re: 30,400

slope: 0.1670   intercept: -0.0589

Harmonic 1:   amplitude= 28.9   phase= +171°
Harmonic 2:   amplitude= 0.82   phase= -132°
Harmonic 3:   amplitude= 0.45   phase= -128°

x value/lambda	Differential Pressure	Average Voltage
3.125E-02	5.374E+00	3.775E-01
6.250E-02	6.635E+00	4.557E-01
9.375E-02	8.522E+00	5.748E-01
1.250E-01	1.251E+01	8.312E-01
1.563E-01	1.672E+01	1.102E+00
1.875E-01	2.142E+01	1.405E+00
2.188E-01	2.492E+01	1.629E+00
2.500E-01	3.057E+01	1.994E+00
2.813E-01	3.512E+01	2.288E+00
3.125E-01	4.048E+01	2.634E+00
3.438E-01	4.657E+01	3.302E+00
4.063E-01	5.642E+01	3.663E+00
4.375E-01	6.004E+01	3.895E+00
4.688E-01	6.068E+01	3.933E+00
5.000E-01	6.537E+01	4.235E+00
5.313E-01	6.216E+01	4.021E+00
5.625E-01	6.230E+01	4.026E+00
5.938E-01	6.231E+01	4.022E+00
6.250E-01	5.893E+01	3.798E+00
6.563E-01	5.654E+01	3.638E+00
6.875E-01	5.100E+01	3.271E+00
7.188E-01	4.697E+01	3.004E+00
7.500E-01	4.187E+01	2.666E+00
7.813E-01	3.493E+01	2.209E+00
8.125E-01	2.900E+01	1.817E+00
8.438E-01	2.342E+01	1.448E+00
8.750E-01	1.802E+01	1.092E+00
9.063E-01	1.521E+01	9.039E-01
9.375E-01	1.026E+01	5.763E-01
9.688E-01	8.156E+00	4.349E-01
1.000E+00	6.312E+00	3.102E-01

TABLE A.3 PRESSURE DATA $2a_d/\lambda = 0.03125$, $\alpha^+ = 0.0029$

Date: June 23,1988

Fluid: Water Temp: 25° C Density: 0.997 g/cm^3 υ: 0.00896 cm^2/s

u^*: 3.87 cm/s a^+: 34.3 Re: 21,600

slope: 0.0922 intercept: -0.0530

Harmonic 1: amplitude= 26.3 phase= +168°
Harmonic 2: amplitude= 1.47 phase= -122°
Harmonic 3: amplitude= 1.06 phase= -88°

x value/lambda	Differential Pressure	Average Voltage
3.125E-02	1.149E+00	6.599E-01
6.250E-02	3.035E+00	7.812E-01
9.375E-02	4.341E+00	8.639E-01
1.250E-01	7.512E+00	1.071E+00
1.563E-01	1.190E+01	1.359E+00
1.875E-01	1.432E+01	1.516E+00
2.188E-01	1.729E+01	1.709E+00
2.500E-01	2.273E+01	2.067E+00
2.813E-01	2.497E+01	2.212E+00
3.125E-01	3.142E+01	2.638E+00
3.438E-01	3.557E+01	2.909E+00
3.750E-01	4.265E+01	3.377E+00
4.063E-01	4.724E+01	3.678E+00
4.375E-01	4.958E+01	3.830E+00
4.688E-01	5.076E+01	3.904E+00
5.000E-01	5.240E+01	4.009E+00
5.313E-01	5.140E+01	3.938E+00
5.625E-01	5.276E+01	4.024E+00
5.938E-01	5.139E+01	3.929E+00
6.250E-01	5.187E+01	3.957E+00
6.563E-01	4.869E+01	3.741E+00
6.875E-01	4.431E+01	3.445E+00
7.188E-01	4.012E+01	3.162E+00
7.500E-01	3.511E+01	2.824E+00
7.813E-01	2.757E+01	2.317E+00
8.125E-01	2.251E+01	1.977E+00
8.438E-01	1.709E+01	1.612E+00
8.750E-01	1.230E+01	1.289E+00
9.063E-01	7.020E+00	9.325E-01
9.375E-01	3.906E+00	7.209E-01
9.688E-01	1.841E+00	5.792E-01
1.000E+00	8.668E-01	5.101E-01

TABLE A.4 PRESSURE DATA $2a_d/\lambda = 0.03125$, $\alpha^+ = 0.0040$

Date: June 25,1988

Fluid: Water   Temp: 25° C Density: 0.997 g/cm^3 υ: .0.00896 cm^2/s

u*: 2.80 cm/s   a$^+$: 24.8   Re: 14,900

slope: 0.0653   intercept: -0.1124

Harmonic 1:	amplitude= 20.3	phase= +169°
Harmonic 2:	amplitude= 2.23	phase= -109°
Harmonic 3:	amplitude= 1.04	phase= -124°

x value/lambda	Differential Pressure	Average Voltage
3.125E-02	7.798E+00	2.074E+00
6.250E-02	8.418E+00	2.100E+00
9.375E-02	1.008E+01	2.177E+00
1.250E-01	1.215E+01	2.272E+00
1.563E-01	1.574E+01	2.440E+00
1.875E-01	1.798E+01	2.544E+00
2.188E-01	1.927E+01	2.602E+00
2.500E-01	2.368E+01	2.808E+00
2.813E-01	2.485E+01	2.862E+00
3.125E-01	2.796E+01	3.006E+00
3.438E-01	3.249E+01	3.219E+00
3.750E-01	3.526E+01	3.348E+00
4.063E-01	3.974E+01	3.558E+00
4.375E-01	4.330E+01	3.725E+00
4.688E-01	4.489E+01	3.797E+00
5.000E-01	4.733E+01	3.910E+00
5.313E-01	4.638E+01	3.862E+00
5.625E-01	4.478E+01	3.783E+00
5.938E-01	4.565E+01	3.822E+00
6.250E-01	4.518E+01	3.796E+00
6.563E-01	4.357E+01	3.716E+00
6.875E-01	4.049E+01	3.567E+00
7.188E-01	3.584E+01	3.342E+00
7.500E-01	3.140E+01	3.128E+00
7.813E-01	2.690E+01	2.911E+00
8.125E-01	2.121E+01	2.637E+00
8.438E-01	1.757E+01	2.461E+00
8.750E-01	1.419E+01	?.296E+00
9.063E-01	1.132E+01	2.157E+00
9.375E-01	5.008E+00	1.853E+00
9.688E-01	4.900E+00	1.845E+00
1.000E+00	4.158E+00	1.807E+00

TABLE A.5 PRESSURE DATA $2a_d/\lambda = 0.03125$, $\alpha^+= 0.011$

Date: July 3,1988

Fluid: Dextrose   Temp: 25° C   Density: 1.20 g/cm^3 υ: .0.0805 cm^2/s

u*:   9.18 cm/s   a$^+$: 9.06   Re: 4690

slope: 0.2515   intercept: -0.0653

Harmonic 1:   amplitude= 12.7   phase= +150°
Harmonic 2:   amplitude= 1.83   phase= -161°
Harmonic 3:   amplitude= 0.46   phase=   +52°

x value/lambda	Differential Pressure	Average Voltage
3.125E-02	4.488E-01	3.221E-01
6.250E-02	8.096E-01	3.702E-01
9.375E-02	1.889E+00	5.347E-01
1.250E-01	3.301E+00	7.528E-01
1.563E-01	5.082E+00	1.031E+00
1.875E-01	6.851E+00	1.307E+00
2.188E-01	8.649E+00	1.588E+00
2.500E-01	1.062E+01	1.896E+00
2.813E-01	1.278E+01	2.235E+00
3.125E-01	1.452E+01	2.507E+00
3.438E-01	1.622E+01	2.771E+00
3.750E-01	1.779E+01	3.016E+00
4.063E-01	1.950E+01	3.282E+00
4.375E-01	2.102E+01	3.518E+00
4.688E-01	2.247E+01	3.742E+00
5.000E-01	2.417E+01	4.007E+00
5.313E-01	2.542E+01	4.200E+00
5.625E-01	2.699E+01	4.442E+00
5.938E-01	2.791E+01	4.582E+00
6.250E-01	2.839E+01	4.649E+00
6.563E-01	2.824E+01	4.615E+00
6.875E-01	2.715E+01	4.428E+00
7.188E-01	2.526E+01	4.112E+00
7.500E-01	2.303E+01	3.741E+00
7.813E-01	1.994E+01	3.231E+00
8.125E-01	1.697E+01	2.739E+00
8.438E-01	1.402E+01	2.252E+00
8.750E-01	1.125E+01	1.793E+00
9.063E-01	8.654E+00	1.363E+00
9.375E-01	6.230E+00	9.600E-01
9.688E-01	4.687E+00	6.999E-01
1.000E+00	3.735E+00	5.357E-01

TABLE A.6 PRESSURE DATA $2a_d/\lambda = 0.03125$, $\alpha^+ = 0.015$

Date: July 1,1988

Fluid: Dextrose   Temp: 25° C   Density: 1.20 g/cm^3 υ: .0.0805 cm^2/s

u*: 6.661 cm/s   a$^+$: 6.57   Re: 3250

slope: 0.1402   intercept: -0.0057

Harmonic 1:   amplitude= 9.8   phase= +149°
Harmonic 2:   amplitude= 1.8   phase= -161°
Harmonic 3:   amplitude= 0.08   phase=   -1°

x value/lambda	Differential Pressure	Average Voltage
3.125E-02	3.438E+00	5.560E-01
6.250E-02	3.734E+00	5.917E-01
9.375E-02	4.310E+00	6.699E-01
1.250E-01	5.559E+00	8.509E-01
1.563E-01	6.959E+00	1.055E+00
1.875E-01	8.416E+00	1.268E+00
2.188E-01	1.000E+01	1.500E+00
2.500E-01	1.157E+01	1.730E+00
2.813E-01	1.191E+01	1.773E+00
3.125E-01	1.376E+01	2.045E+00
3.438E-01	1.502E+01	2.228E+00
3.750E-01	1.668E+01	2.472E+00
4.063E-01	1.767E+01	2.614E+00
4.375E-01	1.903E+01	2.812E+00
4.688E-01	2.023E+01	2.985E+00
5.000E-01	2.170E+01	3.200E+00
5.313E-01	2.165E+01	3.183E+00
5.625E-01	2.278E+01	3.346E+00
5.938E-01	2.429E+01	3.567E+00
6.250E-01	2.477E+01	3.631E+00
6.563E-01	2.463E+01	3.599E+00
6.875E-01	2.418E+01	3.521E+00
7.188E-01	2.326E+01	3.371E+00
7.500E-01	2.113E+01	3.036E+00
7.813E-01	1.870E+01	2.655E+00
8.125E-01	1.637E+01	2.289E+00
8.438E-01	1.378E+01	1.884E+00
8.750E-01	1.146E+01	1.520E+00
9.063E-01	9.263E+00	1.174E+00
9.375E-01	7.174E+00	8.457E-01
9.688E-01	5.883E+00	6.388E-01
1.000E+00	4.735E+00	4.538E-01

TABLE A.7 PRESSURE DATA $2a_d/\lambda = 0.03125$, $\alpha^+ = 0.015$

Date: July 5,1988
Fluid: Dextrose   Temp: 25° C   Density: 1.20 g/cm³ υ: .0.0805 cm²/s
u*: 6.60 cm/s   a⁺: 6.51   Re: 3220
slope: 0.1032   intercept: -0.1766

Harmonic 1:   amplitude= 10.2   phase= +144°
Harmonic 2:   amplitude= 1.38   phase= +173°
Harmonic 3:   amplitude= 0.53   phase= +60°

x value/lambda	Differential Pressure	Average Voltage
3.125E-02	-3.931E+00	8.964E-01
6.250E-02	-3.587E+00	9.537E-01
9.375E-02	-2.766E+00	1.108E+00
1.250E-01	-1.718E+00	1.309E+00
1.563E-01	-3.719E-01	1.571E+00
1.875E-01	1.122E+00	1.862E+00
2.188E-01	2.664E+00	2.164E+00
2.500E-01	4.294E+00	2.484E+00
2.813E-01	5.958E+00	2.810E+00
3.125E-01	7.482E+00	3.108E+00
3.438E-01	8.977E+00	3.400E+00
3.750E-01	1.026E+01	3.649E+00
4.063E-01	1.168E+01	3.925E+00
4.375E-01	1.288E+01	4.157E+00
4.688E-01	1.393E+01	4.358E+00
5.000E-01	1.532E+01	4.628E+00
5.313E-01	1.647E+01	4.851E+00
5.625E-01	1.741E+01	5.029E+00
5.938E-01	1.855E+01	5.250E+00
6.250E-01	1.903E+01	5.333E+00
6.563E-01	1.940E+01	5.396E+00
6.875E-01	1.795E+01	5.088E+00
7.188E-01	1.748E+01	4.979E+00
7.500E-01	1.589E+01	4.641E+00
7.813E-01	1.355E+01	4.152E+00
8.125E-01	1.153E+01	3.726E+00
8.438E-01	9.284E+00	3.256E+00
8.750E-01	7.083E+00	2.794E+00
9.063E-01	4.947E+00	2.345E+00
9.375E-01	3.113E+00	1.953E+00
9.688E-01	1.787E+00	1.674E+00
1.000E+00	1.035E+00	1.508E+00

TABLE A.8 PRESSURE DATA $2a_d/\lambda = 0.03125$, $\alpha^+ = 0.020$

Date: July 2,1988
Fluid: Dextrose   Temp: 25° C   Density: 1.20 g/cm^3 υ: .0.0805 cm^2/s
u*: 5.02 cm/s   a$^+$: 4.95   Re: 2360
slope: 0.1384   intercept: -0.2203

Harmonic 1: amplitude= 7.74   phase= +146°
Harmonic 2: amplitude= 1.57   phase= +174°
Harmonic 3: amplitude= 0.23   phase= +23°

x value/lambda	Differential Pressure	Average Voltage
3.125E-02	1.553E+00	1.723E+00
6.250E-02	1.780E+00	1.737E+00
9.375E-02	2.502E+00	1.795E+00
1.250E-01	3.619E+00	1.888E+00
1.563E-01	5.079E+00	2.011E+00
1.875E-01	5.998E+00	2.086E+00
2.188E-01	7.486E+00	2.212E+00
2.500E-01	8.823E+00	2.324E+00
2.813E-01	9.890E+00	2.412E+00
3.125E-01	1.061E+01	2.470E+00
3.438E-01	1.156E+01	2.548E+00
3.750E-01	1.254E+01	2.629E+00
4.063E-01	1.372E+01	2.727E+00
4.375E-01	1.462E+01	2.801E+00
4.688E-01	1.551E+01	2.873E+00
5.000E-01	1.646E+01	2.952E+00
5.313E-01	1.744E+01	3.032E+00
5.625E-01	1.715E+01	3.001E+00
5.938E-01	1.834E+01	3.100E+00
6.250E-01	1.850E+01	3.108E+00
6.563E-01	1.915E+01	3.160E+00
6.875E-01	1.855E+01	3.102E+00
7.188E-01	1.797E+01	3.045E+00
7.500E-01	1.688E+01	2.944E+00
7.813E-01	1.614E+01	2.873E+00
8.125E-01	1.376E+01	2.658E+00
8.438E-01	1.190E+01	2.489E+00
8.750E-01	9.883E+00	2.305E+00
9.063E-01	7.988E+00	2.133E+00
9.375E-01	6.119E+00	1.963E+00
9.688E-01	4.770E+00	1.838E+00
1.000E+00	4.061E+00	1.770E+00

TABLE A.9 PRESSURE DATA $2a_d/\lambda = 0.0123$, $\alpha^+ = 0.0011$

Date: September 1,1988
Fluid: Water　　Temp: 25° C　Density: 0.997 g/cm^3 v: 0.00896 cm^2/s
u^*: 10.34 cm/s　a^+: 36.0　Re: 66,400
slope: 0.3716　　intercept: -0.0470

Harmonic 1: amplitude= 15.54 　　phase= +173°
Harmonic 2: amplitude= 0.99 　　phase= +176°
Harmonic 3: amplitude= 0.41 　　phase= +79°

x value/lambda	Differential Pressure	Average Voltage
3.125E-02	7.399E-01	2.045E-01
6.250E-02	1.816E+00	3.704E-01
1.250E-01	4.221E+00	5.843E-01
1.563E-01	7.842E+00	9.946E-01
1.875E-01	9.405E+00	1.168E+00
2.188E-01	1.248E+01	1.515E+00
2.500E-01	1.471E+01	1.765E+00
2.813E-01	1.943E+01	2.302E+00
3.125E-01	2.161E+01	2.547E+00
3.438E-01	2.447E+01	2.869E+00
3.750E-01	2.638E+01	3.082E+00
4.063E-01	2.787E+01	3.247E+00
4.375E-01	3.019E+01	3.507E+00
4.688E-01	3.077E+01	3.567E+00
5.000E-01	3.334E+01	3.856E+00
5.313E-01	3.268E+01	3.773E+00
5.625E-01	3.233E+01	3.725E+00
5.938E-01	3.021E+01	3.473E+00
6.250E-01	2.990E+01	3.429E+00
6.563E-01	2.840E+01	3.250E+00
6.875E-01	2.329E+01	2.652E+00
7.188E-01	2.184E+01	2.478E+00
7.500E-01	1.896E+01	2.138E+00
7.813E-01	1.576E+01	1.762E+00
8.125E-01	1.224E+01	1.348E+00
8.438E-01	1.057E+01	1.149E+00
8.750E-01	7.405E+00	7.758E-01
9.063E-01	5.214E+00	5.158E-01
9.375E-01	3.218E+00	2.781E-01
9.688E-01	3.699E+00	3.263E-01
1.000E+00	1.709E+00	8.941E-02

TABLE A.10 PRESSURE DATA $2a_d/\lambda = 0.0123$, $\alpha^+ = 0.00154$

Date: September 3,1988
Fluid: Water   Temp: 25° C   Density: 0.997 g/cm^3 ν: .0.00896 cm^2/s
u*: 7.205 cm/s   a$^+$: 25.1   Re: 43,900
slope: 0.1467   intercept: -0.0244

Harmonic 1: amplitude= 12.59   phase= +172°
Harmonic 2: amplitude= 0.52   phase= +158°
Harmonic 3: amplitude= 0.22   phase= +85°

x value/lambda	Differential Pressure	Average Voltage
3.125E-02	2.347E+00	4.904E-01
6.250E-02	3.548E+00	6.519E-01
9.375E-02	4.462E+00	7.725E-01
1.250E-01	5.770E+00	9.491E-01
1.563E-01	8.167E+00	1.280E+00
1.875E-01	9.091E+00	1.402E+00
2.188E-01	1.234E+01	1.855E+00
2.500E-01	1.441E+01	2.139E+00
2.813E-01	1.772E+01	2.599E+00
3.125E-01	1.994E+01	2.905E+00
3.438E-01	2.218E+01	3.215E+00
3.750E-01	2.383E+01	3.440E+00
4.063E-01	2.489E+01	3.582E+00
4.375E-01	2.646E+01	3.795E+00
4.688E-01	2.674E+01	3.825E+00
5.000E-01	2.842E+01	4.055E+00
5.313E-01	2.870E+01	4.086E+00
5.625E-01	2.814E+01	3.998E+00
5.938E-01	2.665E+01	3.777E+00
6.250E-01	2.659E+01	3.759E+00
6.563E-01	2.487E+01	3.507E+00
6.875E-01	2.288E+01	3.215E+00
7.188E-01	2.022E+01	2.828E+00
7.500E-01	1.798E+01	2.501E+00
7.813E-01	1.573E+01	2.174E+00
8.125E-01	1.323E+01	1.810E+00
8.438E-01	1.177E+01	1.593E+00
8.750E-01	9.128E+00	1.210E+00
9.063E-01	7.130E+00	9.169E-01
9.375E-01	4.122E+00	4.811E-01
9.688E-01	5.280E+00	6.365E-01
1.000E+00	2.539E+00	2.385E-01

TABLE A.11 PRESSURE DATA $2a_d/\lambda = 0.0123$, $\alpha^+ = 0.0020$

Date: August 31,1988
Fluid: Water   Temp: 25° C Density: 0.997 g/cm^3 υ: .0.00896 cm^2/s
u*: 5.483 cm/s   a$^+$: 19.1   Re: 32,100
slope: 0.0795   intercept: -0.1349

Harmonic 1:   amplitude= 10.85   phase= +172°
Harmonic 2:   amplitude= 0.47   phase= -169ˆ
Harmonic 3:   amplitude= 0.13   phase=   +53°

x value/lambda	Differential Pressure	Average Voltage
3.125E-02	2.605E-01	1.550E+00
6.250E-02	1.035E+00	1.656E+00
9.375E-02	1.785E+00	1.758E+00
1.250E-01	2.727E+00	1.889E+00
1.563E-01	4.383E+00	2.126E+00
1.875E-01	5.167E+00	2.234E+00
2.188E-01	7.596E+00	2.586E+00
2.500E-01	9.600E+00	2.875E+00
2.813E-01	1.292E+01	3.360E+00
3.125E-01	1.505E+01	3.668E+00
3.438E-01	1.649E+01	3.873E+00
3.750E-01	1.785E+01	4.067E+00
4.063E-01	1.863E+01	4.174E+00
4.375E-01	2.070E+01	4.473E+00
4.688E-01	2.069E+01	4.461E+00
5.000E-01	2.232E+01	4.695E+00
5.313E-01	2.167E+01	4.590E+00
5.625E-01	2.100E+01	4.480E+00
5.938E-01	1.975E+01	4.283E+00
6.250E-01	2.007E+01	4.323E+00
6.563E-01	1.878E+01	4.121E+00
6.875E-01	1.786E+01	3.974E+00
7.188E-01	1.496E+01	3.532E+00
7.500E-01	1.344E+01	3.297E+00
7.813E-01	1.046E+01	2.842E+00
8.125E-01	8.120E+00	2.485E+00
8.438E-01	7.110E+00	2.325E+00
8.750E-01	5.094E+00	2.015E+00
9.063E-01	3.377E+00	1.749E+00
9.375E-01	2.061E+00	1.544E+00
9.688E-01	-1.331E-01	1.207E+00
1.000E+00	-1.191E+00	1.040E+00

TABLE A.12 PRESSURE DATA $2a_d/\lambda = 0.0123$, $\alpha^+ = 0.0029$

Date: September 2,1988

Fluid: Water   Temp: 25° C Density: 0.997 g/cm^3 υ: .0.00896 cm^2/s

u^*: 3.843 cm/s a^+: 13.4   Re: 21,400

slope: 0.0736   intercept: -0.0319

Harmonic 1:   amplitude= 8.98   phase= +172°
Harmonic 2:   amplitude= 0.74   phase= -175°
Harmonic 3:   amplitude= 0.27   phase= -169°

x value/lambda	Differential Pressure	Average Voltage
3.125E-02	3.793E+00	7.335E-01
6.250E-02	5.064E+00	8.307E-01
9.375E-02	6.166E+00	9.143E-01
1.250E-01	6.705E+00	9.525E-01
1.563E-01	7.861E+00	1.040E+00
1.875E-01	8.996E+00	1.127E+00
2.188E-01	1.172E+01	1.340E+00
2.500E-01	1.276E+01	1.420E+00
2.813E-01	1.478E+01	1.577E+00
3.125E-01	1.631E+01	1.695E+00
3.438E-01	1.782E+01	1.811E+00
3.750E-01	1.868E+01	1.875E+00
4.063E-01	1.865E+01	1.868E+00
4.375E-01	2.120E+01	2.068E+00
4.688E-01	2.166E+01	2.100E+00
5.000E-01	2.250E+01	2.162E+00
5.313E-01	2.319E+01	2.213E+00
5.625E-01	2.139E+01	2.063E+00
5.938E-01	1.864E+01	1.836E+00
6.563E-01	2.008E+01	1.942E+00
6.875E-01	1.930E+01	1.874E+00
7.188E-01	1.682E+01	1.669E+00
7.500E-01	1.539E+01	1.549E+00
7.813E-01	1.356E+01	1.397E+00
8.125E-01	1.144E+01	1.221E+00
8.438E-01	1.072E+01	1.158E+00
8.750E-01	8.800E+00	9.986E-01
9.063E-01	6.463E+00	8.053E-01
9.375E-01	5.283E+00	7.053E-01
9.688E-01	5.176E+00	6.916E-01
1.000E+00	1.353E+00	3.789E-01

TABLE A.13 PRESSURE DATA $2a_d/\lambda = 0.0123$, $\alpha^+ = 0.0039$

Date: September 14, 1988
Fluid: Dextrose   Temp: 25° C Density: 1.122 g/cm^3 υ: .0.0249 cm^2/s
u*: 7.84 cm/s   a$^+$: 9.85   Re: 15,000
slope: 0.2031   intercept: -0.0584

Harmonic 1:   amplitude= 9.78   phase= +163°
Harmonic 2:   amplitude= 0.60   phase= +158°
Harmonic 3:   amplitude= 0.10   phase=   +28°

x value/lambda	Differential Pressure	Average Voltage
3.125E-02	1.181E+00	4.400E-01
6.250E-02	1.930E+00	5.335E-01
9.375E-02	2.635E+00	6.211E-01
1.250E-01	3.602E+00	7.442E-01
1.563E-01	5.184E+00	9.514E-01
1.875E-01	6.546E+00	1.129E+00
2.188E-01	8.579E+00	1.397E+00
2.500E-01	1.047E+01	1.646E+00
2.813E-01	1.181E+01	1.821E+00
3.125E-01	1.379E+01	2.082E+00
3.438E-01	1.551E+01	2.308E+00
3.750E-01	1.723E+01	2.534E+00
4.063E-01	1.882E+01	2.743E+00
4.375E-01	2.041E+01	2.950E+00
4.688E-01	2.117E+01	3.045E+00
5.000E-01	2.254E+01	3.223E+00
5.313E-01	2.067E+01	2.960E+00
5.625E-01	2.127E+01	3.033E+00
5.938E-01	2.094E+01	2.979E+00
6.250E-01	2.110E+01	2.993E+00
6.563E-01	2.048E+01	2.900E+00
6.875E-01	1.973E+01	2.789E+00
7.188E-01	1.736E+01	2.457E+00
7.500E-01	1.636E+01	2.311E+00
7.813E-01	1.318E+01	1.869E+00
8.125E-01	1.126E+01	1.598E+00
8.438E-01	1.022E+01	1.447E+00
8.750E-01	8.603E+00	1.219E+00
9.063E-01	6.634E+00	9.415E-01
9.375E-01	4.679E+00	6.660E-01
9.688E-01	3.568E+00	5.059E-01
1.000E+00	3.550E+00	4.948E-01

TABLE A.14 PRESSURE DATA $2a_d/\lambda = 0.0123$, $\alpha^+ = 0.0059$

Date: September 11,1988
Fluid: Dextrose Temp: 25° C Density: 1.159 g/cm^3 v: .0.0406 cm^2/s
u*: 8.542 cm/s a$^+$: 6.57 Re: 9450
slope: 0.1316 intercept: -0.1415

Harmonic 1: amplitude= 6.79 phase= +162°
Harmonic 2: amplitude= 0.36 phase= -133°
Harmonic 3: amplitude= 0.08 phase= +12°

x value/lambda	Differential Pressure	Average Voltage
3.125E-02	-2.197E-01	8.402E-01
6.250E-02	-7.968E-02	8.599E-01
9.375E-02	3.081E-01	9.438E-01
1.250E-01	9.055E-01	1.082E+00
1.563E-01	1.883E+00	1.318E+00
1.875E-01	2.526E+00	1.468E+00
2.188E-01	3.327E+00	1.658E+00
2.500E-01	4.697E+00	1.996E+00
2.813E-01	6.167E+00	2.360E+00
3.125E-01	7.467E+00	2.679E+00
3.438E-01	8.599E+00	2.955E+00
3.750E-01	9.632E+00	3.206E+00
4.063E-01	1.020E+01	3.337E+00
4.375E-01	1.161E+01	3.686E+00
4.688E-01	1.208E+01	3.790E+00
5.000E-01	1.300E+01	4.010E+00
5.313E-01	1.319E+01	4.044E+00
5.625E-01	1.344E+01	4.091E+00
5.938E-01	1.280E+01	3.911E+00
6.250E-01	1.316E+01	3.986E+00
6.563E-01	1.261E+01	3.827E+00
6.875E-01	1.166E+01	3.567E+00
7.188E-01	1.026E+01	3.188E+00
7.500E-01	7.562E+00	2.458E+00
8.125E-01	6.119E+00	2.068E+00
8.438E-01	5.058E+00	1.778E+00
8.750E-01	3.380E+00	1.328E+00
9.063E-01	2.169E+00	9.983E-01
9.375E-01	9.476E-01	6.663E-01
9.688E-01	5.270E-01	5.412E-01
1.000E+00	3.347E-01	4.750E-01

TABLE A.15 PRESSURE DATA $2a_d/\lambda = 0.0123$, $\alpha^+ = 0.0079$

Date: September 10,1988
Fluid: Dextrose   Temp: 25° C   Density: 1.159 g/cm^3 υ: .0.0406 cm^2/s
u*: 6.35 cm/s   a$^+$: 4.88   Re: 6730
slope: 0.0959   intercept: -0.0573

Harmonic 1:   amplitude= 5.72   phase= +157°
Harmonic 2:   amplitude= 0.52   phase= -127°
Harmonic 3:   amplitude= 0.32   phase=   +44°

x value/lambda	Differential Pressure	Average Voltage
3.125E-02	-7.393E-01	4.401E-01
6.250E-02	-5.819E-01	4.585E-01
9.375E-02	-1.911E-01	5.225E-01
1.250E-01	-1.650E-01	5.152E-01
1.563E-01	7.121E-01	6.744E-01
1.875E-01	1.707E+00	8.565E-01
2.188E-01	2.297E+00	9.596E-01
2.500E-01	2.973E+00	1.080E+00
2.813E-01	4.409E+00	1.348E+00
3.125E-01	5.515E+00	1.552E+00
3.438E-01	6.483E+00	1.729E+00
3.750E-01	6.972E+00	1.812E+00
4.063E-01	7.627E+00	1.928E+00
4.375E-01	8.600E+00	2.106E+00
4.688E-01	8.572E+00	2.088E+00
5.000E-01	9.518E+00	2.260E+00
5.313E-01	1.087E+01	2.512E+00
5.625E-01	1.127E+01	2.579E+00
5.938E-01	1.060E+01	2.434E+00
6.250E-01	1.121E+01	2.543E+00
6.563E-01	1.067E+01	2.424E+00
6.875E-01	1.013E+01	2.305E+00
7.188E-01	8.386E+00	1.952E+00
7.500E-01	6.864E+00	1.642E+00
7.813E-01	6.120E+00	1.484E+00
8.125E-01	5.104E+00	1.273E+00
8.438E-01	4.014E+00	1.047E+00
8.750E-01	2.491E+00	7.369E-01
9.063E-01	1.356E+00	5.024E-01
9.375E-01	5.421E+00	1.285E+00
9.688E-01	7.481E-02	2.270E-01
1.000E+00	-9.929E-02	1.805E-01

TABLE A.16 PRESSURE DATA $2a_d/\lambda = 0.0123$, $\alpha^+ = 0.0099$

Date: September 8,1988
Fluid: Dextrose   Temp: 25° C Density: 1.205 g/cm^3 υ: 0.0740 cm^2/s
u*: 9.23 cm/s   a$^+$: 3.90   Re: 5200
slope: 0.1339   intercept: -0.1560

Harmonic 1:   amplitude= 4.69   phase= +162°
Harmonic 2:   amplitude= 0.38   phase= +175°
Harmonic 3:   amplitude= 0.17   phase=   +10°

x value/lambda	Differential Pressure	Average Voltage
3.125E-02	1.426E+00	1.585E+00
6.250E-02	1.682E+00	1.644E+00
9.375E-02	1.900E+00	1.692E+00
1.250E-01	2.161E+00	1.753E+00
1.563E-01	2.538E+00	1.849E+00
1.875E-01	3.265E+00	2.054E+00
2.188E-01	3.967E+00	2.251E+00
2.500E-01	5.300E+00	2.642E+00
2.813E-01	6.465E+00	2.981E+00
3.125E-01	7.466E+00	3.270E+00
3.438E-01	7.762E+00	3.342E+00
3.750E-01	8.794E+00	3.640E+00
4.063E-01	9.257E+00	3.764E+00
4.375E-01	9.497E+00	3.818E+00
4.688E-01	9.684E+00	3.856E+00
5.000E-01	1.012E+01	3.970E+00
5.313E-01	1.061E+01	4.103E+00
5.625E-01	1.103E+01	4.212E+00
5.938E-01	9.987E+00	3.871E+00
6.250E-01	1.099E+01	4.161E+00
6.563E-01	1.027E+01	3.919E+00
6.875E-01	9.786E+00	3.751E+00
7.188E-01	8.874E+00	3.450E+00
7.500E-01	7.978E+00	3.154E+00
7.813E-01	7.213E+00	2.899E+00
8.125E-01	6.539E+00	2.672E+00
8.438E-01	5.367E+00	2.291E+00
8.750E-01	4.367E+00	1.963E+00
9.063E-01	3.412E+00	1.649E+00
9.375E-01	2.293E+00	1.285E+00
9.688E-01	2.012E+00	1.179E+00
1.000E+00	1.711E+00	1.067E+00

TABLE A.17 PRESSURE DATA $2a_d/\lambda = 0.0123$, $\alpha^+ = 0.0101$

Date: September 7,1988
Fluid: Dextrose   Temp: 25° C Density: 1.205 g/cm^3 υ: .0.0740 cm^2/s
u^*: 9.102 cm/s a^+: 3.84   Re: 5120
slope: 0.1109   intercept: -0.0676

Harmonic 1:   amplitude= 4.45   phase= +156°
Harmonic 2:   amplitude= 0.28   phase= -147°
Harmonic 3:   amplitude= 0.13   phase= +121°

x value/lambda	Differential Pressure	Average Voltage
3.125E-02	5.658E-01	7.914E-01
6.250E-02	6.825E-01	8.107E-01
9.375E-02	1.056E+00	9.229E-01
1.250E-01	1.422E+00	1.033E+00
1.563E-01	2.185E+00	1.286E+00
1.875E-01	2.844E+00	1.501E+00
2.188E-01	3.563E+00	1.739E+00
2.500E-01	4.271E+00	1.972E+00
2.813E-01	4.388E+00	1.991E+00
3.125E-01	5.278E+00	2.291E+00
3.438E-01	6.191E+00	2.598E+00
3.750E-01	6.890E+00	2.828E+00
4.063E-01	7.640E+00	3.077E+00
4.375E-01	8.410E+00	3.333E+00
4.688E-01	8.972E+00	3.514E+00
5.000E-01	9.479E+00	3.674E+00
5.313E-01	9.746E+00	3.748E+00
5.625E-01	9.744E+00	3.724E+00
5.938E-01	8.668E+00	3.312E+00
6.250E-01	9.849E+00	3.716E+00
6.563E-01	9.675E+00	3.630E+00
6.875E-01	9.100E+00	3.399E+00
7.188E-01	8.264E+00	3.073E+00
7.500E-01	7.231E+00	2.676E+00
7.813E-01	6.605E+00	2.427E+00
8.125E-01	5.748E+00	2.094E+00
8.438E-01	4.857E+00	1.748E+00
8.750E-01	3.754E+00	1.326E+00
9.063E-01	2.987E+00	1.025E+00
9.375E-01	2.253E+00	7.359E-01
9.688E-01	1.805E+00	5.510E-01
1.000E+00	1.621E+00	4.614E-01

TABLE A.18 PRESSURE DATA $2a_d/\lambda = 0.0123$, $\alpha^+ = 0.00148$

Date: September 6,1988

Fluid: Dextrose   Temp: 25° C Density: 1.205 g/cm^3 υ: .0.0740 cm^2/s

u*:   6.202 cm/s   a$^+$: 2.62   Re: 3300

slope: 0.0762   intercept: -0.1094

Harmonic 1:   amplitude= 3.72   phase= +164°
Harmonic 2:   amplitude= 0.45   phase= -179°
Harmonic 3:   amplitude= 0.11   phase= -134°

x value/lambda	Differential Pressure	Average Voltage
3.125E-02	3.159E-01	1.497E+00
6.250E-02	8.044E-01	1.601E+00
9.375E-02	9.874E-01	1.631E+00
1.250E-01	9.791E-01	1.613E+00
1.563E-01	1.581E+00	1.745E+00
1.875E-01	2.294E+00	1.904E+00
2.188E-01	2.981E+00	2.056E+00
2.500E-01	3.887E+00	2.262E+00
2.813E-01	4.585E+00	2.418E+00
3.125E-01	5.074E+00	2.522E+00
3.438E-01	5.431E+00	2.594E+00
3.750E-01	6.501E+00	2.824E+00
4.375E-01	7.115E+00	2.959E+00
4.688E-01	7.292E+00	2.987E+00
5.000E-01	7.918E+00	3.125E+00
5.313E-01	7.552E+00	3.020E+00
5.625E-01	7.638E+00	3.025E+00
5.938E-01	4.741E+00	2.301E+00
6.250E-01	7.476E+00	2.954E+00
6.563E-01	7.030E+00	2.829E+00
6.875E-01	7.414E+00	2.908E+00
7.188E-01	6.462E+00	2.659E+00
7.500E-01	4.206E+00	2.092E+00
7.813E-01	4.960E+00	2.261E+00
8.125E-01	4.225E+00	2.066E+00
8.438E-01	3.824E+00	1.952E+00
8.750E-01	2.597E+00	1.636E+00
9.063E-01	1.903E+00	1.451E+00
9.375E-01	7.825E-01	1.161E+00
9.688E-01	4.447E-01	1.063E+00
1.000E+00	-1.913E-02	9.342E-01

APPENDIX B

Data   Analysis   Programs

```
C**********************************************************
C**********************************************************
C******************PROGRAM   PRESS.FOR********************
C**********************************************************
C*   This program reads the binary file created by the Metra-
C*   Byte Analog to Digital conversion board using program
C*   Stream16.  There are two files necessary to run this pro
C*   gram.  The first file, for008.dat, should contain:  the
C*   number of points per file, value of intercept and slope
C*   from pressure transducer calibration, density of fluid,
C*   friction velocity and a listing of the following (at
C*   each x value) : x value(inches), data filename, raw data
C*   output index.  The second file, for009.dat, should con-
C*   tain:  raw output filename and the number of points in
C*   that file(at each x value, if necessary), and the out-
C*   put file name for the plotting file.
C*   The program will convert the binary data to ascii
C*   form with units of voltage.  The dimensionless pressure is calculated
C*   and plotting files are then constructed .
C*   By Dave Courtemanche 3/2/88
C**********************************************************
C**********************************************************

        character*12 filename1(32), routname
        character*12 profilename, fitname
      integer*4 i, j, k, ii, jj, kk, ij, nleft, nrec
       integer*4 ipts, nnleft, nnrec
       integer*4 nopts, nnopts, numpts, ndiff
       integer*2 buffer(256)
      real xval(32), value(30000), val
      real row, ustar, norm
       real delp(10000), totp,totv, a, b, avgp(32),avgv(32)
       real int(32), skew(32), flat(32), delpp(32), intp(32)


C**********************************************************
C*    nnopts is the # of points per file            *
C**********************************************************

      read(8,*) nnopts, a, b, row, ustar
      nnleft = mod(nnopts,256)
      nnrec= nnopts/256
       norm = row*ustar*ustar/2486.2

   do 10 ij= 1, 32


C**********************************************************
C*      xval(ij) is the x value(inches).  (This will be con-*
C*      verted to x/lambda.)  Filename1(ij) is the raw press*
C*      data filename the this x location.  Irawout (ij)     *
C*      should be 1 if you want to output raw data for this x
C**********************************************************
```

```
        read(8,3000) xval(ij), filename1(ij)
c*      @, irawout
3000    format (f8.6, a11, 4i3)
        xval(ij) = xval(ij) / 2.00

        open(unit=10,file=filename1(ij),form='binary',
      @status='old',recl=16, access='direct')

C************************************************************
C*      This part of program unpacks data as voltage, converts
C*      it to pressure(inches of water), and calculates the
C*   average.                           *
C************************************************************

    kj=0
      nopts=nnopts
      nleft=nnleft
      nrec=nnrec +1
    kk=0
    totp=0
    totv=0
     int(ij)=0
     skew(ij)=0
     flat(ij)=0

    do 20 k=1, nrec
      if(k .lt. nrec) then
      read (10) buffer

    do 30 ii = 1, 256
        call unpack (buffer(ii), ichan, val )
      kk = kk + 1
       value(kk) = val
       delp(kk) = a + b * value(kk)
       totp = totp + delp(kk)
       totv = totv + value(kk)

30      continue

    else
      read (10) buffer

    do 40 ii = 1,nleft
        call unpack(buffer(ii), ichan, val)
      kk = kk + 1
       value(kk) = val
       delp(kk) = a + b * value(kk)
       totp = totp + delp(kk)
       totv = totv + value(kk)
```

```fortran
40      continue

      endif
20      continue
        rewind (10)

        avgp(ij) = totp/nopts
        avgv(ij) = totv/nopts

C*      Outputting raw voltage data (if desired).
c*      if (irawout .ne.1 ) goto 3
c*          read(9,3400) routname, irawnum
c*3400    format (a12,i4)
c*          open(unit=27, file=routname,form='formatted',status=
c*      @'new')
c*      do 50 i = 1, irawnum
c*          write(27,3500) value(i)
c*  50    continue
c*3500    format(1pe11.3)
c*   3    continue

C*      CALCULATING THE HIGHER MOMENTS*************************
        do 15 kk=1,nopts
            int(ij)=int(ij)+(delp(kk)-avgp(ij))**2
            skew(ij)=skew(ij)+(delp(kk)-avgp(ij))**3
            flat(ij)=flat(ij)+(delp(kk)-avgp(ij))**4
15      continue
        int(ij)  = sqrt(int(ij)/nopts)
        skew(ij) = skew(ij)/(nopts * int(ij)**3)
        flat(ij) = flat(ij)/(nopts * int(ij)**4)

10      continue

C*      Subtracting mean pressure gradient
      do 37 kk=1,32
          avgp(kk)= avgp(kk) + 2.0305*norm*float(kk)/32.
37      continue

C*   Non-dimensionalizing with wall parameters
      do 16 l=1,32
          delpp(l)=avgp(l)/norm
          intp(l)=int(l)/norm
16      continue

C***      outputting plotting files***********

        read(9,3550) profilename
        read(9,3550) fitname
3550    format(a12)

          open(unit=50,file=profilename,form='formatted',
```

```
       @status='new')
           open(unit=51,file=fitname,form='formatted',
       @status='new')
        write (50,6350)
6350   format('xval/lambda  ',2x,'  delp  ',3x,'    delpp'
       @,3x,'  intp  ',3x,'  avgv ')




    do 100  ll=1,32
        write(50,6400)  xval(ll),avgp(ll),delpp(ll),
     @intp(ll),avgv(ll)
6400    format(6(1pe10.3,2x))
        write(51,6500)  xval(ll),delpp(ll)
6500    format(2(1pe10.3,2x))
 100    continue

17    stop
      end

C*    Subroutine used to unpack data from binary to ascii
          subroutine  unpack (ibin,ichan, val)
        integer*2  ibin
         integer*4  ichan, ival
        real  val, aval

         ichan = iand(ibin, 15)
         if (ibin .lt. 2047) then
         ival = iand(ibin, 65535)

        else

        ival = ibin

        endif

        ival = ival / 16
        aval = ival
         val = (aval/4095.) *5.

         return
        end
```

```
      fit3u.for
C*    This program reads in a two dimensional array
C*    It then fits the second variable of the array to the first
C*..using a three harmonic Fourier series.
C*    A plotting file is output which shows both the first harmonic fit
C*    and the fit using all three harmonics.
      program datfit
        dimension a(20,20),b(20,1)
          dimension  amag(10),z(100),x(100),angd(10),ang(10)
          dimension  work(20000),rat(10),xl(600),f(600)
        dimension ff(600)
          character*12,  filename1,filename2,filename3
        real mean,pi

        print*,' Enter the input file name'
        read(5,22)filename1
        print*,' Enter the number of points (0 to 360 degrees)'
      read*,np
c        print*,' three harmonics will be calculated '

        print*,' Enter harmonic output file name'
        read(5,22)filename3
22     format(a12)
          open(unit=40,file=filename1,form='formatted',status='old')
          open(unit=72,file=filename3,form='formatted',status='new')

      nharmo=3
       n=nharmo*2
      mo=n+1
       pi=4.0*atan(1.0)

      do 1 i=1,mo
      do 2 j=1,mo
2      a(i,j)=0.
1      continue

      do 3 k=1,mo
3      b(k,1)=0.

      do 4 i=1,np
         read(40,433)x(i),z(i)
        x(i)=x(i)*2*pi
    4  continue

      do 5 m=1,np
      ii=0
        b(mo,1)=b(mo,1)+z(m)
       do 6 jj=1,n,2
       ii=ii+1
          b(jj,1)=b(jj,1)+z(m)*sin(x(m)*ii)
          b(jj+1,1)=b(jj+1,1)+z(m)*cos(x(m)*ii)
```

```
      mm=0
       do 7 kk=1,n,2
       mm=mm+1
            a(jj,kk)=a(jj,kk)+sin(x(m)*ii)*sin(x(m)*mm)
             a(jj,kk+1)=a(jj,kk+1)+sin(x(m)*ii)*cos(x(m)*mm)
             a(jj+1,kk)=a(jj+1,kk)+cos(x(m)*ii)*sin(x(m)*mm)
             a(jj+1,kk+1)=a(jj+1,kk+1)+cos(x(m)*ii)*cos(x(m)*mm)
7      continue
          a(jj,mo)=a(jj,mo)+sin(x(m)*ii)
          a(jj+1,mo)=a(jj+1,mo)+cos(x(m)*ii)
        a(mo,jj)=a(jj,mo)
        a(mo,jj+1)=a(jj+1,mo)
6      continue
5      continue

       a(mo,mo)=float(np)
       call  leqt1f(a,1,mo,20,b,0,work,ier)
      print*,' ier= ',ier

   if=0
    do 8 ie=1,n,2
    if=if+1
         amag(if)=sqrt(b(ie,1)**2+b(ie+1,1)**2)
      bb=-b(ie,1)
      bbb=b(ie+1,1)
        ang(if)=atan2(bb,bbb)
         angd(if)=ang(if)*360./(2.*pi)
         rat(if)=amag(if)/amag(1)
8      continue

     zavg=b(mo,1)
     print 100,zavg
         print  101,(ih,amag(ih),angd(ih),rat(ih),ih=1,3)
     write(72,100)zavg
         write(72,101)(ih,amag(ih),angd(ih),rat(ih),ih=1,3)
100    format(//,' mean=',2x,f12.5)
101    format(1x,'harmonic= ',i2,3x,'amp= ',f9.5,3x,'phase= ',f10.3,
    @ 3x,' amp. ratio= ',f7.5)

C**    This section generates a curve of the fourier fit

    print*,' Include the mean? 1=yes '
    read*,reply

  mean=0.0
     if(reply.eq.1)mean=zavg


   do 800 i=1,250
      xl(i)=float((i-1))/249.0
     sum=0.0
```

```
      do 850 j=1,1
            sum=sum+amag(j)*cos(2.0*pi*j*xl(i)+ang(j))
850   continue
      f(i)=mean+sum

    sum1=0.0
    do 860 j=1,3
            sum1=sum1+amag(j)*cos(2.0*pi*j*xl(i)+ang(j))
860   continue
      ff(i)=mean+sum1
800   continue

    do i=1,250
        write(72,433)xl(i),f(i),ff(i)
    end do

433   format(3(1pe10.3,2x))

    stop
    end
```
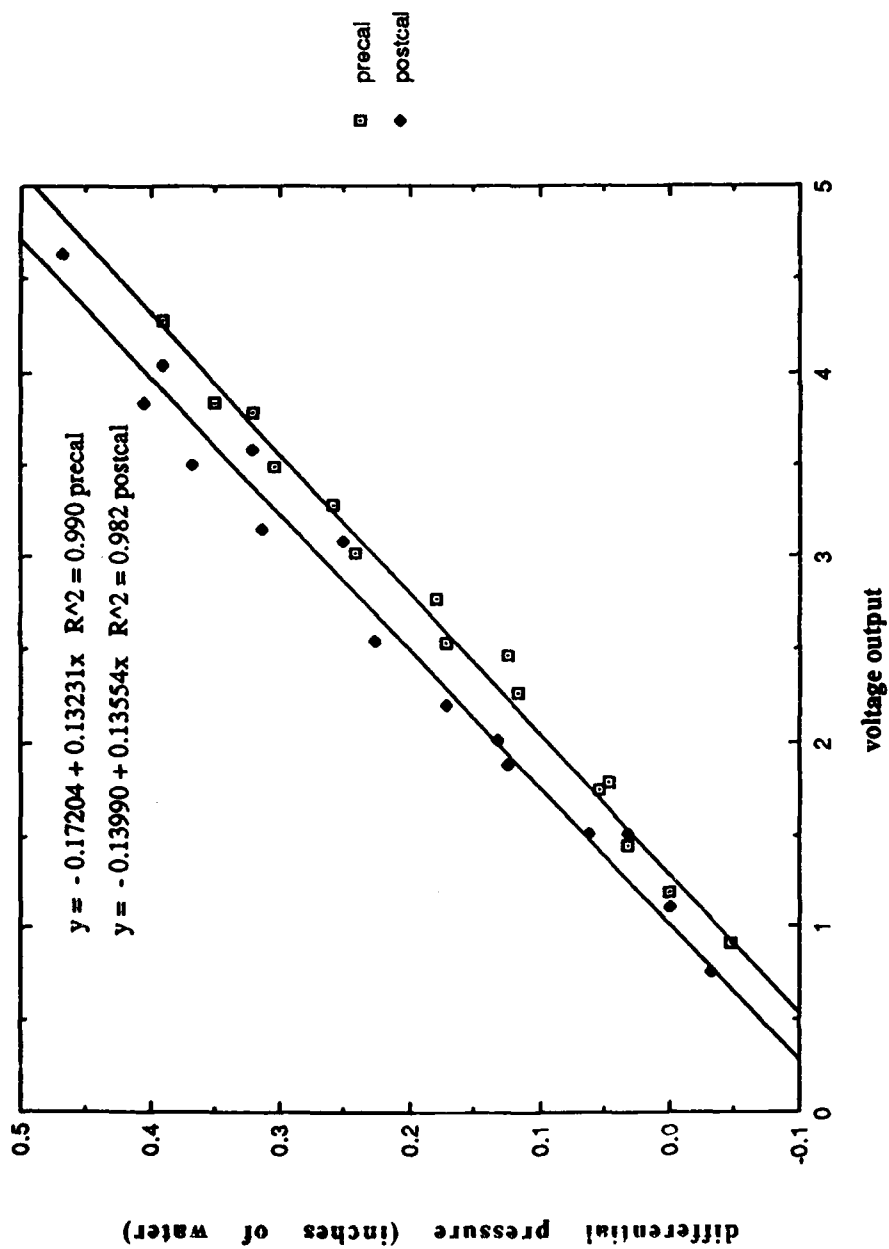
APPENDIX C

Sample   Calibration

precal
postcal

$y = -0.17204 + 0.13231x \quad R^2 = 0.990 \text{ precal}$

$y = -0.13990 + 0.13554x \quad R^2 = 0.982 \text{ postcal}$

voltage output

differential pressure (inches of water)

Figure C.1 Sample Calibration of Pressure Transducer

NOMENCLATURE

A	van Driest parameter
$\overline{A}$	Average van Driest parameter, see equation (3.18)
a_d	amplitude of wave surface (cm)
a_i	amplitude of ith harmonic of non-dimensionalized wave induced surface pressure
a^+	non-dimensional wave surface amplitude
b_i	coefficients in orthogonal transformation
C_f	friction factor
h	average channel half height (cm)
K_1, K_2	non-dimensional empirical constants, see equation (3.18)
K_L	non-dimensional empirical lag constant, see equation (3.19)
p_d	surface pressure (inches H_2O)
p	non-dimensional surface pressure ($p = p_d / \rho u^{*2}$)
p^+	non-dimensional pressure gradient, see equation (3.18)
$p^+{}_{eff}$	effective pressure gradient, see equation (3.19)
Re	Reynolds number, based on bulk velocity and channel half height
R_{ii}	time-averaged stress tensor (g/cm s^2)
S_{ii}	time-averaged rate of strain tensor (1/s)
u	streamwise velocity (cm/s)
u_b	bulk velocity (cm/s)
u'	fluctuating component of streamwise velocity (cm/s)
u^*	friction velocity (cm/s)
v	normal velocity (cm/s)

v'	fluctuating component of normal wise velocity (cm/s)
x	Cartesian streamwise coordinate (cm)
x^+	non-dimensional Cartesian streamwise coordinate
y	Cartesian normal coordinate (cm)
y'	distance to solid surface (cm)
y_t	height of top wall of channel in Cartesian coordinates (cm)

Greek letters

α	wave number (1/cm)
α^+	dimensionless wave number
η	curvilinear normal coordinate (cm)
η_t	height of top wall in curvilinear coordinates (cm)
κ	von Karman constant
λ	wavelength of wave surface (cm)
θ_i	phase angle of ith harmonic of non-dimensionalized wave induced surface pressure
ν	kinematic viscosity (cm^2/s)
ν_t	turbulent eddy viscosity, see equations (3.14-16) (cm2/s)
ε	curvilinear streamwise coordinate (cm)
ρ	density (g/cm^3)
τ	local shear stress (g/s^2)
ψ	stream function, see equations (3.9-10) (cm^2/s)
ω	vorticity, see equation (3.8) (1/s)

REFERENCES

Abrams, J. 1979 A Nonlinear Boundary Layer Analysis for Flow Over a Solid Wavy Surface, M.S. Thesis, Department of Chemical Engineering, University of Illinois, Urbana.

Abrams, J. 1984 Turbulent Flow Over Small Amplitude Solid Waves, Ph.D. Thesis, Department of Chemical Engineering, University of Illinois, Urbana.

Benjamin, T. B. 1959 Shearing Flow Over a Wavy Boundary, J. Fluid Mech., 6, 161-205.

Buckles, J. J. 1979 Interpretation of Pressure Measurements for Separated Flow Over a Wavy Surface, M.S.. Thesis, Department of Chemical Engineering, University of Illinois, Urbana.

Cook, G. W. 1970 Turbulent Flow Over Solid Wavy Surfaces, Ph.D. Thesis, Department of Chemical Engineering, University of Illinois.

Dean, R. B. 1978 Reynolds Number Dependence of Skin Friction and Other Bulk Flow Variables in Two-Dimensional Rectangular Duct Flow. Trans. ASME, J. Fluids Engrg. 100, 215-223.

Frederick, K. 1986 Velocity Measurements for Turbulent Nonseperated Flow Over Solid Waves, Ph.D. Thesis, Department of Chemical Engineering, University of Illinois, Urbana.

Hsu, S. & Kennedy, J. F. 1971 Turbulent Flow in Wavy Pipes, J. Fluid Mech., 47, 481-502.

Kendall, J. M. 1970 The Turbulent Boundary Layer Over a Wall With Progressive Surface Waves, J. Fluid Mech., 41, 259-281.

Kuzan, J. D. 1986 Velocity Measurement for Turbulent Separated and Near Separated Flow Over Solid Waves, Ph.D. Thesis, Department of Chemical Engineering, University of Illinois, Urbana.

Lin, J. C., Walsh, M. J. & Balasubramanian, R. 1984 Drag of Two-Dimensional Small-Amplitude Symmetric and Asymmetric Wavy Walls in Turbulent Boundary Layers. NASA Technical Paper 2318.

Loyd, R. J., Moffat, R. J. & Kays, W. M. 1970 The Turbulent Boundary Layer on a Porous Plate: An Experimental Study of the Fluid Dynamics with Strong Favorable Pressure Gradients and Blowing, Stanford University Thermosc. Div. Rep. HMT-13.

McLean, J. W. 1983 Computation of Turbulent Flow Over a Moving Wavy Boundary. Phys. Fluids 26, 2065-2073.

Miles, J.W. 1957 On the Generation of Surface Waves by Shear Flows Part 1, J. Fluid Mech., 3, 185-204.

Miles, J.W. 1959 On the Generation of Surface Waves by Shear Flows Part 2, J. Fluid Mech., 6, 568-582.

Motzfeld, H. 1937 Die furbulente Stromung on welligen Wanden, Z. angew. Math. Mech., 17, 193-212.

Niederschulte, M.A. 1988 Turbulent Flow Through a Channel, Ph.D Thesis, Department of Chemical Engineering, University of Illinois, Urbana.

Saeger, J. C. & Reynolds, W. C. 1971 Perturbation Pressures Over Traveling Sinusoidal Waves with Fully Developed Turbulent Shear Flow, Report FM-9 Thermosciences Division, Department of Mechanical Engineering, Stanford University.

Shaw, R. 1960 "The Influence of Hole Dimensions on Static Pressure Measurements," J. Fluid Mech., 1, 550-564.

Sigal, A. 1971 An Experimental Investigation of the Turbulent Boundary Layer Over a Wavy Wall; Ph.D. Thesis, Department of Aeronautical Engineering, California Institute of Technology.

Thorsness, C. B. 1975 Transport Phenomena Associated with Flow Over a Solid Wavy Surface, Ph.D. Thesis, Department of Chemical Engineering, University of Illinois, Urbana.

Zagustin, K., Hsu, E. Y., Street, R. L., & Perry, B. 1966 Flow Over a Moving Boundary in Relation to Wind-Generated Waves, Technical Report No. 60, Department of Civil Engineering, Stanford University.

Zilker, D. P. 1976 Flow Over Wavy Surfaces, Ph.D. Thesis, Department of Chemical Engineering, University of Illinois, Urbana.

Distribution List

Editor
Applied Mechanics Review
Southwest Research Institute
8500 Culebra Road
San Antonio, TX 78206

Army Research Office
P. O. Box 12211
Research Triangle Park, NC 27709

Defense Research and Development Attache
Australian Embassy
1601 Massachusetts Avenue, NW
Washington, DC 20036

Mr. Dennis Bushnell
NASA Langley Research Center
Langely Station
Hampton, VA 23365

Dr. Gary Chapman
Ames Research Center
Mail Stop 227-4
Moffett Field, CA 94035

Librarian Station 5-2
Coast Guard Headquarters
NASSIF Building
400 Seventh Street, SW
Washington, DC 20591

Professor Stanley Corrsin
The Johns Hopkins University
Department of Mechanics and
  Materials Sciences
Baltimore, MD 21218

Technical Library
Naval Surface Weapons Center
Dahlgren Laboratory
Dahlgren, VA 22418

Library
David W. Taylor Naval Ship Research
  and Development Center
Code 522.1
Bethesda, MD 20084

Mr. Justin H. McCarthy, Jr.
David W. Taylor Naval Ship Research
  and Development Center
Code 1552
Bethesda, MD 20084

Dr. William B. Morgan
David W. Taylor Naval Ship Research
  and Development Center
Code 1540
Bethesda, MD 20084

Defense Technical Information Center
Cameron Station
Alexandria, VA 22314   12 copies

Engineering Documents Center
University of Illinois
208 Engineering Hall
1308 West Green Street
Urbana, IL 61801   2 copies

Engineering Societies Library
345 East 47th Street
New York, NY 10017

Professor Robert E. Falco
Michigan State University
Department of Mechanical Engineering
East Lansing, MI 48824

Professor H. F. Fasel
Aerospace and Mech. Engr. Dept.
University of Arizona
Tucson, AZ 85721

Professor Thomas J. Hanratty
University of Illinois at Urbana-
  Champaign
Department of Chemical Engineering
205 Roger Adams Laboratory
1209 West California Street
Urbana, IL 61801

Mr. R. J. Hansen
Naval Research Laboratory
Code 8441
Washington, DC 20375

Professor J. H. Haritonides
Department of Aero & Astro.
Massachusetts Institute
  of Technology
Cambridge, MA 02139

Dr. A. K. M. Fazle Hussain
University of Houston
Department of Mechanical Engineering
Houston, TX 77004

Professor R. E. Kaplan
Department of Aero Engineering
University of Southern California
University Park
Los Angeles, CA 90007

Dr. Phillip S. Klebanoff
National Bureau of Standards
Mechanics Section
Washington, DC 20234

Professor Louis Landweber
The University of Iowa
Institute of Hydraulic Research
Iowa City, IA 52242

Professor L. Gary Leal
California Institute of Technology
Division of Chemistry and
  Chemical Engineering
Pasadena, CA 91125

Library of Congress
Science and Technology Divsion
Washington, DC 20540

Professor H. W. Liepmann
California Institute of Technology
Graduate Aeronautical Laboratories
Pasadena, CA 91125

Lorenz G. Straub Library
University of Minnesota
St. Anthony Falls Hydraulic Laboratory
Minneapolis, MN 55414

Professor John L. Lumley
Cornell University
Sibley School of Mechanical
  and Aerospace Engineering
Ithaca, NY 14853

Donald McEligot
Gould Defense Systems Inc.
1 Corporative Park
Middletown, RI 02840

Dr. D. K. McLaughlin
Dynamics Technology Inc.
21311 Hawthorne Blvd., Suite 200
Torrance, CA 90503

Dr. Jim McMichael
Air Force Office of Scientific
  Research/NA
Building 410
Bolling AFB
Washington, DC 20332

Dr. Arthur B. Metzner
University of Delaware
Department of Chemical Engineering
Newark, DE 19711

Professor Richard W. Miksad
The University of Texas at Austin
Department of Civil Engineering
Austin, TX 78712

NASA Scientific and Technical
  Information Facility
P. O. Box 8757
Baltimore/Washington International
  Airport
Maryland 21240

Professor Paul M. Naghdi
University of California
Department of Mechanical Engineering
Berkeley, CA 94720

Technical Library
Naval Costal System Laboratory
Panama City, FL 32401

Technical Library
Naval Missile Center
Point Mugu, CA 93041

Technical Library
Naval Ocean Systems Center
San Diego, CA 92151

Library
Naval Postgraduate School
Monterey, CA 93940

Library
Naval Sea Systems Command A
Code 09GS
Washington, DC 20362

Mr. Thomas E. Peirce
Naval Sea Systems Command B
Code 63R21
Washington, DC 20362

Librarian
Naval Surface Weapons Center
White Oak Laboratory
Silver Spring, MD 20910

Technical Library
Naval Underwater Systems Center
Newport, RI 02840